An Experimental Investigation of the Fire Characteristics of the University of Waterloo Burn House Structure

by

Amanda J. Klinck

A thesis
presented to the University of Waterloo
in fulfilment of the
thesis requirement for the degree of
Master of Applied Science
in
Mechanical Engineering

Waterloo, Ontario, Canada, 2006

I hereby declare that I am the sole author of this thesis. This is a true copy of the thesis, including any required final revisions, as accepted by my examiners.

I understand that my thesis may be made electronically available to the public.

Abstract

This thesis reports on the procedure, results and analysis of four full scale fire tests that were performed at the University of Waterloo's Live Fire Research Facility. The purpose of these tests was to investigate the thermal characteristics of one room of the Burn House structure. A well controlled burn experiment was achieved in addition to an experiment where full room involvement in fire was observed. Comparisons were made of Burn House experimental data to previous residential fire studies undertaken by researchers from the University of Waterloo. This analysis showed similarities in growth rate characteristics, illustrating that fire behaviour in the Burn House is typical of residential structure fire behaviour. The Burn House experimental data was also compared to predictions from a fire model, CFAST. Predictions of upper layer temperatures from the model showed general agreement to experimental upper layer temperature measurements. A sensitivity analysis of the model was performed which indicated that some errors in model predictions could be attributed to user-specified quantities such as heat release rate. Recommendations were made for future work in relation to further investigation of the fire characteristics of the Burn House.

Acknowledgements

This work was completed under the supervision of Dr. A.B. Strong. It is to him that I owe my sincere appreciation for taking me on as his last graduate student and providing me with his undivided attention and help throughout the course of this degree. I would like to thank him for presenting me with the opportunity to participate in this exceptional project, for his guidance and the many hours he contributed to this work. His knowledge in the field of fire research is invaluable and I am forever indebted for having the opportunity to learn from him.

Many thanks to Gord Hitchman and Andy Barber who both provided valuable support needed for the completion of this project. Thanks as well to Professors E.J. Weckman and D. Johnson for their advice and guidance.

I would also like to thank the many co-operative students that worked in the fire research laboratory, as well as the City of Kitchener and Waterloo Fire Departments.

I would like to thank my parents for their unparalleled support and patience. Lastly, I would like to thank Mark for his continual love, support and belief in my abilities.

Table of Contents

List of Tables

List of Figures

List of Symbols, Abbreviations and Nomenclature

A_s	area of wood crib [m^2]
A_w	area of ventilation opening [m^2]
C_p *or* c	specific heat capacity [J/kg·K]
h	convection coefficient [$W/m^2 \cdot K$]
H	height of ventilation opening [m]
HRR	Heat Release Rate [kW or MW]
k *or* k_g	thermal conductivity [W/m·K]
m	mass [kg]
Pr	Prandlt number [dimensionless]
$\dot{Q}$	Rate of heat release [kW]
r	radius [m]
Re	Reynolds number [dimensionless]
t	time [s]
t_o	time to ignition [s]
t_2	time to final transition from slow to fast rate of spread over the upper surface of wood crib [s]
t_3	the time to flaming over the whole of the upper surfaces of wood crib [s]
τ	time (transient) response [s]
T_g	gas temperature [ºC]
α_f	fire growth coefficient [kW/s^2]
π	3.14159 [radians]
°	[degrees]
ρ	density [kg/m^3]
μ	dynamic viscosity at ambient temperature [$N \cdot s/m^2$]
μ_s	dynamic viscosity at surface temperature [$N \cdot s/m^2$]

CHAPTER ONE

Introduction

In the year 2001, 55,323 fires were reported in Canada, resulting in 338 deaths, 2,310 fire related injuries and over a billion dollars in property loss. Of those fires reported, 39% occurred in residential settings and accounted for 81% of all fire fatalities in Canada that year. Of these, 53% occurred specifically in single-family dwellings and accounted for over 300 million dollars in property loss [1]. Three quarters of all structural fires in the United States and Canada combined occur in family residences [2].

The occurrence of residential fires has been greatly reduced (roughly 50%) in the last 20 years. This is mainly due to increased public awareness of fire prevention strategies, improved building techniques, faster response of emergency services and implementation of stricter fire codes [3]. This progress has been abetted by increased knowledge of fire and smoke behaviour in structures due to ongoing fire research activities, which include a combination of large-scale fire testing, laboratory and field-testing and computer modelling.

The study of realistic large-scale fires is expensive and difficult from an experimental standpoint. Until the summer of 2003, a large majority of structural fire research at the University of Waterloo was conducted in the field when there was available condemned housing in which to undertake instrumented burns as joint training and research opportunities in collaboration with municipal fire departments [4]. Accessibility to appropriate instrumentation, along with variations in ambient conditions, geographical locations and sporadic timing was a major inconvenience when attempting to set out a logical research program. As well, it became difficult to obtain comparable and consistent data since structures were of different styles and physical condition. There are many factors that influence the behaviour of fires, for example, factors as simple as room size and ventilation greatly influence fire and smoke behaviour [5-9]. As a result, factors such as ambient and technical difficulties in the field added to the problem of interpretation of results.

In an effort to address these problems, in 2001, the Fire Research Group applied for and received a major grant from Canadian Foundation of Innovation (CFI), Ontario Innovation Trust (OIT) and partners to construct a full-scale fire research facility. The research facility is located on the Waterloo Region Emergency Services Training and Research Complex (known as WRESTRC). In addition to fundamental research into issues of fire science, opportunities exist to collaborate with the local fire service to conduct training exercises and investigate fire suppression techniques. The facility is expected to provide the means for obtaining more reliable and consistent experimental data of structural fires.

A principal feature of the facility is a movable 7 by 7 metre plan area, 4-room, two-story steel Burn House[1] structure that can be situated outside or inside a test

[1] The term Burn House will be used to refer to the full-scale fire test structure where the four experiments presented in this work were undertaken.

enclosure. When situated inside the enclosure, the ambient conditions surrounding the house can be controlled. The facility is equipped with a wind generation system, consisting of six variable speed fans, banked three across by two high, which are independently controlled and can supply up to a total of 472 m^3/s of air through the enclosure. The uniform wind profile can be varied from about zero to 14 m/s with a cross sectional area of 10 by 14 metres at the fan plenum exit. The wind generation system will be used in future research to study wind pressure distribution on the burn structure and how this affects fire behaviour and heat and smoke movement inside the structure [10].

The ability to understand and quantify the thermal development of compartment (room) fires is of great significance to the fire protection industry. Knowledge of compartment fire temperatures allows for prediction of hazardous conditions, property and structural damage, ignition of objects, changes in burning rate and the onset of flashover[2] [11].

This thesis will report on four experimental burns undertaken in one room of the Burn House. The data will be analysed to demonstrate that the Burn House facilitates, in the gross sense, residential structural fire experiments by comparing the overall behaviour of the current fires with data from representative real house fires performed by the Fire Research Group of the University of Waterloo. The initial conditions for the four fires were not reproducible, thus the effects of several features of structural burns will be observed and discussed such as vitiation[3] and flashover.

[2] Flashover is the simultaneous ignition of room combustibles and precludes fully developed fire conditions.
[3] Vitiation is when the fire becomes ventilation controlled, meaning the compartment conditions are fuel rich and under ventilated. The rate of air supply is insufficient (oxygen depletion) to continue burning the fuel vapours in the compartment.

A secondary exercise will be to compare the present data with predictions from a commonly used and simple, but highly empirical mathematical computer fire model, CFAST (Consolidated Fire growth And Smoke Transport) [59].

Computational analysis using advanced fire modelling techniques is becoming a valuable tool for predicting fire behaviour, however, modelling fire scenarios is a relatively complex problem that requires a great deal of computational resources. This is both a time consuming and costly solution. As well, models which use varying degrees of empirical correlations require comparison with experimental data to assess their accuracy. Therefore a balance of computer modelling and experimentation is required to develop models that reliably predict fire behaviour in structures, which can then be used to improve fire prevention and safety systems and fire suppression methodologies. The role of this thesis, however, is not to further *validate* the CFAST model for use as a predictor for structural fire behaviour, as this has already been the focus of much research, [12-14]. Rather, the purpose of model and experimental comparisons in this thesis will be to demonstrate CFAST's relative *accuracy* as a predictive tool, as well as aid in the demonstration of the experimental data as representative of structural fire behaviour. This will be done only for the best controlled fire experiments.

Finally, there is little experience available for the design of burn rooms for structural fires tests which survive large (2 to 5 MW) peak fires, that are reusable for a number of burns without requiring extensive and costly post-burn reconstruction and in some cases, destruction of the entire facility. For future researchers in this facility this thesis will provide a brief recounting of the behaviour and effectiveness of the wall linings chosen for these fires based on observations during and after the burns (Appendix B)

1.1 Purpose and Focus of Thesis

The purpose of this thesis is to present and evaluate the temperature data obtained from four real, full-scale fire tests performed in the Burn House at the University of Waterloo Live Fire Research Facility. This information will be used to characterize the thermal development in a first floor compartment of the Burn House for the entire fire growth process from ignition to decay and will be compared to real structural fire data from previous studies where appropriate.

Experimental data will be compared to CFAST model predictions. The data will be used to demonstrate the relative accuracy of the model for predicting a representative fire in the Burn House.

The data will be archived and available to other researchers for future burn house experimentation.

1.2 Presentation of Thesis

The thesis is divided into five Chapters. The following Chapter will outline the major physical processes and theories relevant to compartment fires. It will also discuss previous and relevant experimental and laboratory work, as well as developments in computer modelling of fire scenarios. Chapter Three outlines the experimental set up in the Burn House and demonstrates the results obtained from the full-scale experiments performed at the WRESTRC site. A summary of observations of the behaviour of the wall linings of the burn room will also be provided. Chapter Four will compare experimental results and CFAST model predictions. The last Chapter in this thesis will be used to summarize the main conclusions and achievements of this thesis and to discuss future work. All figures will be presented at the end of each chapter.

1.3 Objective of Thesis

The objective of this thesis is to report the results of a commissioning study of four burn experiments, undertaken in the new University of Waterloo, Fire Research Group Burn House. The purpose was to determine the operating parameters and thermal characteristics of the main burn room as a working model for realistic full scale structural fire tests.

This will be achieved by:

- Instrumentation, data collection and analysis of four burn scenarios with particular attention to the effects of ventilation, fire loading, and consumable wall linings on the ensuing burn behaviour of the room
- Comparison of fire growth during the initial growth period against other structural fire data
- Comparison of data with predictions from the CFAST fire growth model,
- An evaluation of the effectiveness of, and problems with, protective liners and material used to line the steel structure
- A summary of suggested operating parameters and recommendations for future burn experiments

CHAPTER TWO

The Literature in Review

2.1 Introduction to Problem

Compartment fires are fires in enclosed spaces, usually rooms, or similar enclosures within a structure which may have, and indeed require, ventilation pathways. For the purpose of this thesis, discussion will be limited to room fires that exist in typical multi-compartment residential structures which the University of Waterloo's Burn House is designed to model.

In a multi-compartment building, the physical processes of fire behaviour in one burn room *can* be influenced by the presence of adjacent rooms. These effects will be negligible, however, if the burn room can somehow be isolated from adjoining rooms.

Any experiment undertaken in a single room enclosure is still a challenge to the researcher due to the complex physical processes involved; however knowledge of fire

behaviour in a single compartment can be extended to understanding the fire behaviour in much more complex experimental arrangements, such as residential structures [4].

Single Compartment Fire Theory

The physical processes behind fire dynamics in a room can, for simplicity, be broken down into five major stages [5]. These stages are (1) Ignition stage, (2) Growth stage, (3) Flashover, (4) Fully Developed Fire and (5) Decay. The first three stages are often lumped together and referred to as the 'Growth Period'. This is shown in Figure 2.1 where the stages of a compartment fire are depicted generically using fire heat release rate as a function of time.

The first stage, the Ignition stage, is the stage when the fuel source has been ignited and the fire begins to burn. Various methods are used to ignite the fuel source in experimental compartment fires. These include torches, lighters and cigarettes and (sometimes involve) the use of an accelerant such as gasoline.

After localized burning has been established one of three things may happen [5]:

(1) The fire may burn itself out after the fuel load is consumed without involving other items of combustible material, particularly if the fuel load is isolated from other room combustibles.
(2) If there is insufficient ventilation (inadequate supply of oxygen), the fire may self-extinguish. The fire will then be considered to have vitiated. This situation may arise if there are insufficient ventilation openings in the

enclosure, if a hot layer[4] has developed past the sill of any openings or if the rate of air supplied to the plume exceeds the influx of ambient air to the enclosure [4]. Alternately, the fire may continue to burn, but at a very slow rate, dictated by the availability of oxygen (this situation may contribute to the phenomenon called backdraft[5]) [4].

(3) If there is sufficient fuel and ventilation the fire may progress to the "Growth Stage" and burn out as the fuel load is consumed or proceed to full room involvement if the room is sufficiently hot to initiate pyrolysis of ceiling, wall or furnishings as the case may be.

This study is concentrated on the fire behaviour as it relates to the last point – where it develops into the Growth Stage and in some cases on to the Fully Developed Stage.

Compartment fire growth can generally be approximated as having a parabolic growth rate, called a t^2 fire, given by the following equation [5]:

$$\dot{Q} = \alpha_f (t - t_o)^2 \qquad \text{(kW)} \qquad (2.1)$$

where $\dot{Q}$ is the rate of heat released during the fire(kW), α_f is the fire growth coefficient (kW/s^2) and t_o (s) is the incubation period[6]. Values for the fire growth coefficient can be estimated from data obtained for a number of combustibles. The slower the burning rate

[4] Hot layer are the combustion gases that have risen to the ceiling and formed a 'layer' which increases in size with continued fire growth

[5] Backdraft – The phenomenon that occurs when a fire has been burning under vitiated (oxygen depleted) conditions for a prolonged period of time and then is suddenly exposed to a fresh ingress of air, which causes unburnt fuel and vapours to burn rapidly, producing a 'backdraft'.

[6] The incubation period is a function of the ignition source type, its location in the room and the properties of the item ignited

of the combustibles, the smaller the value of the growth coefficient. Table 2.1 lists values of the coefficient for different growth rates [5].

Table 2.1: Fire Growth Coefficients for Various Growth Rates [5]

Growth Rate	Growth Coefficient, α_f (kW/s^2)
Ultra Fast	0.1876
Fast	0.0469
Medium	0.01172
Slow	0.00293

It is during the Growth Stage that the hot products of combustion form a plume, which, due to buoyancy, rises, toward the ceiling [11]. As the plume rises, it draws in cool air from within the compartment, decreasing the plume temperature and increasing the volume flow rate. The fire plume will develop and grow in strength as the fire grows in size. When the plume reaches the ceiling, it spreads out and forms a ceiling jet. This ceiling jet will flow outwards until it reaches the wall of the compartment. Thus begins the formation of the hot upper gas layer which grows in depth with time, as the plume gases continue to flow into it. The boundary between the hot upper layer and the air in the lower part of the compartment is often referred to as the interface[7]. The only interchange between the air in the lower part of the room and the hot upper layer is assumed through the plume. As the hot layer descends to an opening in the compartment walls, (such as doors or windows) hot gas will flow out the openings and ambient air will flow into the openings. In an opening, the surface formed between the outflow of hot gases and the inflow of ambient air is called the neutral layer [11].

A two layer or zone model (such as CFAST) is often used to describe this development in single (and multiple) compartment fire(s), where the room stratification is modeled as a hot 'upper' gas layer and a cold 'lower' layer that continues to supply the plume. While variations in temperature, gas concentration and other properties exist in each of these layers they are considered to be adequately modeled by two zones represented by an average 'upper layer' temperature and an average 'lower layer' temperature. Figure 2.2 shows a visual representation of a two-layer model.

In multi-compartment buildings, the developing hot layer in the burn room will vent to the ambient air as well as to the adjacent rooms, which also develop hot layers [4]. Gases from adjacent rooms will also be drawn into the lower layer of the burn room. These gases will be associated with greater enthalpies and warmer temperatures than entrained ambient air due to the radiative heating from the upper layers in the compartments and mixing between stratified layers at the ventilation openings.

The boundary that lies between the upper and lower layer during the Growth Stage is frequently referred to as the layer interface or interface height. An interface height is distinguishable only until fully developed conditions are reached. While temperature stratification may still be present under fully developed conditions, a distinct boundary between a hot upper and cold lower layer becomes difficult to identify. Understanding the development of the hot gas layer, or the location of the interface height is helpful in developing fire suppression techniques, understanding fire growth, spread and protecting individuals from harmful conditions.

Towards the end of the Growth Stage, a large quantity of combustion gases will have built up in the room, particularly at the ceiling. Temperatures of hot gases can

[7] Researchers attempt to define this interface however there is no agreement on what criteria should be used to define it.

escalate to 600 ºC or above whereby the gas has exceeded the autoignition temperature of the room materials. At this point, thermal radiation from the gases in the smoke layer and the flames will ignite all of these combustible items simultaneously and eventually involving the entire room in fire. It only takes a few seconds for a room to flashover. This is one of the many descriptions of the onset of flashover [15, 16]. Other studies defined the onset of flashover as the emergence of flames from an opening, while the 1968 Waterman [5] experiments concluded that a heat flux of 20 kW/m^2 at the floor level was required for flashover to occur from the ignition of paper. This is lower than the heat flux required to ignite larger solid fuel sources however this was more than enough to promote pilot ignition and rapid flame spread at the surface of most combustible materials. Waterman speculated that most of this heat flux came from radiation in the heated upper surfaces of the room, rather than the flames above the burning fuel, however, later studies determined that there are actually four sources of radiative flux in a compartment that will vary throughout the course of the fire [5]:

i) from vertical flames above the fire;
ii) from the hot surfaces in the upper part of the enclosure;
iii) from flames under the ceiling;
iv) from hot combustion products trapped under the ceiling.

The dominating flux at flashover will depend on the nature of the fuel and amount of ventilation available.

The onset of flashover is of particular importance to the study of fire prevention as it is the time at which fire enters the Fully Developed Stage or in firefighter terminology ‘the fully involved stage’ and will cause the majority of damage to the structure, occupants and firefighters. During the Fully Developed Stage, the fire will have the greatest heat release and temperatures will reach a maximum. In some cases, the flame temperatures will exceed 1000 ºC. Firefighters usually withdraw from a

building and undertake an exterior attack during this stage and as well, attempt to mitigate fire spread and damage by protecting the exposures[8]. During this state, the rate of burning is often controlled by the rate at which air can flow into the compartment, which is determined by the available ventilation pathways and the ambient wind conditions. This is termed a 'ventilation-controlled' fire.

If, however, the ventilation opening is large so as to supply a surplus of oxygen, the burning rate will become dependent only on the surface area and burning characteristics of the fuel. This situation is referred to as 'fuel-controlled', which continues as the fuel is consumed. The transition from ventilation-controlled to a fuel controlled fire is characteristic of the Decay Stage. During this stage, heat release and temperatures will drop as the fuel is consumed. Flaming will eventually stop, leaving behind glowing embers which will continue to smoulder, for some time, maintaining high local temperatures [5].

2.2 Review of Experimental Work

For the purposes of the following discussion, four types of fire testing facilities, as they have been identified in the literature, will be defined here.

Residential (Real) Structures: This definition refers to any pre-existing houses, dwellings or buildings where a fire test is performed. The results of fire tests in these settings often lead to a total destructive loss of the structure; therefore, in this case, repeatability of experiments is not possible.

[8] Exposures – a term used to identify buildings or objects that are adjacent to the fire and which might cause further fire spread if ignited.

Full-Scale (Large-Scale) Test Enclosures: This definition refers to facilities that have been purposely constructed with the intent of withstanding repeated fire testing and have been built to a scale similar to that of residential structures or houses. The University of Waterloo Burn House is, by this definition, a Full-Scale Test Enclosure.

Room Test Enclosures: Room Test Enclosures are single compartments, usually constructed inside larger laboratory facilities. These are often built to the dimensions of an ISO standard room fire test structure[9], however, the size of the test enclosure will depend on the preference and objectives of the individual researcher. Room Test Enclosures are similar to Full-Scale Test Enclosures in that they are, in general, built with the intention of withstanding repeated fire testing, however, due to the relatively lower cost associated in constructing them (compared to Full Scale Test Enclosures) this is not a requirement.

***Laboratory (Bench-Scale) Tests*:** Laboratory and Bench-Scale Testing refers to testing of materials or samples on a scale much smaller than the size of the actual item using laboratory instrumentation. The purpose of these tests is often to determine properties of the specimen. For example, the Heat Release Rate of materials can be determined in a laboratory using a cone calorimeter. These tests are performed in isolated laboratory environments and not in real, end-use settings in which they will normally be found.

Some testing facilities might not exactly meet any one of these four definitions. In this situation, the most closely fitting definition will apply. For example, some testing facilities may be referred to as Full or Large-Scale, but are not built, in their entirety, to a scale the size of an actual house. For the purposes of this thesis, any structure which is represented by more than one room, but is not a pre-existing residential (real) structure, will be considered a Full or Large-Scale Test Enclosure.

[9] ISO standard room fire test dimensions: 2.4m by 3.6m by 2.4 m high with a 0.8 m by 2.0 m doorway [17]

CHAPTER TWO – THE LITERATURE IN REVIEW

To date, many institutions around the world have undertaken structural fire studies in full-scale and room test enclosures, laboratories and residential buildings. This section will discuss and compare the various experimental set-ups, objectives and results of some of these experiments. Whether performed in residential structures, labs or enclosures, many of these studies demonstrate similar objectives with regards to fire research; however, results often vary due to the uniqueness and arrangement of each structure, as well as limitations inherent with each experimental set up. The purpose of this discussion is to give a brief overview of major fire research activities whose objectives are to study fire behaviour in residential-type structures. A description of fire test facilities will be provided and compared to the Burn House structure. This will aid in comparison of results.

The University of Waterloo Burn House is a full-scale test enclosure which is similar to other test enclosures currently used for fire research; however, its distinguishing feature is the wind generation system which presents the ability to study more closely the effects of wind conditions on fire behaviour in structures through experimentation. Studying the effects of wind generation on Burn House fires will be of particular interest for future experimentation at the University of Waterloo.

While there has been much research performed to study the effects of wind on fire behaviour [6, 7, 8, 9], to date, results of fire studies performed in full-scale test enclosures like the Burn House with comparable wind generation capabilities have not been published. Many of the results obtained from initial fire experiments in the Burn House may be comparable to results of the studies presented in this section.

For the purposes of this thesis, the following section will exclude discussion on laboratory or small-scale (bench-scale) experiments. These types of experiments, while valuable, are often only useful for characterizing a material's fire performance under controlled laboratory conditions without regard to end use in a building (uncharacteristic

of real fire situations). Even recent attempts in predicting large-scale burning behaviour of materials from bench-scale test results have met with only limited success for items of furniture and with less success for other, more generic materials [4].

Residential Structures

Original compartment fire studies led by Japanese researcher Kawagoe [17] began as early as 1948 with fully developed fire experiments in small-scale rooms and later in larger cubical enclosures which eventually led to a series of compartment fire experiments undertaken in real structures between 1956 and 1975 as part of the research program at the Ministry of Construction's Building and Research Institute (BRI) in Tokyo, Japan [4]. Through his work at the BRI, Kawagoe encouraged other researchers to pursue fire behaviour through experiments that simulated real fire situations [18].

Of the 15 buildings reported in the compartment fire tests, 10 were large commercial or industrial buildings, 2 were apartment buildings, 2 were hospitals and 1 was a residential structure. Since then, the BRI's Department of Fire Engineering has performed various fire experiments in real structures and in its full-scale test facility with a focus on finding methods for ensuring the safety of people in case of fire in a building or city, and methods for minimizing the economic loss caused by fires [19]. The department investigates the physical behaviors of materials, components, and structures at elevated temperatures during fires, analyzes evacuation behaviors of people, and researches and develops comprehensive methods for fire safety evaluation.

The most recent full-scale residential fire studies to come out of the BRI are two apartment fire experiments, in 1991 and 1996 [18] where researchers attempted to assess the fire safety of a three-story apartment building (Figure 2.3) in a densely populated

urban area. As summarized in a report by the UJNR[10] [18], a three storey wooden apartment building had been constructed in the BRI's Fire Test Field for the first experiment in 1991. The purpose of this study was to evaluate the risk of fire spread from a dwelling unit to other units and to adjacent structures. The results of the first experiment showed that the impact of this type of fire in an urban scenario had not been fully quantified, thus, in 1996 a similar experiment was performed with two additional wooden, two-story buildings located behind the apartment building in order to better assess the risk of fire spreading to adjacent buildings. (Figure 2.4)

Temperature measurements were made in each room of the dwelling, within major load bearing separation walls and external walls surfaces using K-type thermocouples. Heat flux, gas sampling, static pressure and smoke density measurements were made, as well as visual infrared and video images. A pool fire of n-heptane was used as a fuel source, along with 6 propane burners to simulate remaining fires of collapsed buildings. Each floor of the three storey building contained 30 kg wood crib fire loadings.

In 1991, the University of Waterloo's Fire Research Group performed a series of residential house fire tests, called HFOS[11] I [20]. The first of these experiments were conducted with heat-activated sprinkler suppression of typical residential fires in a two storey dwelling west of Edmonton, Alberta. The motivation for these experiments came from recognizing the lack of information available on sprinkler and household smoke detector operation and effectiveness during realistic residential fires as well as the importance of early suppression systems as a means to further reduce residential fire risk.

[10] In 1964 'The United States and Japan Cooperative Program in Natural Resources (UJNR)' was established. The Fire Research and Safety Panel of the UJNR perform collaborative research activities that focus on understanding and predicting fire behavior and its effects on life and property.
[11] HFOS – House full of sprinklers.

The studies were designed to characterize the environments in various rooms of a residence with time after onset of the fire, with simultaneous determination of the times to activation of common household smoke detectors and typical residential sprinklers. In the first portion of HFOS I, sprinkler suppression of a kitchen grease fire, a fire developed from ignited bedclothes, and smoldering and open fires in the living room of a single family dwelling were examined. A residential sprinkler system was installed, with ceiling mounted heads in the centre of the kitchen and bedroom ceilings respectively, and three ceiling mounted and one pendant (wall-mounted) sprinkler head in the living room. Commercial smoke alarms were positioned on the bedroom ceiling, the living room ceiling near the entrance to the upstairs stairwell and on the ceiling of the upstairs landing. Ceiling level gas sampling pipes and floor level heat flux monitors were installed and several thermocouples were positioned in each room. Through these, the development of temperature profiles, ceiling layer CO concentrations, particulate formation and heat flux were monitored in the various rooms over time, during the initial growth of the fire, as well as during suppression of the fires by the sprinklers. The results of these experiments have led to preliminary indications of the effectiveness of these systems and a better understanding of initial fire growth during typical residential fires under the specific fire scenarios studied.

The objective of the second part of HFOS I was to study the development of a living room fire in an unsprinklered setting. More specifically, the goal was to obtain more detailed results on the development and spread of heat and toxic gases during the fire tests. In this experiment, three living room fire tests were conducted, each started with newspapers ignited on a couch and surrounding furnishings. Twenty K-type thermocouples were positioned throughout the dwelling as well as gas sampling tubes and heat flux monitors.

In addition to providing detailed time-temperature plots for the duration of the fire, comparisons were made to model predictions using the two-zone model, CFAST. Results from these tests and the model will be used for comparison in Chapter 4.

Similar to the first set of HFOS I tests performed by the University of Waterloo, the Santa Ana Fire Department of Santa Ana, California, (in conjunction with NIST) conducted a series of fire experiments in a vacant, one storey, single family dwelling in July 1994 [21]. The focus of the experiments was to measure the activation time of typical residential-type sprinklers.

The building was of wood frame construction with gypsum board interior walls and ceiling. Floor to ceiling thermocouple arrays were positioned throughout the living room to measure temperature stratifications. Room furnishings were used as the fuel load and a plastic wastebasket as the ignition source.

Due to failure of the living room thermocouple tree shortly after full room fire involvement, the temperature data from the burn room could only be provided up to 120 seconds. Observation of plots from other rooms indicates, however, that this data encompasses the entire growth phase. Temperatures in the hallway and second floor room were provided for the duration of the fire.

The University of Waterloo Fire Research Group performed five fire tests in two residential structures as described in a thesis by Poole in 1995 [4, 22, 23]. The purpose of the tests was to collect information relating to the development of hot layers in residential structures. These results were compared to computer fire model predictions to identify possible limitations for prediction of hot layer growth during real structural fires. The report describes the importance of testing more comprehensive fire models with data from controlled fires in real structures in order to describe real fire effects such as leakage, ambient wind and failure of windows and doors. Twenty K-type thermocouples were located throughout each structure, located near the ceiling or at an elevation of 1 m above the floor to monitor the development of the hot layer. Mattresses and wood cribs were used as fuel sources. The results from the tests are compared with predictions from three fire models, CFAST, ASET-BX and McCaffrey [5, 23]. The results of CFAST comparisons will be discussed in Chapter 4.

In 2001, the University of Waterloo's Fire Research Group performed another set of residential house fire experiments in collaboration with the Centre for Forensic Sciences and the Waterloo Fire Team [23]. The experiments were designed such that they would expose new fire fighters to fire fighting activities and experimental equipment would be tested so that competence would be gained in the field of live fire data collection. The original objective of the experiments was to make preliminary comparisons of three of the leading foam/water additives for structural Class A fire fighting fire suppressants, however, ultimately the data provided the opportunity to gain insight into the behaviour of a Class A house fire throughout its growth phase.

K type thermocouples were positioned in the main burn room at heights of 14, 27, 34, 49, 60, 72, 84 and 95" (0.356, 0.686, 0.863, 1.245, 1.524, 1.829 and 2.413 m) above the floor level and stratified temperature data was collected using a data acquisition system and computer. Class A combustibles were used as a fuel source. Ten fire tests were performed in total and nine sets of reliable data were acquired for analysis.

Analysis of the data first required an estimation of the beginning and end of the growth phase of fire development. The experimental report identifies that there is no correct or standard method for establishing this criteria and the decision is left to the individual researcher. The start of the growth phase was determined as the time when the temperature at the lowest thermocouple, 14" (356 mm) above floor level, reached 30 degrees Celsius. This temperature was used because it represented a deviation from ambient conditions by 10 degrees Celsius, which would surely be the result of presence of a growing fire and not due to fluctuations in ambient temperatures. The end of the growth phase for these tests was chosen to be 100 seconds whereby most of test data began to depart from the model of growth phase fire incubation (see previous section).

Results indicate a high degree of comparability of data for all tests, with some large variances in ceiling level temperatures. Measurement errors were suspected with one thermocouple located 72" (1.829 m) above the floor level. The temperature data

obtained using this thermocouple demonstrated temperatures much lower than those positioned closer to the ceiling level. As well, difficulties with the data acquisition system prevented data collection for the third test. Detailed results of these experiments will be presented for comparative purposes in Chapter 4.

In a report by the Building and Fire Research Laboratory at the National Institute of Standards and Technology (NIST) a residential fire experiment was undertaken in 1998 for the purpose of developing a fire investigation training tool [24]. The experiment was performed in an unoccupied, two story wood frame, single family dwelling with gypsum board interior walls and ceilings. The living room served as the fire room for the experiment. The majority of doors and windows were closed throughout the experiment, with a few remaining open to provide ventilation pathways.

Temperature measurements were made from the floor to the ceiling in several rooms with K-type thermocouples. Heat flux was measured at the floor level. The contents (furnishings) of the house were used as fuel, with two cycle engine fuel used as an accelerant. The results demonstrated detailed time-temperature profiles at various heights in the room of fire origin. These results will be used for comparative purposes in Chapter 4.

To date, few experimental fire studies have been undertaken in residential structures due to high costs, limited availability of test structures and due to the destructive nature of testing and often uncontrolled ambient conditions. As a result, structures used for experimental work on compartment fires have traditionally been full or laboratory scale, single, or to a lesser extent, multiple room enclosures built to mimic fire behaviour in residential structures [4].

Performing fire tests in residential structures will undoubtedly produce results most like actual fire situations; however, there are some advantages to using full-scale and room test enclosures over real structures. Often, when using full-scale enclosures,

experimental parameters, such as ambient conditions can more easily be controlled and monitored which allows for repeatability of experiments and aids in comparing results. In addition, these structures are often capable of withstanding frequent testing, which makes experimentation less costly than using real structures. The results of full-scale and room fire testing have been readily applied to fire behaviour in real structures, with much success.

The ability to construct and experiment in re-useable full-scale (and room) test enclosures rather than residential structures has led to an increase in research related to e structural fire behaviour .which has greatly increased the fire research community's knowledge of fire behaviour in structures and helped progress contemporary Compartment Fire Theory. Due to the quantity of available information on full-scale testing and structures, the following discussion will be limited to more recent studies and in particular, those which will be and have been performed in facilities most similar in arrangement to the Burn House structure.

Full Scale Structures and Room Enclosures

The Fire Research (FR) program at the National Research Council (NRC) in Ottawa, Canada, provides research services to a broad range of clients, including industry and all levels of government. It undertakes research on a wide range of fire related issues from studying the behaviour of people in fires and emergency situations, through to studies of the behaviour of materials and systems when exposed to fire challenges. The program also undertakes research in the areas of fire/smoke detection, fire suppression and smoke management. Finally, the program conducts research and development in the area of computational fire models and the development of computer-based fire safety engineering tools. The research facilities at NRC include an ignition strength and cigarette test facility, column, wall and floor test furnaces, an intermediate scale test furnace, thermal conductivity apparatus and cone calorimeter. Recently, Carleton

University, in partnership with NRC[12] and the Toronto Transit Commission, with resources from the CFI (Canada Foundation for Innovation) and OIT (Ontario Innovation Trust), have recently completed construction (March 2005) of full-scale fire research facilities adjacent to existing facilities at NRC, in Almonte, Ontario, Canada [25].

The new facilities include a 10-story atrium for investigating smoke management in high rise buildings and large volume spaces. A new burn hall with dimensions of 20 by 20 by 12 m high will be used to investigate fire scenarios involving large fires. A tunnel measuring 10 m wide, 5.5 m high and 37 m long will be used to conduct tests that realistically simulate fires in roadway and mass transit tunnels. Smoke produced in all three facilities can be collected and exhausted through a high capacity fan system to measure heat release rates.

Researchers in the Civil Engineering department at the University of Canterbury in New Zealand have designed a standard, two room test enclosure at the McLeans Island test facility where they have studied numerous pre and post-flashover conditions in compartments using gas burners [26, 27, 28]. The rooms are 2.4 m wide by 3.6 m long by 2.4 m high as shown in Figure 2.5. Figure 2.6 shows a photograph of the LPG burner used in the experiments. A graduate thesis by Rutherford [26] discusses the results of 23 pre-flashover fire experiments with fuel loadings of 60 kW, 120 kW and 180 kW conducted at the University of Canterbury's McLeans Island testing facility between December 2002 and January 2003. The experiments were conducted to later use in validating zone and field computer modelling programs used for simulating fire scenarios. The two room enclosure was constructed inside a building at the testing facility. The room consists of a rigid steel box section frame with steel studs at 23.6" (0.599 m) centres. Wooden joists were attached to the frame at a spacing of 23.6" (0.599

[12] NRC – National Research Council

m) to provide the basis for the ceiling, floor and walls. Figure 2.7 shows a picture of the experimental set up.

The door between compartments was opened (at various angles) for seven of the fire experiments. To obtain temperature profiles in the compartment, seven thermocouple arrays were installed with K-type thermocouples along the centreline of the two-room compartment. Each thermocouple tree consisted of 14 thermocouples at specific heights in the compartment. Two more thermocouple arrays, each with 16 thermocouples, were placed from the side walls. Figure 2.8 shows a schematic of the room instrumentation.

A three minute base line in ambient conditions was recorded for each of the experimental runs. The pilot flame and then burner were ignited, followed by a period of 10 minutes to allow a steady state to be reached in the two-room compartment. The gas measurement location is changed every three minutes. After measuring the gas concentrations from each location, the gas measurement position is then changed back to the topmost probe in the doorway for another three minutes to check for experimental reproducibility. The gas supply to the burner is then shut off, and another 3 minutes of data is logged. At this point the data logger is also stopped.

Only results from the fifth experiment (120 kW fire) were reported. Time-temperature plots are provided for the thermocouple trees located at the doorway and in the burn room. The report identifies a thermocouple located 40" (1.016 m) below the ceiling level which experiences a wide range of temperatures throughout the experiment. This thermocouple is suspected to be in the neutral plane. Maximum fire temperatures reached in the burn room were approximately 200 ºC.

In addition to the study of pre and post flashover conditions in the two room enclosure, much research at the University of Canterbury has been focused on behaviour

of structural elements and materials when exposed to fire as well as modelling fire behaviour using field and zone fire model programs [29, 30, 31].

Researchers at NIST (National Institute of Research and Technology), Gaithersburg, Maryland have performed *numerous* fire experiments in standard ISO room test structures and laboratory settings [32]. The Building and Fire Research Laboratory (BFRL) at NIST has studied building materials; computer-integrated construction practices; fire science and fire safety engineering; and structural, mechanical, and environmental engineering. Products of the laboratory's research include measurements and test methods, performance criteria, and technical data that support innovations by industry and are incorporated into building and fire standards and codes. This information is free and available in a database maintained on the NIST website. The information published by NIST serves as an invaluable resource to the fire research community [32].

In conjunction with NIST, the Department of Fire Protection Engineering at the University of Maryland performed a series of fire tests on the first floor of a burn tower [33]. The room was lined with furnishings and glass windowpanes. The room was instrumented to measure temperature, heat flux and gas concentrations. The fire in the room was initiated and data acquisition began when an ignited book of matches was placed underneath four newspapers on a chair. Repeatability of such experiments is often low due to the complexity of the fuel load composition and arrangement. It is difficult to extract information from these test results and compare them to situations where the fuel loads are not identical or where ambient conditions may vary.

Concrete on a steel frame was used to construct the Experimental Building Fire Facility at the Centre for Environmental Safety and Risk at the Victoria University of Technology in Australia. This facility has been used to study full-scale multi-room compartment fire scenarios using polyurethane foam mattress fuel loads. The floor plan

is much like that of a multi-story apartment building and is comprised of four rooms and a corridor connecting the rooms [34, 35]. No indication has been given as to the external ambient conditions that the test structure is exposed to. Two reports outline flashover and non-flashover experiments that have been performed at the facility and used for comparison to CFD models [34, 35].

Recently, many large-scale studies have been performed by the Swedish Rescue Agency [36]. The objective of these tests was to study the effects of fire ventilation during fire fighting operations.

One report [36] describes three live fire tests performed in a three-storey building with a cellar, attic and wooden roof. The objective of these tests was to try out an explosive cutting frame, to make an initial study of natural and forced (positive pressure) ventilation to identify important and measurable variables in conducting live fire tests. The fire test indicated the danger of ventilating concealed spaces where the fire conditions are not entirely known, as well as the importance of co-ordinating ventilation with fire extinguishing. Use of positive pressure ventilation techniques demonstrated very good results [36].

In a second live fire experiment, researchers aimed to investigate the effect of positive pressure ventilation on firefighting abilities and rescue services when responding to a fire in a small apartment [37]. A fire fighter training facility was used for the experiments, which consisted of three rooms on the first level and a basement of an apartment-style dwelling, attached by a staircase. Fifteen different scenarios were investigated, using a heptane pool fire. The fire tests showed that the risk of fire spread and flash-over will increase if the distance between the fire and the ventilation opening is large. The possibility of survival for victims trapped inside the apartment will then decrease. Positive pressure ventilation increases the burning rate. This is more significant if the fan is located outside the staircase (as in the case of the pressurization of

the staircase). Fire fighters may have a significant influence on pressure and flow patterns inside a burning apartment.

A third report presents the results of the computer model, CFAST that was used to study the effects on the height of the smoke layer and temperature when simulating a positive pressure ventilation scenario. Nine different scenarios were simulated using a three room structure modelled after the fire training facility used in actual live fire tests [38]. The results indicated that fans cannot be accurately simulated with the model and that live fire tests in a full scale fire fighter training facility require pressure relief when the fire exceeds 1.0 MW.

The Swedish National Testing and Research Institute has one of the largest fire testing facilities in Europe. Research and development constitute approximately 40% of their activities with financing provided from Swedish and international industry as well as from research councils and foundations and the European Commission. Their Fire Technology department performs many experiments with focus in areas of CFD modelling, cable fires, chemical analysis of fire gases, extinguishing systems (including sprinkler systems), flame spread, fire investigation, material evaluation and vehicle fires [39].

Their facilities include a main burn hall 18 m wide by 22 m long by 19 m high with a maximum ventilation capacity of 250,000 m^3/h and two calorimeters with peak capacity of 2 MW and 15 MW, respectively. The main burn hall is used for custom designed large scale fire tests. Figure 3.9 shows the main burn hall. A smaller burn hall is used to study custom designed intermediate-sized burn tests, as shown in Figure 2.10. This room is 8.5 m wide by 13.5 m long by 11m high with a maximum ventilation capacity of 100,000 m^3/h. In the Large Scale Reaction to Fire laboratory, intermediate scale international fire tests are performed using an ISO 9705 Room Corner test apparatus, an IEC 60 332-3 Full scale cable tests and an EN 13823 SBI. The maximum

calorimeter capacity in this facility is 2 MW. A furnace testing hall is also provided for testing building facades. A vertical furnace is used to study structures of 3 m by 3 m, while a horizontal furnace is used to study structures up to 3.2 m by 5.2 m.

Similar to NIST, their website offers a large database available with fire test data from many of their projects. As well, reports and articles from the most recent published projects are available but unfortunately mostly in Swedish [39].

2.3 Review of Theoretical Work

The objective of this thesis is not to provide a detailed analysis of fire modelling. As it has been discussed in previous sections, one of the purposes of this work is to ascertain whether the Burn House mimics real structural fire behaviour, by observing and analysing the results of four full-scale fire experiments. Comparisons with the data from the aforementioned live fire structural burns are considered the best method to confirm this. However as a secondary exercise it is useful to compare results from actual fire data to predictions from a much-used and tested fire model, such as CFAST.

Much work has been done to validate and evaluate the predictive capabilities of CFAST for use in fire test scenarios. While not the focus of this work, this information can be found extensively in published literature [4, 12, 13, 14, 22]. One of the best discussions of the CFAST model is provided in the thesis of Poole [4]. The purpose of using CFAST results in this thesis is for comparative purposes only and model predictions will be used to provide insight into CFAST as a modelling tool. Comparisons will be made to model results, in Chapter 4, from other fire experiments to aid in this objective. To this end, a brief discussion on fire modelling will be provided in this section along with a description of the CFAST model used.

Fire Modelling Methods

A fire in a compartment can be modeled using either empirical correlations based on observations from experiment or mathematical methods.

Empirical correlations are predictive methods of determining fire behaviour in a compartment based on previous experimental data. Empirical correlations can be useful when attempting to gain a general indication of the conditions in a burn room but cannot be used for specific fire configurations where data does not already exist. Empirical correlations can be used quite accurately to predict the mass loss rate or pyrolysis rate of a variety of fuel sources. They can also be used to give quantitative insight into the likely behaviour of developing room fires for the purpose of risk assessment and hazard analysis [5]. The difficulty lies in predicting the detailed physical and chemical processes that take place simultaneously in a compartment.

Mathematical models are commonly divided into two categories: probabilistic and deterministic models [40]. Deterministic models predict fire development based on solutions to equations that describe the physical and chemical behaviour of the fire [40]. Two main types of deterministic compartment fire models exist: field models and zone models. Zone models can also be divided into two categories: one-zone and two-zone models. Probabilistic fire models are not discussed in this thesis.

One-zone models are widely used in the analysis of post-flashover fires and smoke movement in rooms remote from the burn room. Early research showed that gas temperatures in an enclosure after flashover could be estimated as nearly uniform after flashover had occurred [5] which makes an analysis based on a one zone model reasonable. The one zone model was based on an energy balance taken about a control volume that encompasses the entire enclosure. The gas properties could then be approximated as spatially uniform, which was very easy to solve numerically. Kawagoe [17] is responsible for the development of the single zone approach for a post flashover

compartment fire. His work has led to the creation of many single zone models still used today. An overview of available one-zone models is presented in a report by Benichou and Bounagui, 2003 [41]. A number of these models are used to predict the smoke movement and concentration in a building and the impact of the temperature on the building structure.

Two-zone models are used to predict the behaviour in a pre-and post-flashover compartment fire. A two-zone model approach for modeling of pre-flashover fires emerged in the mid 1970's with the publication of the work by Fowkes and Emmons [42, 43]. It wasn't until the late 1970's and early 1980's that useful models became available [5].

As mentioned in Chapter 1, pre-flashover conditions in a compartment encompass three distinct stages: (1) The Ignition Stage, (2) The Growth Stage and (3) Flashover. As the fire develops beyond the Ignition Stage, a hot 'upper' region and cold 'lower' region is formed. These layers exist until the fire becomes fully developed.

In two- zone models the compartment is divided into two control volumes, representing the hot upper layer and cold lower layer, respectively, which are considered to be internally uniform[13]. Conservation of mass, momentum and energy equations, as well as the ideal gas law, are then used to develop a series of ordinary differential equations, which are then used to resolve the conditions in each of the zones. (See Table 2.2) The physical details of the gases within each region are not considered, while the mass and energy transport between zones is calculated by modeling the relevant sub-processes: combustion, fluid flow and heat transfer [44]. One of the advantages of zone models over empirical models is that the equations they incorporate are correct and any

[13] Internally uniform – Properties such as temperatures and gas and species concentrations are considered to be the same at every point within the region or zone.

errors that are made by the model will be based on incorrect user inputs, simplified assumptions or by compartment fire processes which have been left out [13].

Table 2.2: Conservative Zone Modeling Differential Equations (Reproduced from [40], page 6)

Variables	Differential Equations for i'th layer
Mass	$\frac{dm_i}{dt} = \dot{m}_i$
Pressure	$\frac{dP}{dt} = \frac{\gamma - 1}{V}(\dot{h}_U + \dot{h}_L)$
Volume	$\frac{dV_i}{dt} = \frac{1}{\gamma P}\left((\gamma - 1)\dot{h}_i - V_i \frac{dP}{dt}\right)$
Density	$\frac{d\rho_i}{dt} = \frac{1}{C_p T_i V_i}\left(-(\dot{h}_i - C_p \dot{m}_i T_i) + \frac{V_i}{\gamma - 1}\frac{dP}{dt}\right)$
Temperature	$\frac{dT_i}{dt} = \frac{1}{C_p \rho_i V_i}\left((\dot{h}_i - C_p \dot{m}_i T_i) + V_i \frac{dP}{dt}\right)$
Internal Energy	$\frac{dE_i}{dt} = \frac{1}{\gamma}\left(\dot{h}_i + V_i \frac{dP}{dt}\right)$

Many two-zone compartment fire models exist; however, the only model considered in this study is the Consolidated Fire and Smoke Transport (CFAST) model developed by NIST [32]. This model has undergone much testing, modification, and development since its inception and is supported by a large contingent of researchers and engineers at NIST and through development grants to external agencies. Of the two-zone models currently available, CFAST has a simple interface, which is capable of providing up to a 30-room configuration with a fan and duct system in each. CFAST allows for modeling of a wide variety of ventilation scenarios, room geometries, multiple plumes and fires, sprinklers and detectors and up to one flame spread object. As well, it has the capabilities to track up to ten toxic species concentrations and a diverse materials and pyrolysis database. The CFAST model provides the potential to compare to a large

number of experimental configurations and parameters. It requires only a moderate amount of computational power and for this reason can be used on personal computers.

Field models have been given much attention with the development of faster and more robust computers. Early development began in the 1980's but due to the intensive computational power required; zone models and empirical models were given much more consideration. Field or 'CFD' (Computational Fluid Dynamics) models present a higher resolution approach to compartment fires than zone models. They can divide the compartment into thousands or millions of cells and therefore provide the capability to resolve very accurate localized effects in a burn room. The density, velocity, temperature, pressure and gas concentrations can be found for each cell based on the conservation laws of mass, momentum and energy. Models such as FDS (Fire Dynamics Simulator) allow a variety of room and material configurations. A description as well as other references to these models is provided in [40].

CFD models are very complex and can permit much insight into fire behaviour, especially in large-scale situations; however, they still require much longer run times and more computational power than zone models. CFD models are required when important local effects must be traced and when a detailed analysis of fire behaviour in a burn room is needed. Future experimentation at the Burn House may eventually require more robust CFD models to resolve burn room details on a sub-grid level depending on the level of detail required or specification of overall trends; however, emphasis in this study will be placed on the predictions from the much used and tested two-zone model, CFAST.

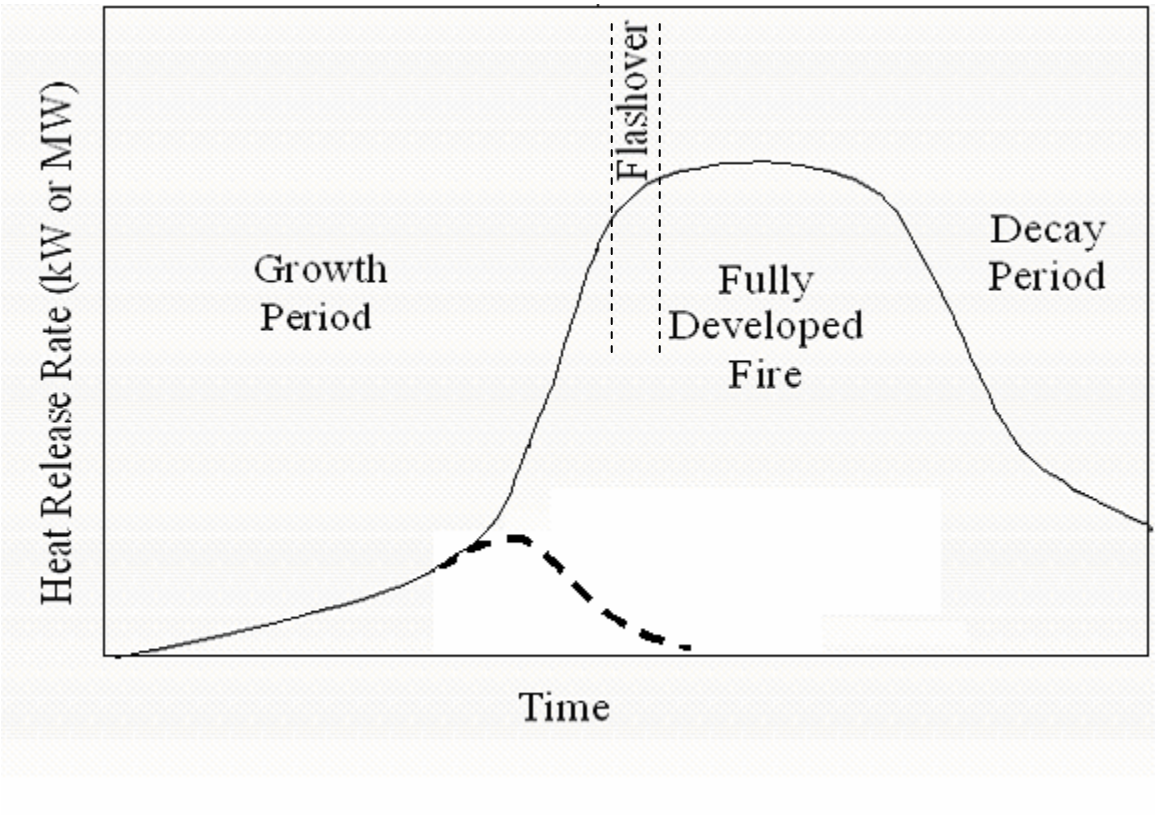

Figure 2.1: Course of a Well Ventilated Compartment Fire[14] (Reproduced from Drysdale [5])

[14] The bold broken line represents the event in which the heat release rate of the fire is not sufficient to cause flashover.

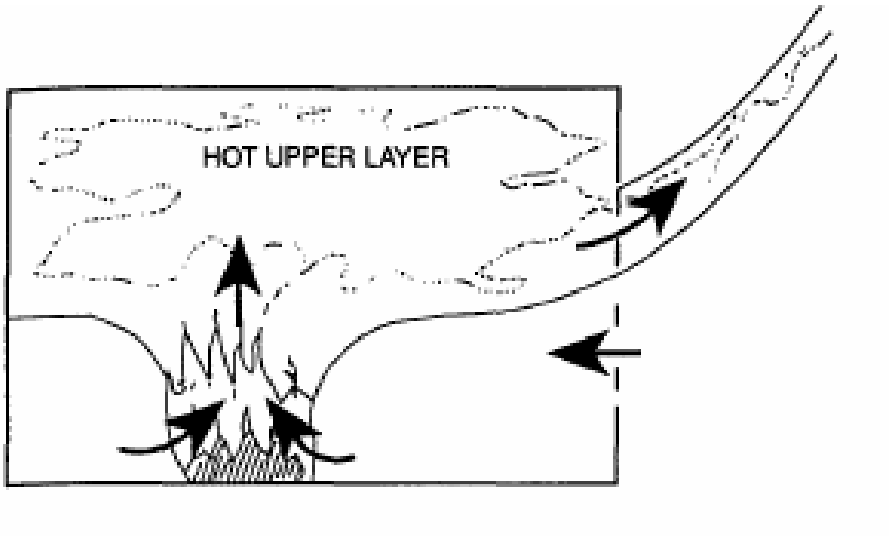

Figure 2.2: Two Layer Zone Model with Openings to Outside (Reproduced from [41])

Figure 2.3: Building and Research Institute, 1991 Fire Test Structure (Reproduced from [18])

Figure 2.4: Building and Research Institute, 1996 Fire Test Structure (Reproduced from [18])

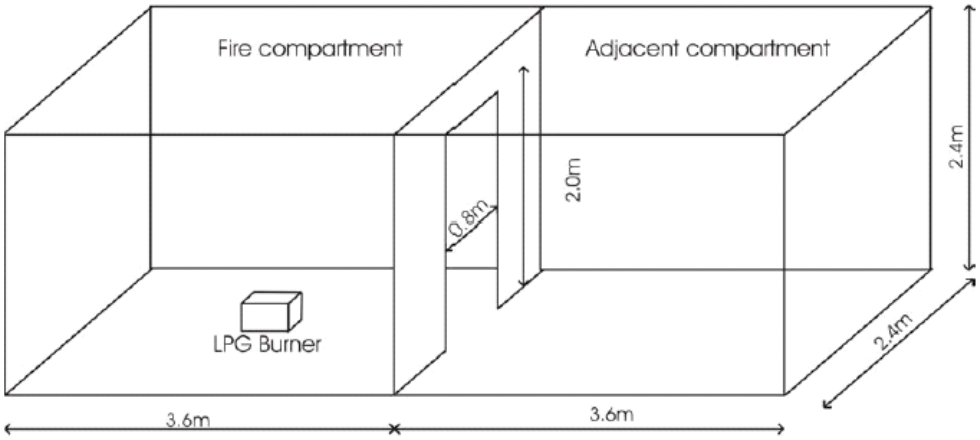

Figure 2.5: Schematic of Two Room Enclosure: University of Canterbury Fire Experiments. (Reproduced from [26])

Figure 2.6: LPG Burner used in Room Fire Experiments at the University of Canterbury [27]

Figure 2.7: Experimental Set up of Two Room Enclosure at the McLean's Island Testing Facility [27]

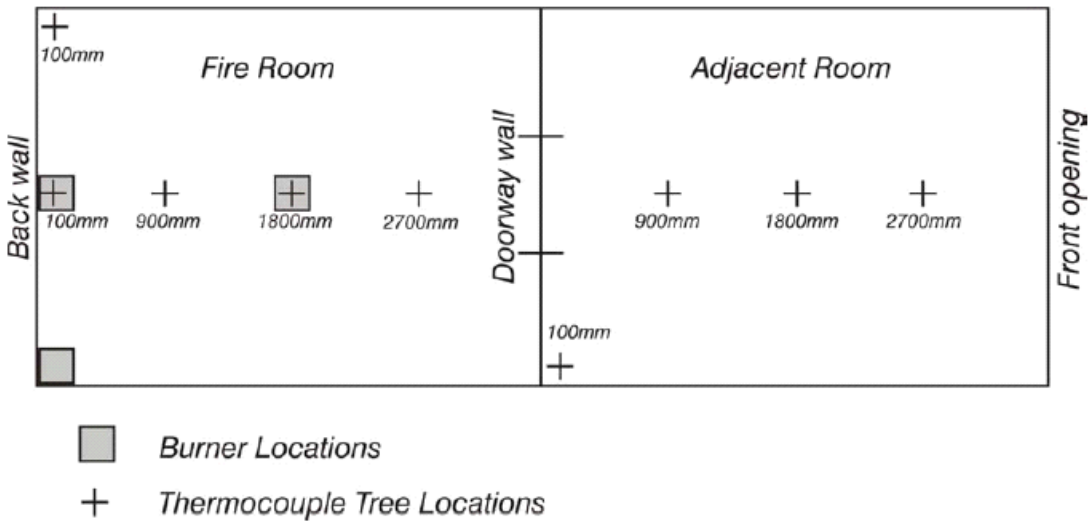

Figure 2.8: Instrumentation and Experimental Setup for University of Canterbury Pre-Flashover Experiments [27].

Figure 2.9: Main Burn Hall, Swedish National Testing and Research Institute [39].

Figure 2.10: Small Burn Hall, Swedish National Testing and Research Institute [39].

CHAPTER THREE

Experimental Setup, Procedure and Presentation of Results

This chapter provides a description of the experimental setup and procedures and presents the results for the four full-scale fire tests performed at the Burn House. As discussed in previous sections, the purpose of these tests was to obtain temperature data that would be used to characterize the thermal development of one room of the Burn House. This characterization comes from recording thermocouple data measured during the fire growth and development phases of four burns. Observation of the fire provided by a digital video camera also aided in the interpretation of the fire behaviour.

A second, but related objective was to use temperature data to compare to model predictions from CFAST. These comparisons are not intended to provide a detailed evaluation of the accuracy of CFAST but rather to demonstrate the veracity of CFAST as an 'off-the-shelf' predictive tool. A third part of the objective of this work will involve

comparisons of the present data with previous field data to determine if burn house fires do indeed demonstrate typical real structural fire behaviour.

Model results and any comparisons will be discussed in the following chapter along with experimental uncertainty and error.

The next section in this chapter discusses the Burn House experimental setup, followed by a description of the thermocouple instrumentation layout, with experimental procedures and results presented in subsequent sections.

In this and subsequent chapters all figures will be presented at the end of the respective chapters.

3.1 Burn House Experimental Setup: Overview

As previously mentioned, the Burn House is a movable, two-storey steel structure that can be situated inside (as shown in Figure 3.1) or outside a test enclosure. For these four experiments the Burn House was situated outside the test enclosure and exposed to ambient conditions. Ideally, ambient conditions would have been better controlled from the impact of variable ambient conditions had these tests been undertaken *inside* the enclosure; however, an existing experimental set-up prevented this arrangement. The schematic on the right in Figure 3.1 shows the floor plan of the second floor of the Burn House, which is identical in its layout to the first floor, as shown in Figure 3.2. The red squares (Figure 3.1) indicate the location of the burn pads (2.3 m x 2.3 m) and the blue square indicates the two-storey instrumentation shaft where the thermocouple modules for the data acquisition system were mounted. The four experiments were performed in Room 1 as indicated in the schematic of Figure 3.1 by the yellow dashed line. Room 1 is

approximately 3.6 m by 7.2 m by 2.15 m high. A side and isometric view of the Burn House are shown in Figures 3.3 and 3.4, respectively.

Figure 3.5 demonstrates a typical fuel load for each experiment: wood pallets, newspaper and straw. The Region of Waterloo limits the type of fuel used to Class A[15] fuels only. The fuel load is located on the burn pad in Room 1 for each of the experiments. The burn pad is constructed of firebrick on a steel frame and sits approximately 10" (0.254 m) above the burn room floor. Figure 3.6 shows a rendered drawing of the burn room.

The procedure for initial experiments was to limit the size of the fuel load so as to produce approximately 1.0 MW of heat released at peak fire intensity [45]. Fuel loads of this size regularly produce relatively small fires considering that a modest sized house, when fully involved in a fire, could release up to 45 MW of energy [46]. The purpose of keeping the fires small, at least for initial experimentation, was to ensure that damage to the structure would be minimal by keeping hot layer and surface temperatures relatively low. When exposed to high fire temperatures, the thermal expansion of the steel will be significant. If not adequately protected, the differential in thermal expansion from the floor to the ceiling on the sheet steel will cause welds to break, sheets to deform, and windows and doors to warp.

In addition, the Burn House has a rigid welded steel sheet skin affixed to a steel frame which will result in very large thermal stresses. Material properties of the steel, such as modulus of elasticity, ultimate strength and yield strength will also be adversely affected by high temperatures. For example, the yield strength of mild structural steel will maintain 80 percent of its room-temperature value until approximately 500 ºC;

[15] Class A fuels are ordinary combustibles, for example, paper, wood, etc.

however by 600 ºC the yield strength will have dropped to 60 percent of its room-temperature value [47]. Typical maximum design loads produce about 60 percent of yield stress so collapse of a fully loaded member could occur once this temperature (600 ºC) is reached, although most steel structures would be much more lightly loaded during a fire and would not fail until higher temperatures were achieved. It would be unlikely that a wood fuel fire producing approximately 1.0 MW peak heat release, would produce temperatures as high as 600 ºC on the structural steel[16] [48] and this would be a safe operating limit for initial tests. In addition to limiting fire size, however, a protective thermal barrier was affixed to further reduce high temperature exposure to the burn room structure.

The Burn House structure was 0.125" (3.18 mm) sheet steel on a 4" (102. mm) H and I beam steel frame. The liner adopted for the first fire (Jan 9/04) for the exposed wall and ceiling was 0.75" (19.1 mm) plywood overlaid with 3 x 5’ (0.914 x 1.524 m) sheets of 0.375" (9.53 mm) cement board (commercial name Durock®) to protect the steel framework of the house from damage and act as a thermal barrier to the ambient. The ceiling was overlaid with 0.5" (12.7 mm) 4 x 8 ft (1.219 x 2.438 m) sheets of plywood as a sacrificial liner.

The doorway connecting rooms 1 and 2 (see Figures 3.1 and 3.2) in the Burn House was closed off with cement board to prevent fire spread, protect material being stored and to limit ventilation to and from the burn room. (See after Experiment #1 assessment in Appendix B) The door connecting Room 1 with the hallway was exposed plywood (see after burn 1 assessment in Appendix B). The window located on the east wall of the burn house was sealed off and covered with cement board to limit ventilation pathways. The window on the south wall was partially blocked with cement board but

[16] This information is based on previous experimental testing however, it depends on ambient conditions and liner materials used.

one side of the sash was left exposed to allow partial opening of the window to about 2" (50.8 mm). The purpose of this opening was to allow sufficient oxygen to enter the burn room for combustion of the fuel load. The door from the outside to Room 1 was opened during the experiments, as required, if the fire showed signs of vitiation in the early stages of fire development.

The window located on the north wall of the burn room was covered with a 0.75" (19mm) plywood sheet with a hole so a digital video camera could be mounted and used to visually record the experiments. The digital camera was connected to a monitor in the control room of the test facility so that the conditions in the burn room could be observed during the experiment.

This summarizes the basic room preparation in terms of liners, doors and windows. Appendix B provides more technical detail on the construction and thermal design of the liner construction as well as a summary of its observed effectiveness during the four burns and modifications undertaken as the experiments progressed. The effects of fire on the lining material were evaluated on the basis of visual observations via the digital camera images and the post fire observations.

3.2 Thermocouple Layout and Instrumentation

To characterize the thermal development in Room 1 it was necessary to measure the temperature at many locations and positions. K-type chromel alumel thermocouples with ceramic fibre (Nextel) insulation and inconel sheathing were used because of their durability and ability to withstand repeated exposure to high fire temperatures. (1000 – 1200 °C) These thermocouples have been found to withstand harsh environments in previous field fire studies [21, 23, 27-31]. Based on this experience, the thermocouples were not expected to need replacing over the course of experimentation. They are

however susceptible to shorting due to water penetration during suppression and are not mechanically robust.

In order to minimize intermediate connections in the thermocouple system, it was decided that single lengths of thermocouple wire would be run from the measurement location back to the data acquisition backplane in the instrumentation shaft. The required locations of the thermocouples in the burn room were predetermined and the corresponding lengths of wire were measured and cut. K-type thermocouples, (made of nickel-chromium and nickel-aluminum) were welded together to form a bead, or junction using a commercial TIG-Argon gas micro-welder (THERM-X® Model258B). This junction then generates a voltage that can be related to temperature [49].

Figure 3.7 shows a schematic of the final distribution of thermocouples in the burn room. Two thermocouples (51, 52 in Figure 3.8) were placed on the ceiling (affixed to copper plates) above the burn pad. Thermocouples were also placed near sources of ventilation such as above the north and south windows and in front of the doorway. Thermocouples were placed in these locations in anticipation of providing a good indication of the maximum fire temperatures at the ceiling, remote locations in the room, of the fire plume and of the exhaust gases leaving the room through ventilation sources. (These thermocouples are not shown in the figures, but were labelled 72, 54 and 53.) Before the wall materials were affixed in the burn room, thermocouples were placed on the steel frame of the structure so that the heat conduction through the material could be observed and potential fire spread beneath the walls could be monitored. These thermocouples are labelled 46, 48, 49 and 50 in Figure 3.7.

For the **first experiment (Jan20/04)** the burn room was instrumented with one thermocouple rake[17] (Rake 1). The rake consisted of nineteen thermocouples from the burn pad, approximately 10" (254 mm) above the floor, to the ceiling, approximately 85" (2.159 m) above the floor. The thermocouples were spaced 5" (127 mm) apart; however, this spacing was reduced to 0.5" (12.7 mm) near the ceiling and at 36" or 'three foot level' (0.914 m) to resolve greater detail of the temperature stratification in these regions. The rake was then positioned at the southwest edge of the burn pad as shown in Figure 3.8.

For the **second experiment (June9/04)** another rake (Rake 2 in Figure 3.8) was added to verify temperature data obtained from the first rake. It was suspected that the first rake contained faulty thermocouples that could not all be replaced in the time frame of the tests, as will be discussed in more detail in the following section. Another purpose of the second rake was to capture additional data, providing a more detailed description of the distribution of temperatures in the burn room. Twenty- five thermocouples were used in the second rake, spaced approximately 3" (76.2 mm) apart, except near the ceiling and three-foot (0.914 m) level where, as with the first rake, their spacing was reduced to approximately 0.5" (12.7 mm). A total of fifty-five thermocouples were used for the second experiment. Figures 3.8 and 3.9 shows the positioning of both rakes around the burn pad for the second, third and fourth experiments.

To better track the development of the hot gas layer in the room, **for the third and fourth burns (Sept 20 /04 & Nov 25/04),** thermocouples were added at five locations along the length of the room (north to south) positioned at the ceiling, 8" (203 mm) down and 16" (406 mm) down, as shown in Figure 3.10. The purpose of these

[17] A thermocouple rake is a set of thermocouples that are positioned at intervals from ceiling to floor (the height) in a burn room to measure temperature stratification during fire growth. In this work, this has been done by affixing the thermocouples at set heights along a hanging chain, then running the wires in a bundle to back to the data acquisition system.

measurements was to provide an indication of the thermal stratification in the upper layer (just below the ceiling) on a plane down the centre of the burn room. There were 71 thermocouples in total for the last two experiments. (This will be discussed in more detail in Section 3.3.4.)

Thermocouple rakes and individual thermocouples were hung from the ceiling using brackets. (See Figures 3.8, 3.9, 3.10) The thermocouples were then fed through a hole on the west wall of Room 1 to the instrumentation shaft.

Datalogging was achieved using National Instruments's Compact FieldPoint programmable automation controller, which samples the individual 8-channel Compact FieldPoint temperature modules (backplanes) via an ethernet connection. All seventy one thermocouples were connected to nine backplanes (model FP-TC-120) mounted in the instrumentation shaft of the Burn House. The datalogger was set to a sampling rate of 1 Hz. The controller was programmed and data was converted using LabView RealTime software from National Instruments using a personal computer. Raw data was viewed and saved to an output file using FieldPoint Explorer software.

The following section will outline experimental procedures and temperature data obtained from the four Burn House experiments, followed by a section which discusses uncertainty and error with thermocouple measurements. Further analysis of the data, model results and comparisons will be presented in the next chapter.

3.3 Experimental Procedure

The experimental data for each of the tests were recorded to a text file located on a computer in the control room at The University of Waterloo Live Fire Research Facility.

Matlab Version 6.1 [49] was used to present all data in this study. The program files used to manipulate the experimental data are found in Appendix A.

As previously discussed, the objective of preliminary experimentation was to create a set of data from baseline fire tests with limited numbers of variables affecting fire behaviour in the burn room. This would facilitate development of an understanding of the fire characteristics of the structure, and would build a strong basis for further research into house fire behaviour. By limiting the variables studied for initial tests an experimental protocol and set of data could be obtained and used as a reference for future experiments. To this end, the ventilation in the room (sealing off doors and windows to adjacent rooms and to the ambient) was limited, the size of the fuel load was restricted and fairly repeatable and only basic wall lining materials were incorporated into the test structure.

Before experimentation, the walls of the burn room were lined with 0.75" (19.1 mm) plywood and 0.375" (9.53 mm) cement board on the steel frame of the Burn House. In addition, a 0.5" (12.7 mm) layer of plywood was affixed to the ceiling. The purpose of the wall lining material was to reduce heat losses through the steel walls and act as thermal barrier. For the first experiment, the purpose was to provide simple lining materials which would not contribute to the fuel load of the experiments, however, wall materials were altered for successive experiments.

For the first experiment, the burn room was instrumented with one rake and wall and ceiling thermocouples for a total of thirty temperature measurements. The rake contained thermocouples that had been previously used in experiments. Some of these thermocouples had frayed sheathing, which could have exposed the thermocouple wires inside, leading to damage from moisture or debris. The extent of the damage to the wire, if any, could not be determined from visual inspection so they were individually tested

using a blowtorch and observing the temperature response on Field Point Explorer. All of the thermocouples *appeared* to be functioning properly for this first experiment.

The fuel load for this experiment was comprised of approximately 3 wood pallets of varying size (42 kg hardwood), 6 kg of plywood, 4 kg of miscellaneous softwood, 1/5 bale of straw and some newspaper and cardboard.

The fire was started with a propane torch, igniting the newspaper and straw first. The datalogger on the computer was started when the fuel load was ignited. This was initiated via radio communication from firefighters in the burn room to personnel in the control room of the fire test facility. The temperatures on the computer were monitored closely and the digital video images were observed for any signs of vitiation in the burn room so that a window or door could be opened to supply more oxygen if necessary. The window on the south wall of Room 1 was kept open 2" (50.8 mm) to allow sufficient air to enter the burn room and maintain the fire in near steady state conditions.

Figure 3.11 shows a view of the burn room as set up for the second experiment. An additional thermocouple rake was introduced for the second experiment to obtain more burn room data and so that suspected faulty thermocouples in the first rake could be identified.

The fuel load for this experiment consisted of 51.6 kg of hardwood, of which 6 kg was plywood and the rest wooden pallets (approx. 3 wood pallets). The fuel loading was slightly more than that of the first experiment. Miscellaneous softwood made up 6 kg of the load, along with 1/3 of a bale of straw. Paper and cardboard were added for ignition. Figure 3.11 shows the fuel loading. A similar procedure was followed as in Experiment 1, where a propane torch was used to ignite the paper and cardboard material. In addition to data acquisition, a digital video camera was used to capture images of the burn room

throughout the experiment. The first few minutes of the experiment were used to observe the room carefully for any signs of vitiation or smouldering.

For the third experiment, the plywood ceiling was removed to limit additional fuel sources for the fire. In the first two experiments the ceiling plywood was observed to burn which, particularly in the second experiment, resulted in significant thermal jets of very hot air throughout the room which led to ignition of exposed plywood on the camera window (north wall) and the door between room 1 and the hallway. (See Appendix B for further discussion) It was decided that for Experiment #3 all exposed consumables would be reduced to a minimum single source fire load so that the thermal development of the room would be unaffected by other sources. The wall materials were returned to the same construction materials as the first experiment (cement board on plywood). See Appendix B for a more detailed discussion. Figure 3.12 shows this set up. Several thermocouples were added down the centre plane of the burn room. At five locations along the ceiling thermocouples were placed at the ceiling height, 8" (203 mm) below the ceiling and 16" (406 mm) below the ceiling. The purpose of these additional measurements was to gain a better understanding of the thermal stratification just below the ceiling down the central cross section of the burn room. This can be seen in Figure 3.10 and Figure 3.12. A few of the thermocouples on the first rake were replaced with new ones based on the measurements observed from the data of the first two experiments. In addition, Rake 2 was moved slightly farther away from the fire than in the second experiment to ensure that the rake was not positioned directly in the flames. There were a total of 77 temperature measurement locations for this experiment.

The fuel load was comprised of 32 kg of hardwood (2 wooden pallets), 6 kg of plywood, 3 kg of softwood, paper and cardboard and 1/5 of a bale of straw, as shown in Figure 3.12. As usual, the fire was initiated using a propane torch. The south window was kept ajar 2" (50.8 mm) to allow more oxygen to enter the room.

For the fourth and last experiment, the walls and ceiling were again lined with a sacrificial plywood layer 3/4" thick. This time, the material was extended farther down the wall, as shown in Figure 3.13. As shown in the figure, small wood slabs were added to the wall construction so that the vertical extent of char could be identified during post-experiment analysis.

The fuel load for this experiment consisted of 42.7 kg of hardwood (two large and one small wooden pallet), 6 kg of plywood, 2 kg of softwood, paper, cardboard and 1/5 of a bale of straw. Approximately 8 kg of fuel was added during the burn to speed up the rate of fire growth and increase the burn room temperatures. Figure 3.14 shows the fuel load for this experiment.

The burn room instrumentation was identical to the September 30th experiment and the fire was again started using a propane torch. The south window and door to the burn room were left open 2" (50.8 mm).

The following table summarizes the fuel loading for each of the four experiments.

Table 3.1: Fuel Loadings for Burn House Experiments

Experiment No.	Hardwood (kg)	Softwood (kg)	Straw (bale)	Added during burn (kg)
1	42.0	4	1/5	-
2	51.6	6	1/3	-
3	32.0	3	1/5	-
4	42.7	2	1/5	8

The following table summarizes the ambient conditions for each of the experiments.

Table 3.2: Ambient Conditions for Burn House Experiments

Experiment No.	Ambient Temperature (ºC)	Wind Speed (m/s)	Wind Direction	Relative Humidity (%)
1	-13.0	3.2	NE	75.0
2	27.6	2.4	SE	73.5
3	15.4	1.6	SW	76.3
4	-2.2	2.1	SW	96.8

The ambient temperature will have the greatest effect but only on the initial fire growth rate and maximum temperatures achieved because of the thermal sink of a colder building from experiments performed during cooler weather. The wind effects should be negligible since the burn room was minimally ventilated. None of these condition variations should impact significantly on the thermal behavior during burns.

3.4 Experimental Results

Experiment 1, Results

Figure 3.15 shows the time evolution of the temperatures in the burn room for thermocouples on the ceiling, 0.5, 5 and 10" (12.7, 127 and 254 mm) below the ceiling and at 42" (1.067 m) above the floor. Temperatures at all heights increased until approximately 8 minutes (490 seconds) into the fire. At this time, temperature measurements at 0.5" below the ceiling in the burn room indicated a maximum value of approximately 875 ºC as shown by the triangular symbols in Figure 3.15. At this time, temperatures directly on the ceiling and 5" (127 mm) below reached approximately

675 ºC while temperatures at 10" (254 mm) below the ceiling reached just above 600 ºC. Maximum temperatures were observed on the ceiling and at 42" (1.067 m) above the floor later in the burn, at approximately 510 seconds. Ceiling temperatures at this time peaked to 700ºC while temperatures at 42" (1.067 m) above the floor level were observed to be 450ºC.

Once temperatures reached their maxima there was a rapid decrease in burn room temperatures because the majority of the fuel load had been exhausted. Temperatures at the ceiling levelled off at 750 seconds to approximately 500 ºC and then began to gradually decrease just before 1000 seconds. All other temperature measurements demonstrated a similar profile. Measurements at 5 and 10" (127 – 254 mm) below the ceiling, and 0.5" (12.7 mm) below the ceiling levelled off at 375ºC, 350ºC and 300 ºC, respectively. The fire was allowed to burn to extinction and data acquisition was terminated at 3000 seconds.

A measurement was taken at the floor level on the second storey above the burn room to estimate heat conduction through the ceiling. Temperatures were observed to be relatively low (no greater than 50 ºC) and indicated no cause for concern during future experiments at this level of fuel loading.

Figure 3.16 illustrates the thermal stratification in the room at various times during the burn as measured by thermocouple Rake 1. Observation of the profile at 240 seconds shows the development of a hot upper layer, as temperatures start to increase rapidly approximately 30" (0.762 m) above the floor towards the ceiling. Temperatures in the lower layer, floor to 30" (0.762 m) above, remain relatively steady at approximately 50 ºC. At this time, upper layer temperatures range from about 100 ºC to 500 ºC. Similarly to Figure 3.15, Figure 3.16 shows the maximum temperature in the burn room was approximately 875 ºC at 0.5" below the ceiling at 480 seconds. As time increases, Figure 3.16 demonstrates a decrease in all burn room temperatures.

It was anticipated that the stratified temperatures would show a relatively smooth increase in upper layer temperatures for Experiment 1. As discussed in Chapter Two, as the fire grows, hot gases will begin to rise towards the ceiling and a hot layer will form and grow, descending towards the floor as gases continue to build up at the ceiling. Upper layer temperatures would increase from the boundary between the upper and lower layer to the ceiling of the burn room during fire growth. Due to the complexities and number of uncontrollable variables in a realistic scenario fire scenario, there may be many reasons why a smooth increase in upper layer temperatures at increasing heights might not be observed. For example, the circulation of hot gases throughout the burn room could cause temperature fluctuations at various heights or a thermocouple rake positioned close to the fire could result in random spikes in temperature due to impinging flames from the plume.

Figure 3.16 demonstrates some skewed measurements at heights above 65" (1.651 m) from the floor for $t > 600$ seconds and a few random spikes in temperature at approximately 20 and 30" (0.508 and 0.762 m) above the floor for each temperature profile. There are several likely possibilities for this occurrence. This information could indicate potential thermocouple measurement error due to short-circuiting due to insulation breakdown caused by kinking of the wires during handling or water penetration through the insulation as they had already been used in previous for experiments and could have been damaged from fire and water exposure. Ventilation leaks or thermally generated gas flows are another potential cause of the skewed profile. They are observed as 'pulling' of the temperatures at various levels in the temperature stratification. These leaks can occur through sources of ventilation such as gaps in windows or doors and provide a means for fresh air to enter or hot exhaust gases to exit the burn room.

An attempt would be made to rule out error from these sources in the second experiment by sealing up doors and windows and replacing suspected faulty thermocouples.

Experiment 2, Results

Figures 3.17 and 3.18 show temperature-time plots of data from thermocouple rakes 1 and 2, respectively, for the second experiment. Immediately after ignition (t=0 s), the fire grew, but temperatures then levelled off to a nearly constant value of 40ºC until 250 seconds. At this point, burn room temperatures began to decrease because the fire began to smoulder, as observed from the digital video. The southwest window was opened to 6" (152 mm) to increase the ventilation in the room. Previously it had only been open 2" (50.8 mm). At roughly 550 seconds, temperatures began to rapidly increase as the fire began to grow. Two maximum temperature peaks were observed for this burn, as shown in both of Figures 3.17 and 3.18.

In Figure 3.17 thermocouple Rake 1 shows that the first peak occurred at approximately 775 seconds, reaching 675 ºC after which several small dips and spikes in temperature were observed until the second peak occurred at 1300 seconds where temperatures rose to approximately 750ºC. The maximum temperature for the first peak was recorded by the thermocouple situated 10" (254 mm) below the ceiling, while the second temperature peak occurred at 0.5" below the ceiling.

In Figure 3.18 the second rake shows both peaks occurring at slightly higher maximum temperatures. The first peak is observed at almost 800 seconds and 700ºC and the second peak is 775ºC at 1200 seconds, occurring at 0.5" below the ceiling. A possible reason for the higher temperatures observed by Rake 2 may have been due to the fact that the second rake was situated slightly closer to the fire.

The cause of the two temperature peaks and fluctuations between them could not be determined by simple observation of the experimental data; however images from the digital video of the burn provided some insight into the events that caused the double peaks in Figures 3.17 and 3.18. The digital images indicated that the sacrificial plywood ceiling was ignited around 700 seconds which essentially made additional fuel available for the fire to continue to grow and burn. As the plywood layer was consumed, overall temperatures in the burn room would have increased as the fire grew. After ignition, the digital video showed intermittent bursts of flames across the ceiling as the plywood burned which may correspond to the temperature fluctuations observed in Figures 3.17 and 3.18. It is speculated that these flames bursting across the ceiling are a result of the burning characteristics of the plywood ceiling material. Due to high temperatures at the ceiling, the plywood pyrolized, potentially creating pockets of hot unburned gases at the ceiling. When these pockets ignited and burned, the flame appeared to explode from the main fire plume travelling across the ceiling and contributing to large, rapid temperature fluctuations like those seen in Figures 3.17 and 3.18. These figures show the largest fluctuations in temperature occurring for thermocouples within 10" (254 mm) of the ceiling which could indicate that these thermocouples were positioned directly in the flames.

Unfortunately the fluctuations observed between peaks cannot be fully explained due to the complexities involved with the burn room dynamics and burning characteristics of the plywood.

The fire begins to decay somewhere between 1200 and 1300 seconds into the burn. Just after 1600 seconds, a large drop in temperature can be seen in Figure 3.17 and 3.18. At this time, a fire fighter had entered the burn room and sprayed water onto the flaming ceiling, cooling burn room temperatures for a period of time, before the fire continued to burn and smoulder. The data logging was stopped around 1800 seconds and the fire was suppressed until it had been put out.

Figure 3.19 shows the temperatures recorded by a thermocouple located on the ceiling (near the door) and at a point 8" (203 mm) down from the ceiling on the north wall (farthest point from the fire). Surprisingly, temperatures near the door rise to just below 700 ºC; not too different than the values recorded for the first peak by the thermocouples in each of the rakes. The peak value observed in Figure 3.19 occurs at just before 800 seconds, consistent with observations from the digital images which suggest that the ceiling had been ignited by this time. The digital video also indicates that once the plywood ceiling had ignited, flames spread along the ceiling as far as the doorway, causing the high temperatures recorded there. Large temperature fluctuations near the doorway can also be observed on this plot caused by a combination of ceiling jets and ventilation of hot gases from the doorway. Fluctuations are present, but less marked for the thermocouple situated 8" (203 mm) below the ceiling along the north wall than for the thermocouple near the doorway. These smaller fluctuations are likely due to the fact that the ceiling material did not extend as far as the north wall, preventing flames from travelling along the ceiling to this point. In addition, this thermocouple was situated at the farthest point from the fire as well as in front of the north wall window, where hot gases from the fire could exhaust and some fresh, cooler air could recirculate into the room. Observation of the curves in Figure 3.19 shows that temperatures at the doorway decreased much more rapidly than temperatures recorded at the north wall, however, by 1400 seconds, they both began to decrease at relatively the same rate. Due to the relatively low thermal inertia of the burn room lining materials, once the fire had burned out (as observed by the large decrease in temperatures at the doorway), the temperatures in the room decreased at a relatively slow rate.

Figure 3.20 shows four digital images that were captured from the video of the fire experiment. In the first frame (top left), the flames are shown beginning to char the plywood on the ceiling over the fire load. In the second frame (top right), a mere 18 seconds later, the plywood ceiling over the fire has ignited and the flames begin to spread outwards across the ceiling. By the fourth frame (bottom right), 29 seconds later, the

flames have completely engulfed the ceiling. The time stamps on the digital images in Figure 3.20 were traced back to times recorded by the data logger and the events were correlated with the temperature-time data in Figures 3.17 and 3.18. The first frame occurred at approximately 669 seconds into the fire, the second frame 687 seconds, the third frame occurred at 690 seconds and the last frame at 716 seconds.

Figure 3.21 illustrates the temperature stratification at varying times throughout the fire measured by Rake 1. The temperature profiles at 60, 120, 240 and 480 seconds appear to be relatively uniform from floor to ceiling which corresponds to the time frame in Figures 3.17 and 3.18 where the fire temperatures have increased to only 40ºC and then levelled off. It has been shown that a smouldering fire will have very little effect on the development of the hot layer [9].

Observation of the temperature stratification at 600 seconds in Figure 3.21 shows a marked increase in upper layer temperatures, starting at 30" (0.762 m) above the floor and upwards towards the ceiling, which corresponds to the fire growth observed in Figures 3.17 and 3.18 after 550 seconds and before the first temperature peak. The data at the next two time intervals show a continued increase in upper layer temperatures with maximum temperatures occurring at 0.5" below the ceiling at 1200 seconds into the fire. Lower layer temperatures appear to be quite steady for all heights up to 30" (0.762 m) above the floor, with the exception of temperatures directly at the floor level. Measurements at the floor show an increase of 100 ºC over the next highest thermocouple measurements. The reason for this increase is unknown; however, one possibility is that the enclosed thermal plume may have travelled down the wall and back across the floor, affecting the thermocouple measurements. By 1500 seconds into the burn, all the temperatures have decreased, and by 1800 seconds temperatures have decreased even further, which indicates that the fire is in the Decay stage.

Figure 3.22 shows thermal stratification in the enclosure as measured using thermocouple Rake 2. Comparison of Figure 3.21 and Figure 3.22 indicates that slightly higher temperatures were recorded at 0.5" below the ceiling for Rake 2 than for Rake 1. This could be due to the fact that Rake 2 was situated slightly closer to the fire or perhaps flames from the plume impinged on the thermocouples in Rake 2. It is difficult to estimate the cause of this measurement difference as it may also depend on the overall room circulation of the hot gases which cannot be determined from this information. Similar to Figure 3.21, the temperature in Figure 3.22 is not stratified but uniform with a value of approximately 50ºC at 60, 120, 240, and 480 seconds. This indicates relatively uniform mixing throughout the room in the early stages of fire growth. By 600 seconds, the formation of a hot upper layer can be observed for measurements 20" (0.508 m) above the floor. For successive time series' it is more difficult to resolve a boundary between an upper layer and a lower layer as the temperatures appear to increase linearly from the floor to the ceiling. This result might again, be due to the fact that Rake 2 was situated close to the fire resulting in temperature measurements of the impinging flames of the plume rather than of the hot gases in the room. A maximum temperature of 775ºC occurs at 05" below the ceiling at 1200 seconds which corresponds to the information observed in Figure 3.18.

As previously mentioned, Rake 2 was positioned slightly farther away for the third experiment based on the results of the second experiment.

Experiment 3, Results

Figure 3.23 is a plot of the temperature-time profile for thermocouple Rake 1 throughout Experiment 3. Figure 3.23 shows that burn room temperatures increased and reached their peak at around 300 seconds, where they began to level off except for some small

fluctuations. A maximum temperature of just below 500 ºC was recorded for Rake 1 at 1" (25.4 mm) below the ceiling. By 800 seconds the fire began to slowly decay.

Figure 3.24 shows the temperature-time traces recorded for thermocouple Rake 2. The curves show similar results as those shown in Figure 3.23. Temperatures reached a maximum of 400 ºC at approximately 300 seconds, levelling off until 800 seconds and then began to decay. The maximum temperatures recorded by Rake 2 were slightly lower than those recorded at the ceiling for Rake 1. This might be because Rake 2 was positioned slightly farther away from the centre of the fire than Rake 1.

A few dips can be observed in the profile for Rake 2 near the ceiling once the fire has become fully developed. This is likely caused by ceiling jets (flames) propagating out from the fire plume similar to those observed at the ceiling in Test 2. Smaller dips can also be seen for profiles at other heights. Again, occurrence could be due to flames from the plume in addition to ventilation effects or circulating hot gases.

Figure 3.25 and Figure 3.26 show the temperature stratification in the room for thermocouple Rakes 1 and 2, respectively. Figure 3.25 shows relatively uniform temperatures of 20ºC from floor to ceiling at 60 seconds. At 120 seconds, upper layer temperatures start to increase approximately 40" (1.016 m) above the floor. By 240 seconds upper layer temperatures have increased significantly ranging from 100ºC at 30" (0.762 m) above the floor to 430ºC at 1" (25.4 mm) below the ceiling. Very similar profiles are observed at 480 and 600 seconds with maximum temperatures occurring near 500ºC just below the ceiling. Observation of the data in Figure 3.23 shows that temperatures remain relatively steady from 300 to 800 seconds which explains the similar profiles at 480 and 600 seconds. Temperatures decrease for profiles at 900, 1200 and 1500 seconds, as the fire begins to decay.

Similarly to Figure 3.25, Figure 3.26 illustrates uniform temperatures of approximately 20ºC at 60 seconds. Upper layer temperatures are beginning to increase 70" (1.778 m) above the floor at 120 seconds. By 240 seconds, upper layer temperatures have increased substantially, however, many temperature fluctuations can be observed throughout the profile. Measurements at 480 and 600 seconds have very similar temperature profiles which can be attributed to the steady temperatures observed in the fully developed region (300 to 800 seconds) of Figure 3.24. Profiles at 900, 1200 and 1500 seconds decrease at all heights as the fire begins to decay.

Figure 3.27 shows the temperature-time curves for thermocouples that were placed at five locations down the centre plane of the burn room for Experiment 3. (Figure 3.7 from Section 3.2 can be used as a reference for the thermocouple placement in the room) The temperature profiles are similar in shape to those for Rakes 1 and 2. After ignition at t=0, the fire grew until approximately 300 seconds, where temperatures became relatively steady. Maximum temperatures recorded for thermocouple #66 are just above 600ºC, higher than maximum temperature measurements at the ceiling for Rakes 1 and 2. Thermocouple #66 was situated over the burn pad, almost directly in the centre of the fire plume. Temperature fluctuations can be observed for this curve and are a result of flames from the plume impinging on the thermocouple as well as circulating hot gases at the ceiling level. Temperature fluctuations can also be observed for thermocouple #63, which had also come in contact with flames at the ceiling, as observed through digital video images of the fire. Thermocouple #63 was situated above the burn pad, but slightly farther away from the centre of the fire than thermocouple #66. This accounts for the lower maximum temperatures observed for thermocouple #63. After fire growth, thermocouple #63 recorded steady temperatures of approximately 450ºC until just before fire decay, where a temperature spike of 500ºC was observed. As shown in Figure 3.27, all other ceiling temperature profiles decreased with increasing distance from the plume.

Figure 3.28 demonstrates the ceiling temperatures as a function of distance from the south wall of the burn room at various times throughout the experiment. The data is plotted to show the ceiling temperature distribution across the burn room from fire growth to decay. At 60 seconds, temperatures across the room are fairly constant. At 120 seconds temperatures above the burn pad are starting to increase more rapidly. From 240 to 600 seconds, fire temperatures above the burn pad have reached a maximum with a gradual decrease in temperatures towards either end of the burn room. By 900 seconds the fire has burned out and temperatures across the room are again relatively constant.

Figure 3.29 shows similar information for thermocouples located 8" (203 mm) lower than those at the ceiling. The maximum temperatures recorded at this height were approximately 550º C. Figure 3.30 demonstrates the temperatures of the thermocouples 8" (203 mm) down versus distance from the south wall of the burn room. This figure demonstrates similar trends to those seen in Figure 3.28; however, from 240 to 900 seconds, temperatures across the room are relatively constant, with the exception of the thermocouple directly above the burn pad. Hot gases have circulated and mixed causing relatively constant temperatures across the room at 8" (203 mm) below the ceiling.

Figures 3.31 and 3.32 display temperature measurements for those thermocouples located 16" (0.402 m) below the ceiling down the centre plane of the room. These figures illustrate that the maximum temperatures that occur anywhere in the burn room (approximately 675ºC) occur at a height 16" (0.402 m) below the ceiling for thermocouple #68. This may be due to the fact that thermocouple #68 was positioned directly in the fire plume. Another possibility is that a potential cold jet could have passed above the plume, cooling the thermocouples near the ceiling and 8" (203 mm) below, or perhaps this is a result of high heat transfer to the ceiling. This information could not be verified from the experimental data obtained or from the digital video images of the burn experiment. Figure 3.32 shows that relatively constant temperatures

occurred across the burn room between 240 and 900 seconds, with the exception of those recorded by the thermocouple placed directly over the burn pad.

Figure 3.33 shows the temperature profiles for all thermocouples positioned on the ceiling throughout the burn experiment. The results show similarly shaped profiles and close-ranged temperature measurements for all thermocouples with the exception of those placed directly over the burn pad (#63, #66) which registered significantly higher temperatures. As previously discussed, these latter two profiles also show fluctuations in the fully developed region which could be attributed to flames propagating from the fire plume.

Experiment 4, Results

Figures 3.34 and 3.35 illustrate the temperature-time plots for thermocouple Rakes 1 and 2, respectively for the fourth experiment. After ignition, at t= 0, the fire began to grow very slowly until approximately 450 seconds, where the temperature levelled off below 200ºC. Observation of the digital video indicated that the fire was still burning and had not smouldered, however, by 600 seconds burn room temperatures had still not increased. Just after 600 seconds, another pallet of wood (approximately 8 kg) was added to the fuel load in an attempt to increase the rate of fire growth. Within two minutes (by 700 seconds), temperatures in the burn room began to escalate rapidly as the fuel load and additional pallet began to burn.

Figure 3.34 shows a temperature of 850 °C recorded at 800 seconds for the thermocouple located at 1" (25.4 mm) below the ceiling. This was quickly followed by a large dip in temperature and then a gradual increase until about 1300 seconds. Figure 3.35 shows a peak temperature of approximately 700ºC at the end of the fire growth stage. Temperatures remain relatively steady until 1000 seconds, where a gradual

increase is observed until about 1400 seconds. The increase is particularly marked for thermocouples 23" (0.584 m) above the floor.

It is suspected that the ceiling material has caught fire just before 700 seconds, and the entire plywood lining material has become engulfed in flames by the first peak at 800 seconds. The time period following these events and leading up to the second peak at 1300 seconds is likely where the majority of the lining material is consumed in the fire. These predictions cannot be verified from the experimental data alone so confirmation will come from analysis of the digital video of the fire.

The images in Figure 3.36 were captured from the digital video of the fire experiment. The first frame (top left) shows the flames beginning to char the ceiling. Thirty-three seconds later, the ceiling material has been ignited and ceiling jets are propagating outwards from the top of the fire plume. By the third frame (bottom left), another thirty-four seconds later, the entire ceiling is engulfed in flames and the flames are beginning to spread down the walls. One minute and twenty-four seconds later, the lining material on both walls and on the ceiling is burning.

The events in Figure 3.36 occur over the course of approximately 3 minutes. The time stamps on these images were correlated back to the experimental data. The data acquisition system was started just after the propane torch was lowered to ignite the paper and straw which occurred at approximately 7 minutes, 34 seconds on the digital video.

The first frame of Figure 3.36 occurs at 668 seconds into the burn. Observation of Figures 3.34 and 3.35 show that this is where temperatures start to rapidly increase – roughly a minute after the additional fuel has been added to the fire. At this point, flames are beginning to reach the ceiling. The second frame (top right) in Figure 3.36 occurs at 701 seconds into the fire. Temperatures at this point have increased by over 100 °C as the ceiling material starts to catch fire. The third frame corresponds to approximately

735 seconds where the fire has spread and the entire ceiling is fully involved in flames. Temperatures near the ceiling have increased to nearly 500 °C. The last frame occurs at 819 seconds into the burn where the first large temperature spike can be observed for Rake 1 in Figure 3.34. This point is where the fire plume has extended across the ceiling and down the walls so that the ceiling *and* wall material are completely burning.

In a similar way, as discussed in the results for the second experiment, the thermocouples situated within 10" (254 mm) of the ceiling show fluctuations in temperature measurements from 800 seconds until the fire begins to decay at approximately 1400 seconds. This is likely a result of the ignition hot unburned gas pockets at the ceiling created by the pyrolysis of the plywood material.

Figure 3.37 shows the behaviour of the fire about half way through the fully developed stage at 1140 seconds. The fire has spread extensively and progressed down the walls of the burn room. The fire plume is still burning strong. Figure 3.38 shows the fire at a later time, towards the onset of the decay stage at 1522 seconds. This image shows fire plume has diminished in size but observation of Figures 3.34 and 3.35 indicate that temperatures within 10" (0.254 m) of the ceiling, although starting to decrease, are still relatively high between 600 and 700°C. Parts of the lining material are still burning and some material has fallen to the floor.

Figures 3.39 and 3.40 illustrate the vertical stratification of temperature in the burn room for various times after ignition. Fairly uniform temperatures are observed until 240 seconds into the fire, with slightly higher temperatures within 15" (0.381 m) of the ceiling. Similar profiles are observed at 480 and 600 seconds which correspond to the region discussed in Figures 3.34 and 3.35 where temperatures in the room levelled off soon after ignition. At these times, temperatures in both the lower and upper layers have increased and demonstrate a relatively linear profile from floor to ceiling.

Figure 3.39 shows that ceiling temperatures remain relatively constant around 800ºC from 800 to 1200 seconds. During this time, lower layer temperatures show a much smaller increase in temperature at successive thermocouple heights than upper layer temperatures. Due to this difference in temperature increase, a boundary between layers is developed at approximately 30" (0.762 m) above the floor. Similar information is illustrates in Figure 3.40 for thermocouple Rake 2.

In Figures 3.41 through 3.46 the temperatures measured by thermocouples placed down the centre plane of the burn room are plotted.

As shown in Figure 3.41 all the thermocouples placed at the ceiling measured similar temperature-time profiles. Temperatures closest to the south wall, experienced the lowest maximum temperatures, at 600ºC, while temperatures directly above the burn pad (#63, #66) achieved the highest maximum temperatures of approximately 775ºC.

Figure 3.42 shows, as expected that the highest temperatures occur directly over the burn pad (#63, #66) and are approximately 775ºC. The temperatures remain quite high for the other thermocouples in the room as well. This is due to extent of the hot fire plume and the burning ceiling material.

A sudden large increase in temperature is observed for the thermocouple #67 at 1100 seconds into the burn as shown in Figure 3.43. This thermocouple is positioned over the burn pad at 8" (203 mm) below the ceiling. This thermocouple is likely entirely surrounded by flames because of its location and the large temperature increase could be a result of ceiling and wall material burning and hot gases circulating in the upper layer. Figure 3.44 shows constant temperatures across the burn room, with the exception of higher temperatures directly over the burn pad, approximately 70" (1.778 m) from the south wall.

Large temperature spikes are observed in Figure 3.45 for the thermocouple 16" (0.406 m) below the ceiling, positioned over the burn pad (#68). This may due to the fact that it is positioned within the fire plume. Maximum temperatures of approximately 850ºC are observed. The temperature-time plot shown in Figure 3.45 shows very similar profiles for other thermocouples positioned 16" (0.406 m) below the ceiling across the burn room. Figure 3.46 also illustrates that almost constant temperatures exist across the burn room at various time throughout the fire, with the exception of slightly higher temperatures over the burn pad.

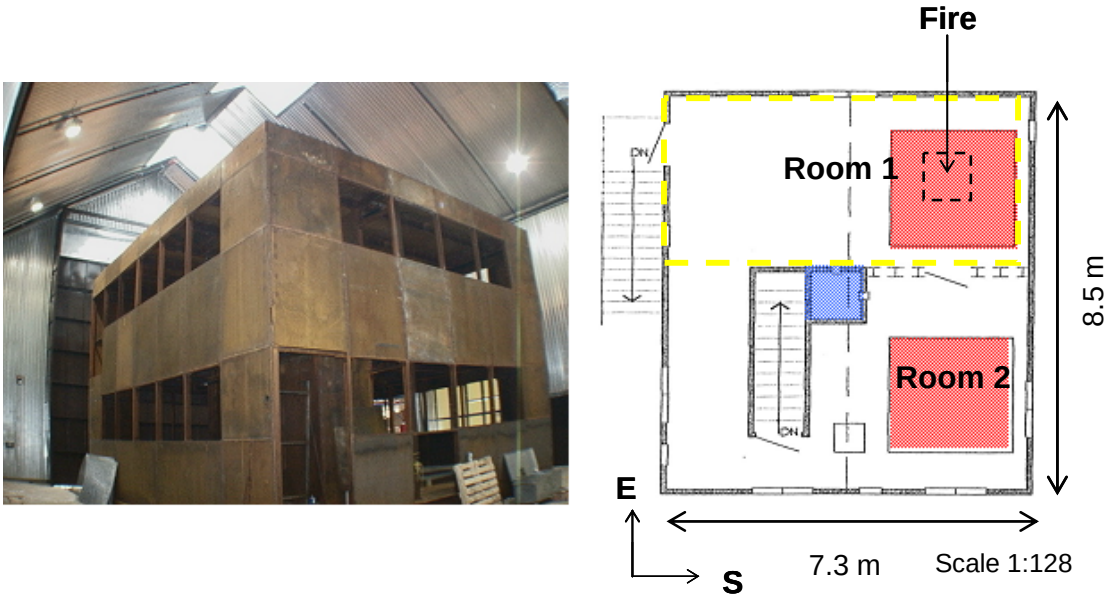

Figure 3.1: Burn House Situated inside the Test Enclosure (left) and Second Floor Schematic of the Floor Plan (right)

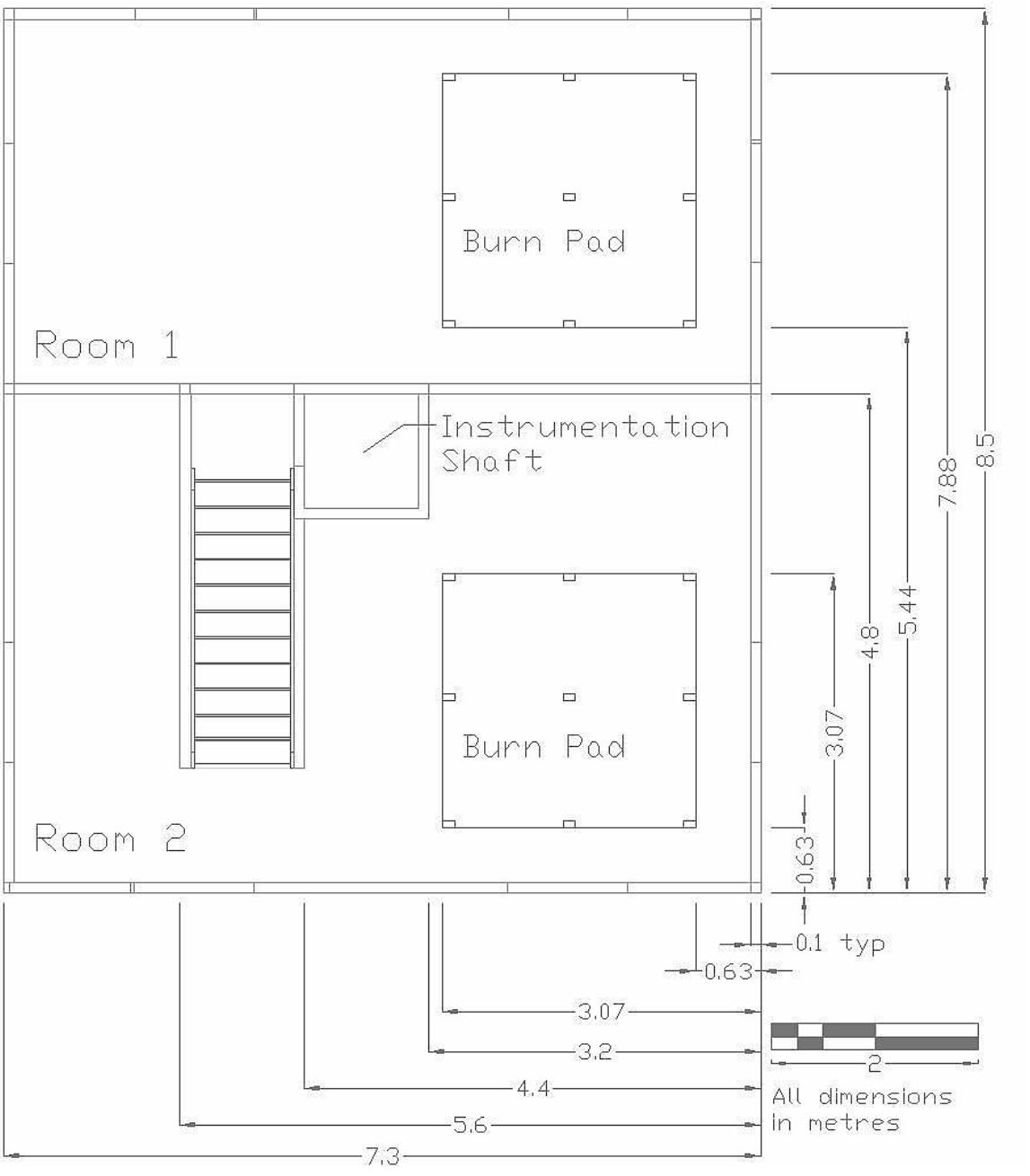

Figure 3.2: First Floor Schematic of Burn House

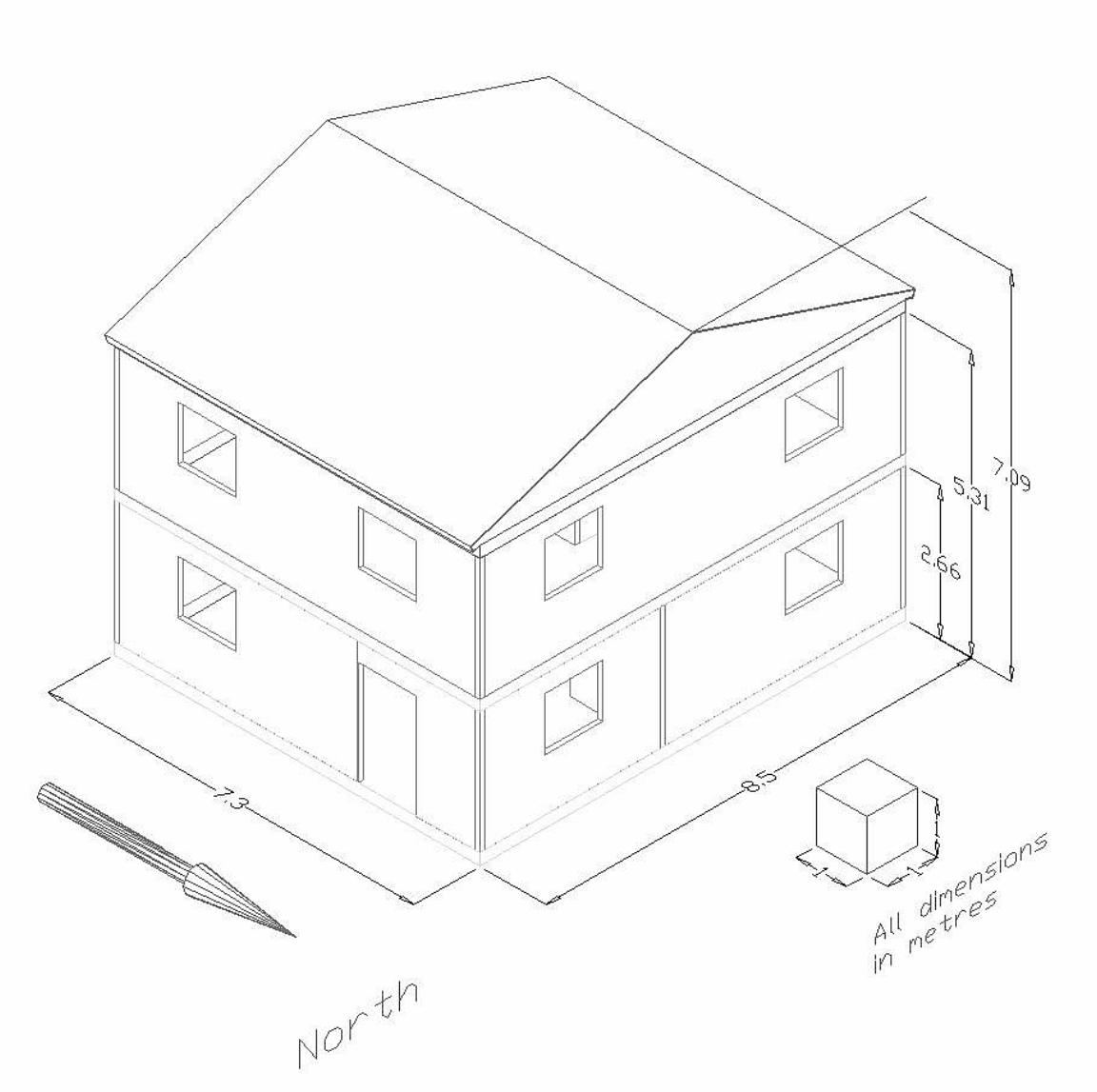

Figure 3.3: 3D Isometric View of Burn House

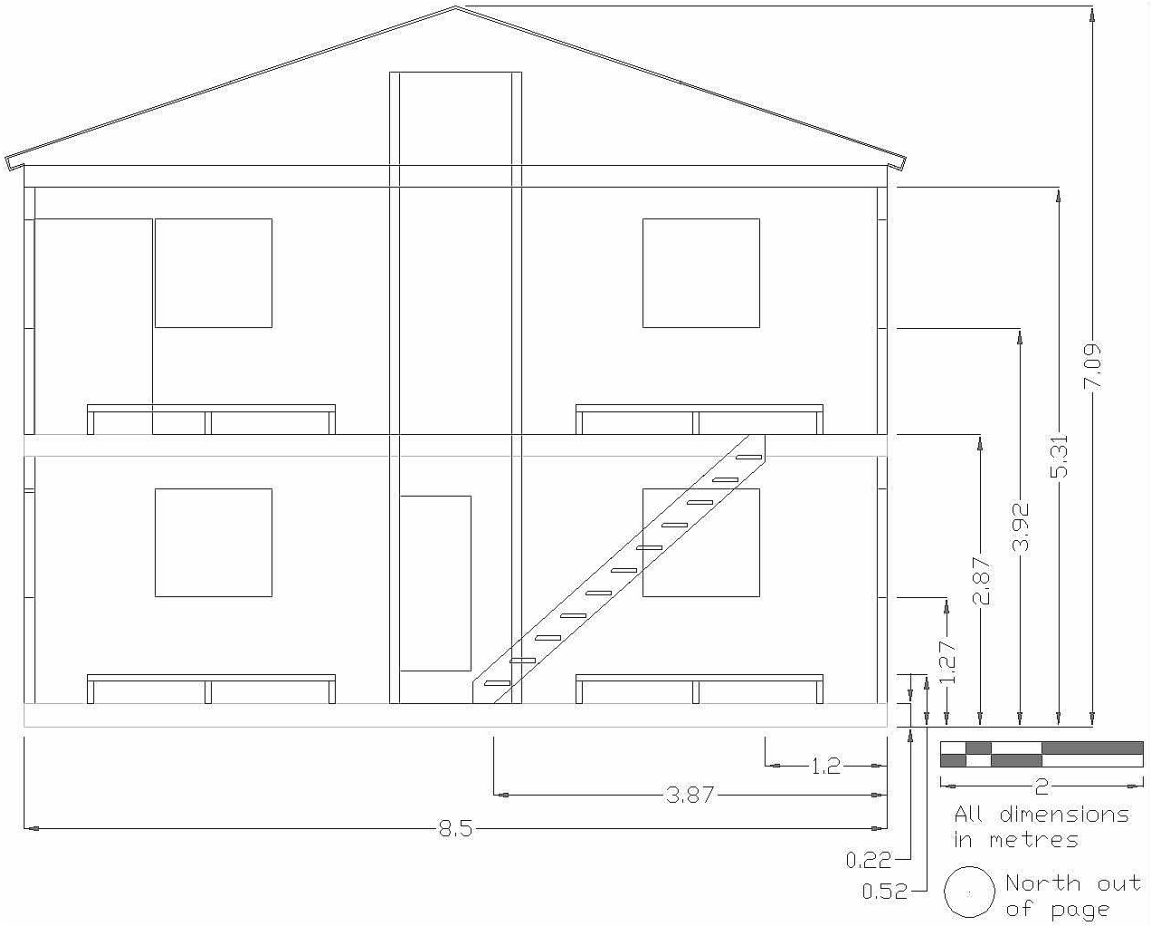

Figure 3.4: Side View of Burn House

Figure 3.5: Typical Fuel Load for Fire Experiments, Located on Burn Pad

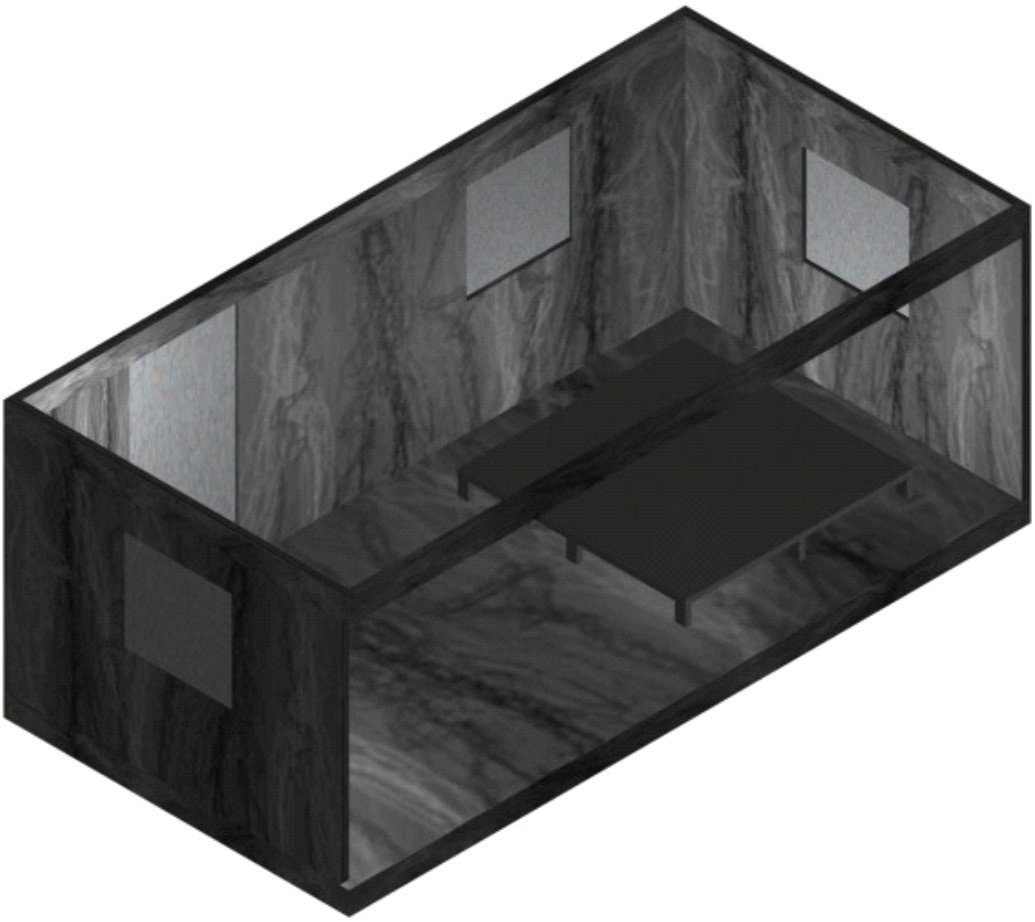

Figure 3.6: AutoCad rendering of Room 1 in Burn House

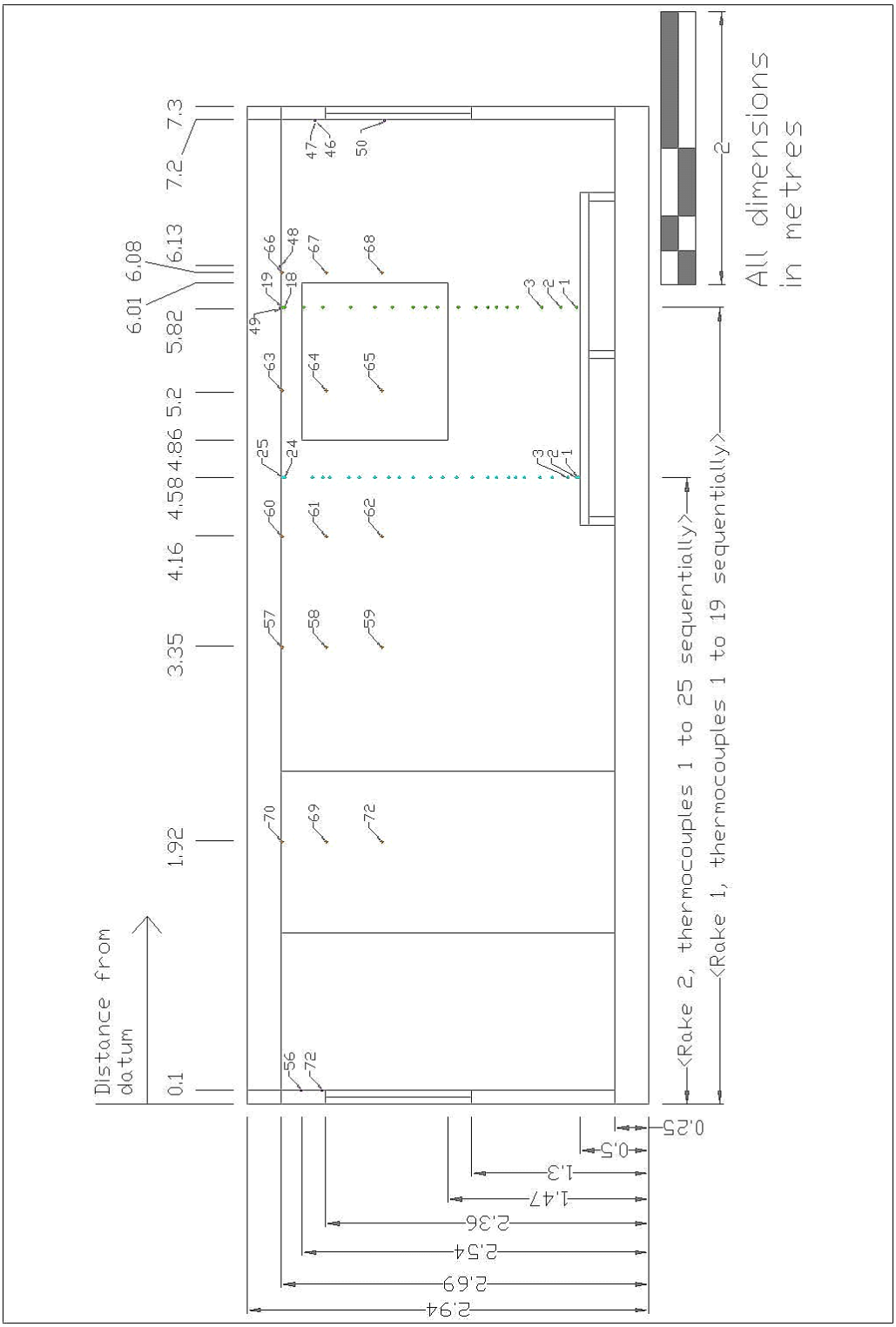

Figure 3.7: AutoCad Schematic of Thermocouple Locations in Room 1

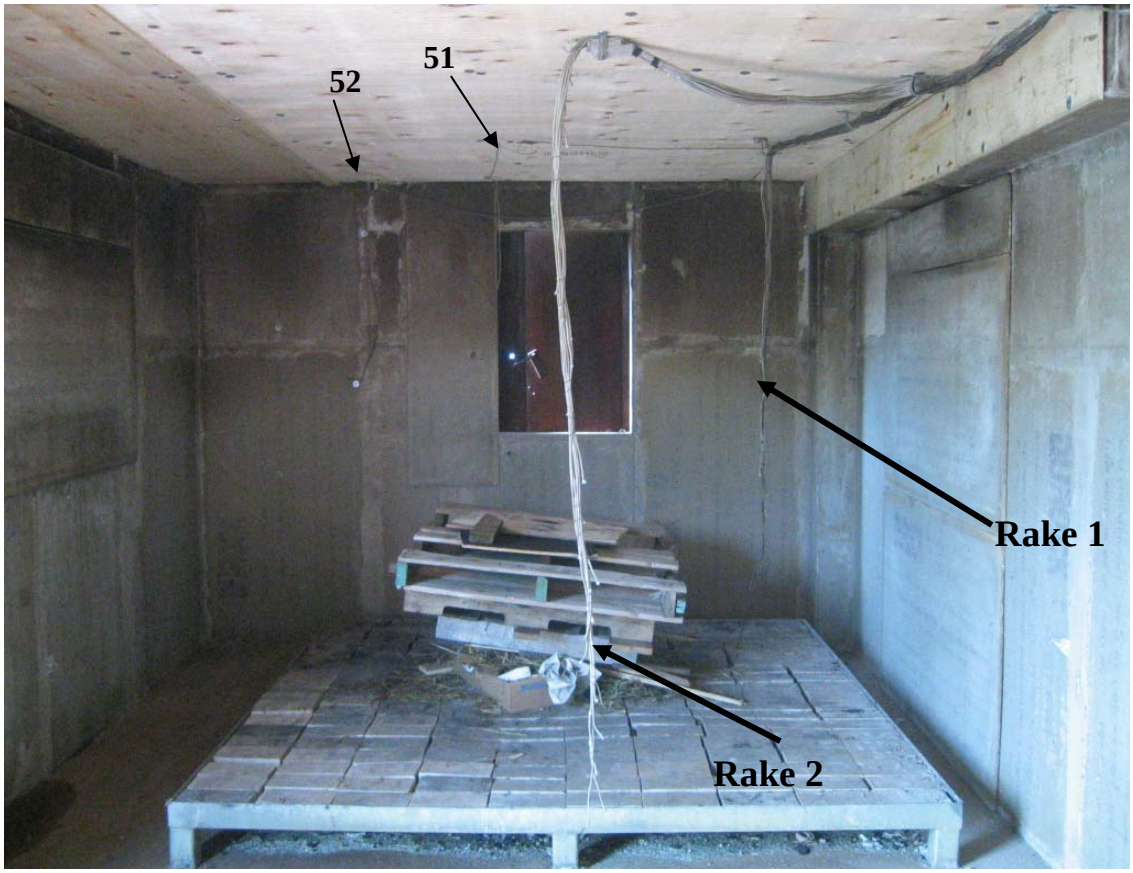

Figure 3.8: Positioning of Both Thermocouple Rakes around Burn Pad

Figure 3.9: Thermocouple Positions in Rake 2 and Ceiling Hangars

Figure 3.10: Thermocouples Positioned at Ceiling, 8" (203 mm) and 16" (406 mm) Down from Ceiling for Third and Fourth Experiments

Figure 3.11: Experimental Setup, June 9, 2004

Figure 3.12: Experimental Setup, September 30, 2004

Figure 3.13: Burn Room Interior Wall Construction, November 25, 2004

Figure 3.14: Fuel Load, November 25, 2004

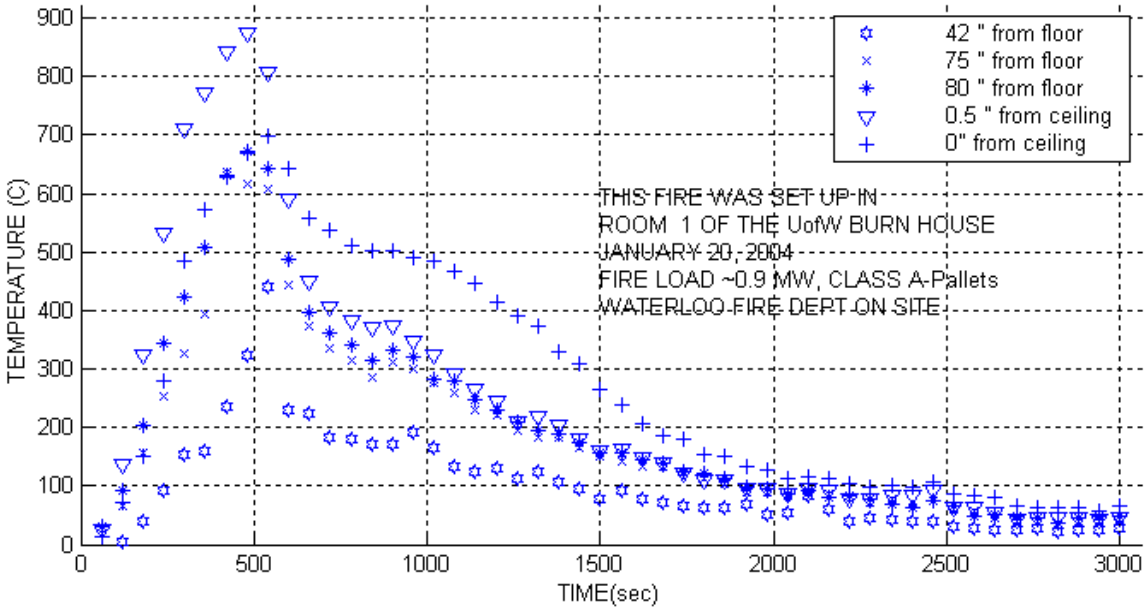

Figure 3.15: Temperature vs Time, Rake 1, January 20, 2004

Legend with SI Units

42” (1.067 m) from floor
75” (1.905 m) from floor
80” (2.032 m) from floor
0.5” (12.7 mm) from ceiling
0” (0 mm) from ceiling

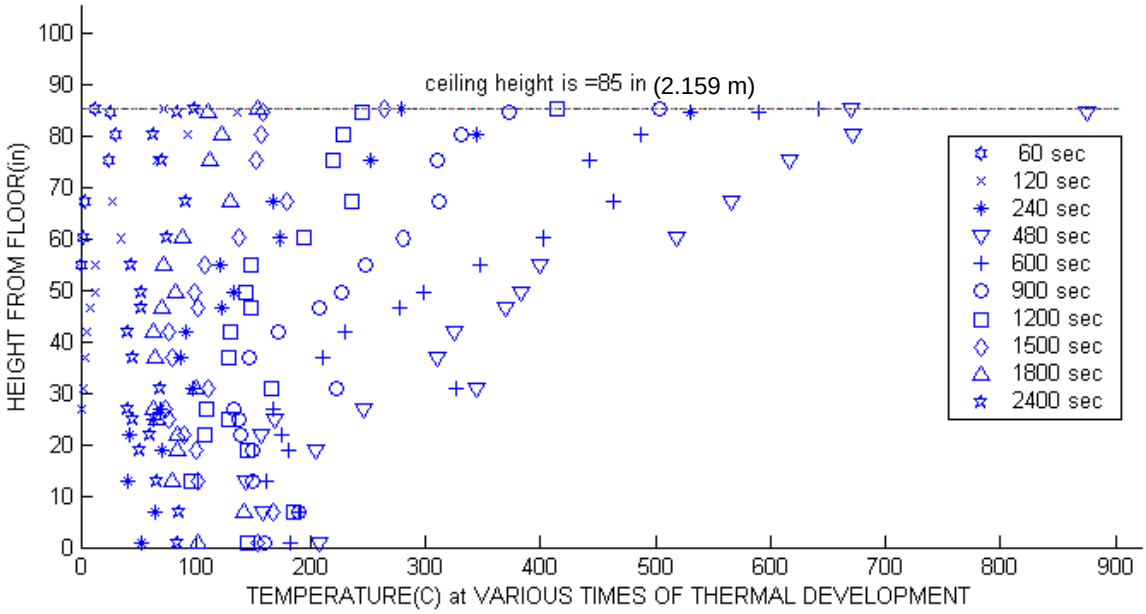

Figure 3.16: Temperature Stratification for Rake 1, January 20, 2004

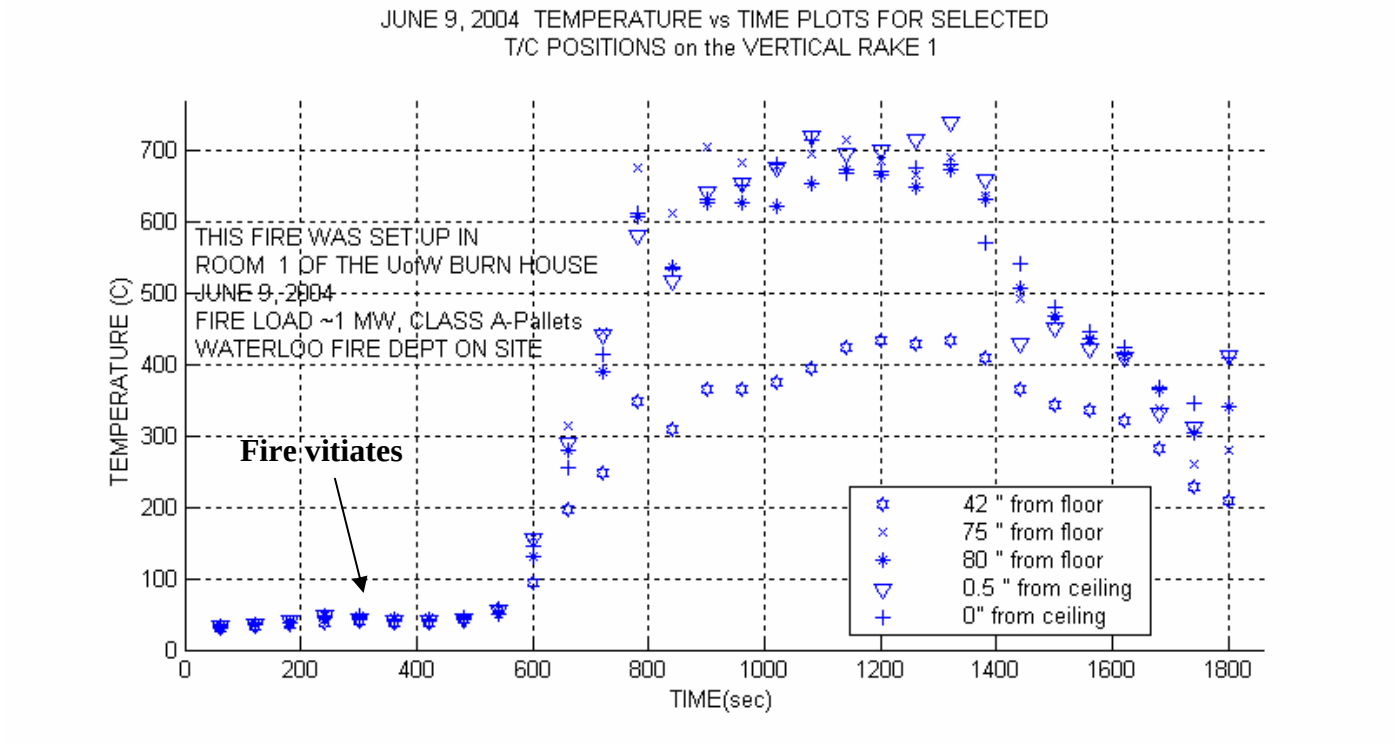

Figure 3.17: Temperature vs Time, Rake 1, June 9, 2004

Legend with SI Units

42” (1.067 m) from floor

75” (1.905 m) from floor

80” (2.032 m) from floor

0.5” (12.7 mm) from ceiling

0” (0 mm) from ceiling

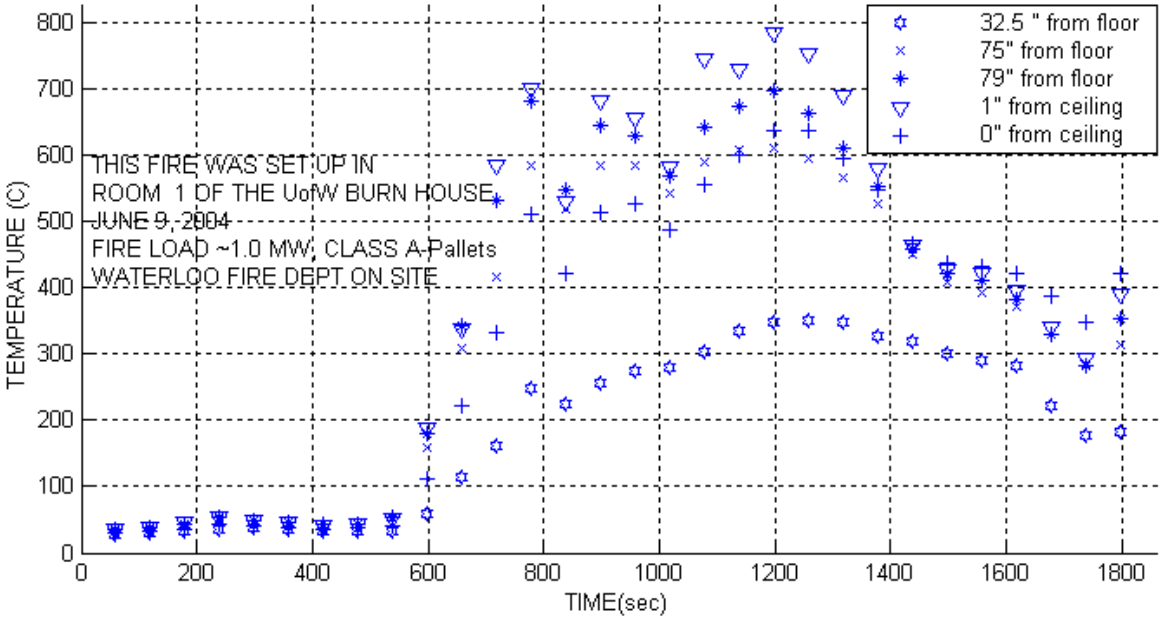

Figure 3.18: Temperature vs Time, Rake 2, June 9, 2004

Legend with SI Units

32.5” (0.826 m) from floor
75” (1.905 m) from floor
79” (2.007 m) from floor
1” (25.4 mm) from ceiling
0” (0 mm) from ceiling

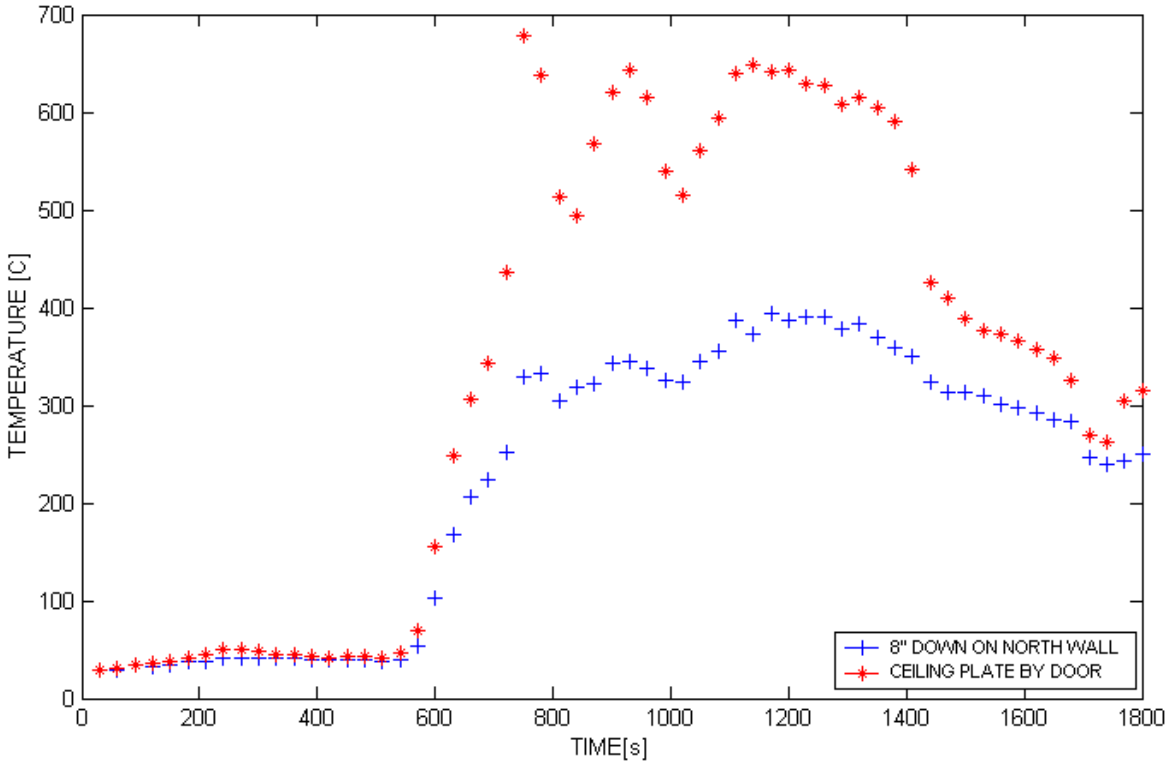

Figure 3.19: Temperature vs Time, Ceiling and North Wall Thermocouples

Legend with SI Units

8” (203 mm) DOWN ON NORTH WALL

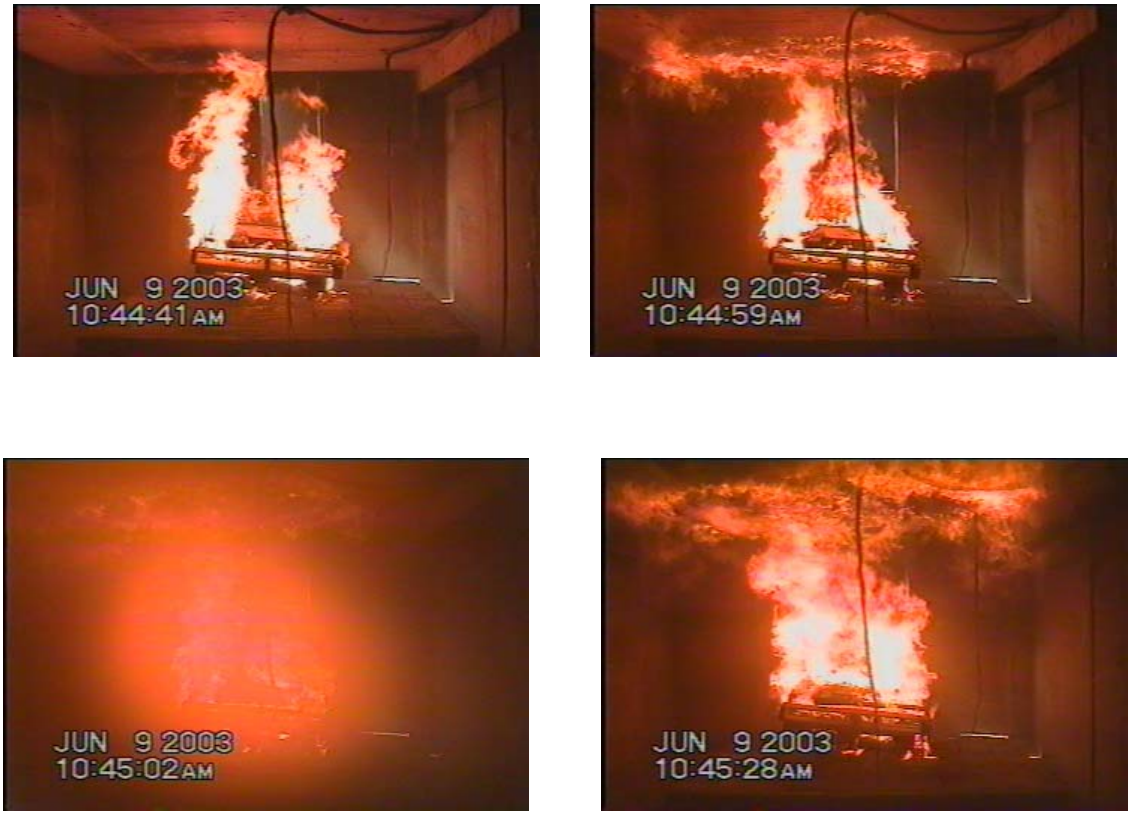

Figure 3.20: Digital Video Images of Fire, June 9, 2004

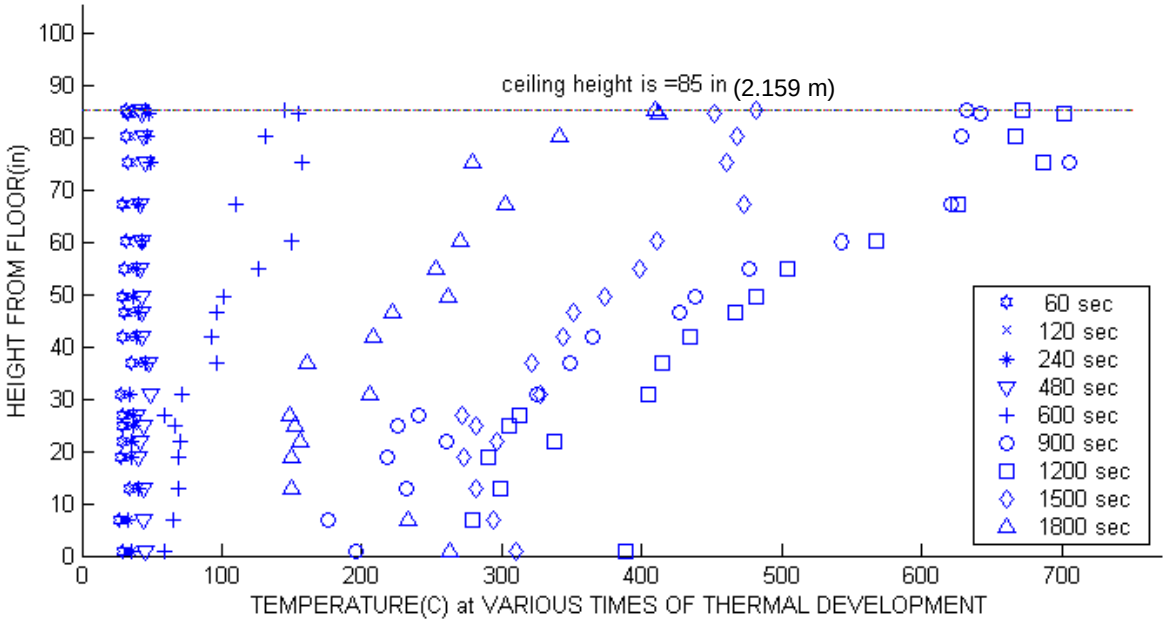

Figure 3.21: Temperature Stratification for Rake 1, June 9, 2004

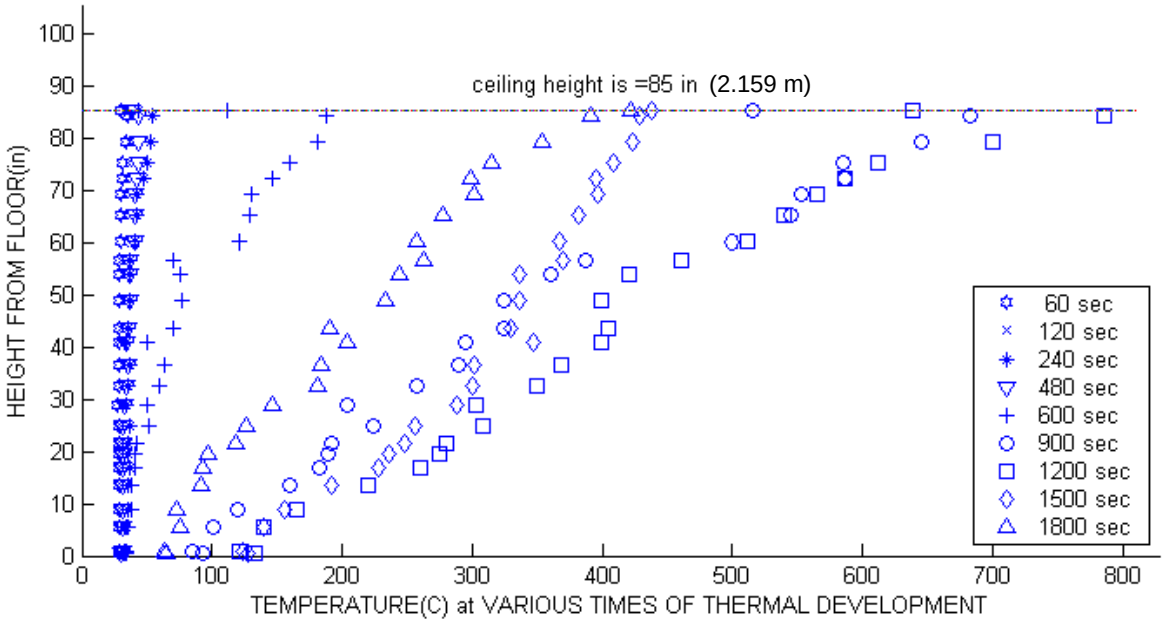

Figure 3.22**:** Temperature Stratification for Rake 2, June 9, 2004

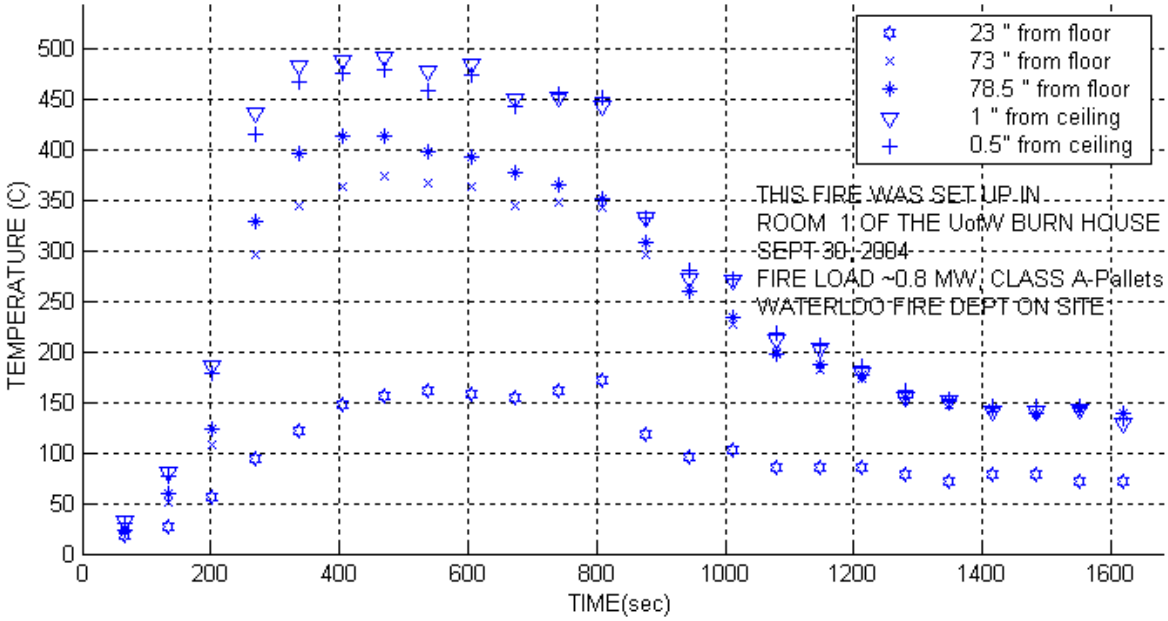

Figure 3.23: Temperature vs. Time, Rake 1, September 30, 2004

Legend with SI Units

23” (0.584 m) from floor
73” (1.854 m) from floor
78.5” (1.994m) from floor
1” (25.4 mm) from ceiling
0.5” (12.7 mm) from ceiling

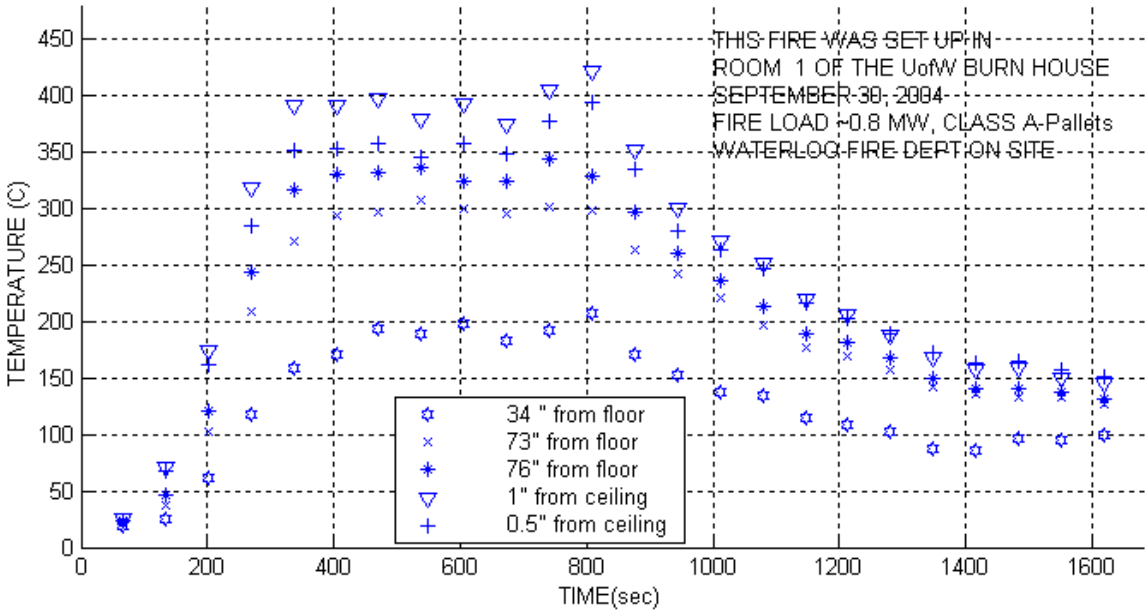

Figure 3.24: Temperature vs Time, Rake 2, September 30, 2004

Legend with SI Units

34” (0.864 m) from floor
73” (1.854 m) from floor
76” (1.930m) from floor
1” (25.4 mm) from ceiling
0.5” (12.7 mm) from ceiling

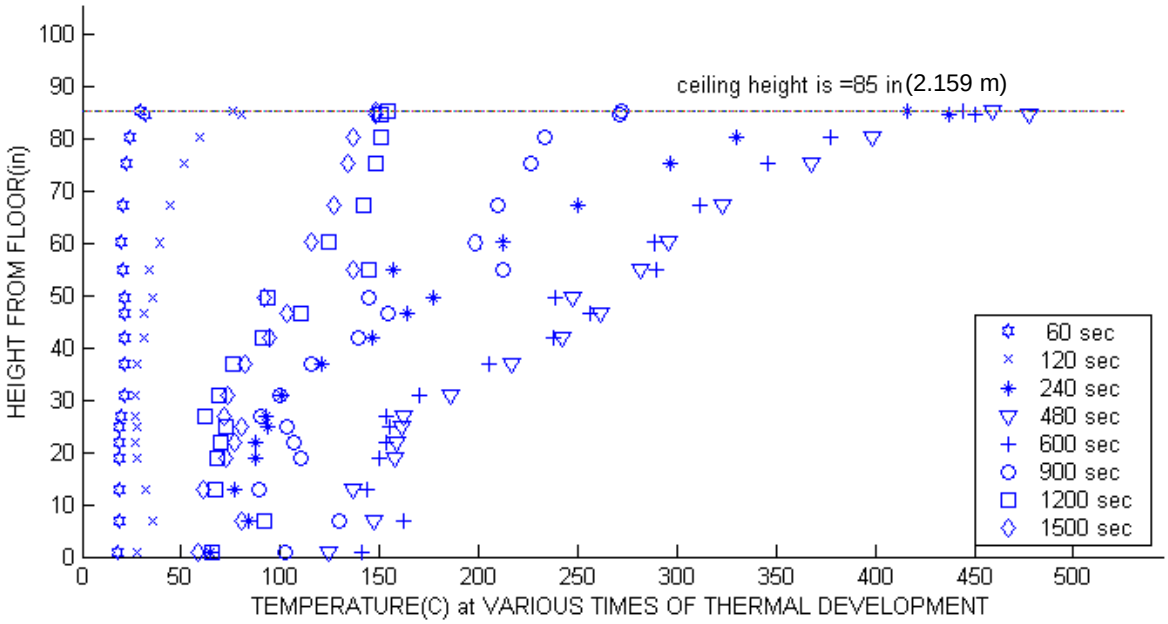

Figure 3.25: Temperature Stratification, Rake 1, September 30, 2004

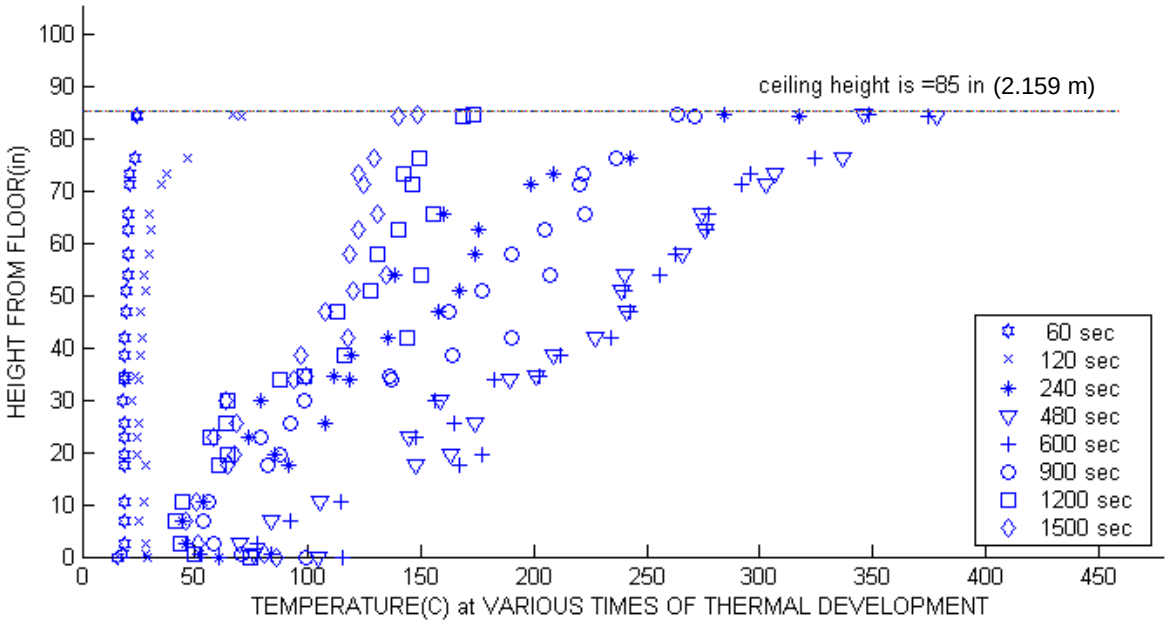

Figure 3.26: Temperature Stratification, Rake 2, September 30, 2004

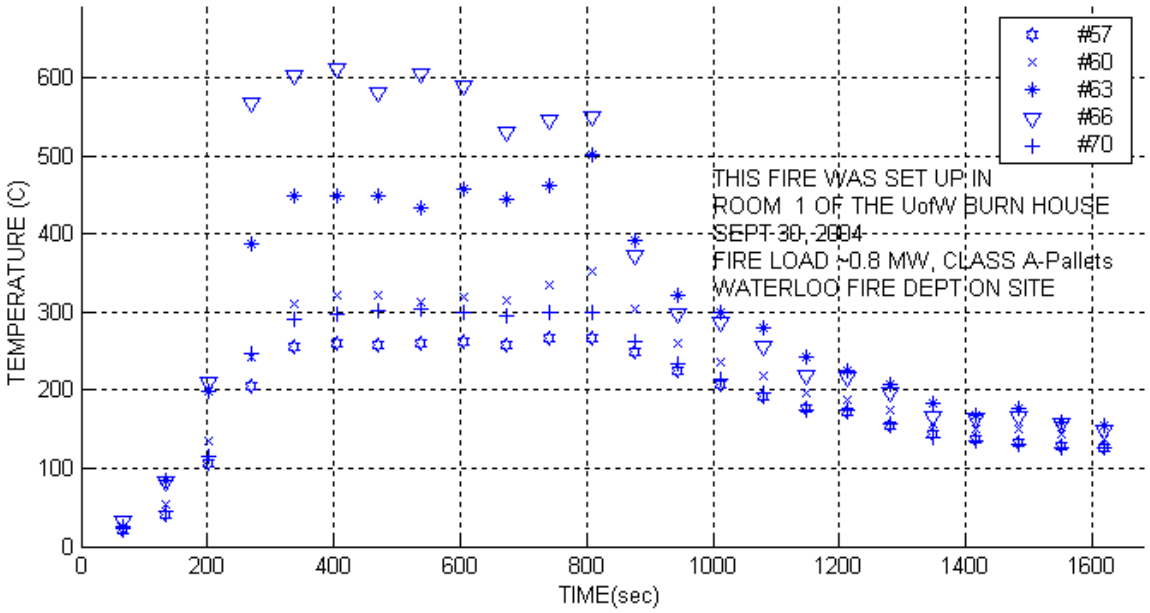

Figure 3.27: Temperature vs Time, Ceiling Thermocouples (Centre Plane), September 30, 2004

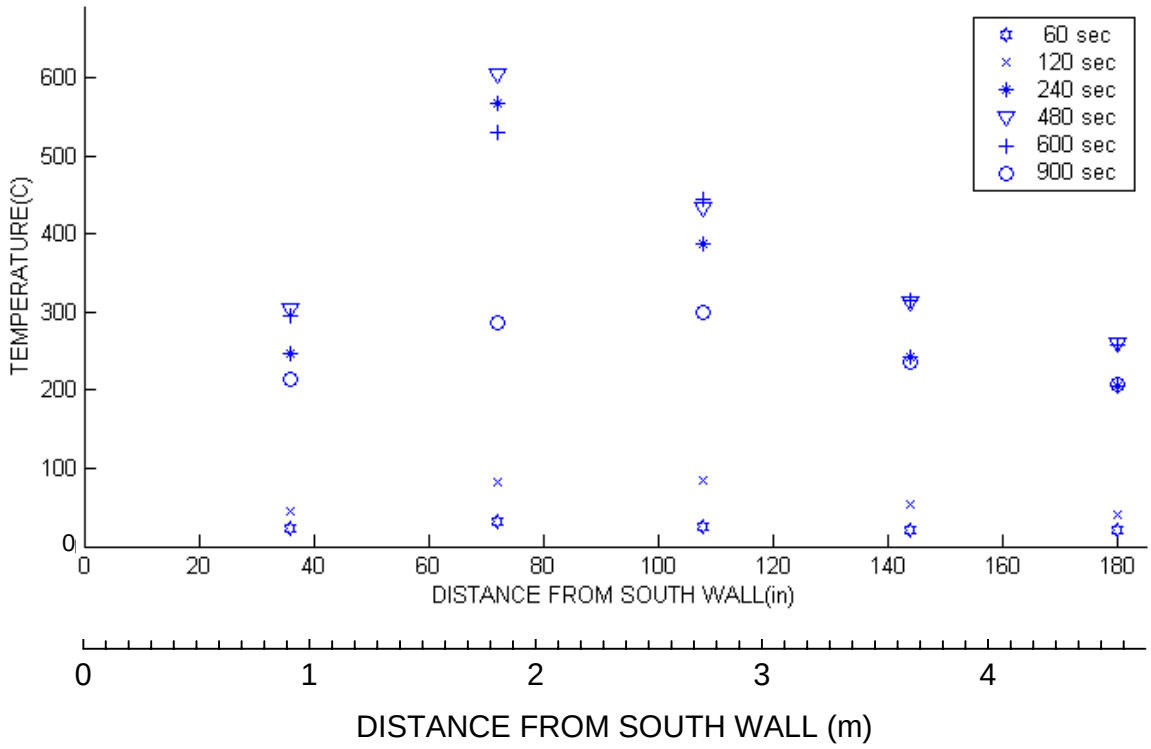

Figure 3.28: Temperature of Ceiling Thermocouples (Centre Plane), September 30, 2004

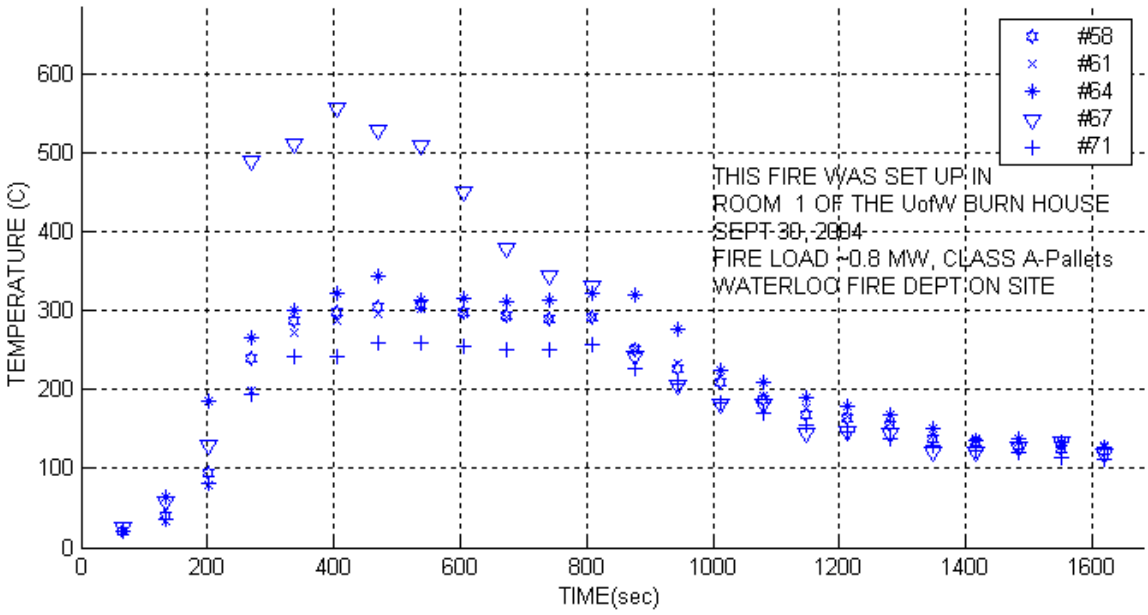

Figure 3.29: Temperature vs Time, Thermocouples 8" (203 mm) Below Ceiling, September 30, 2004

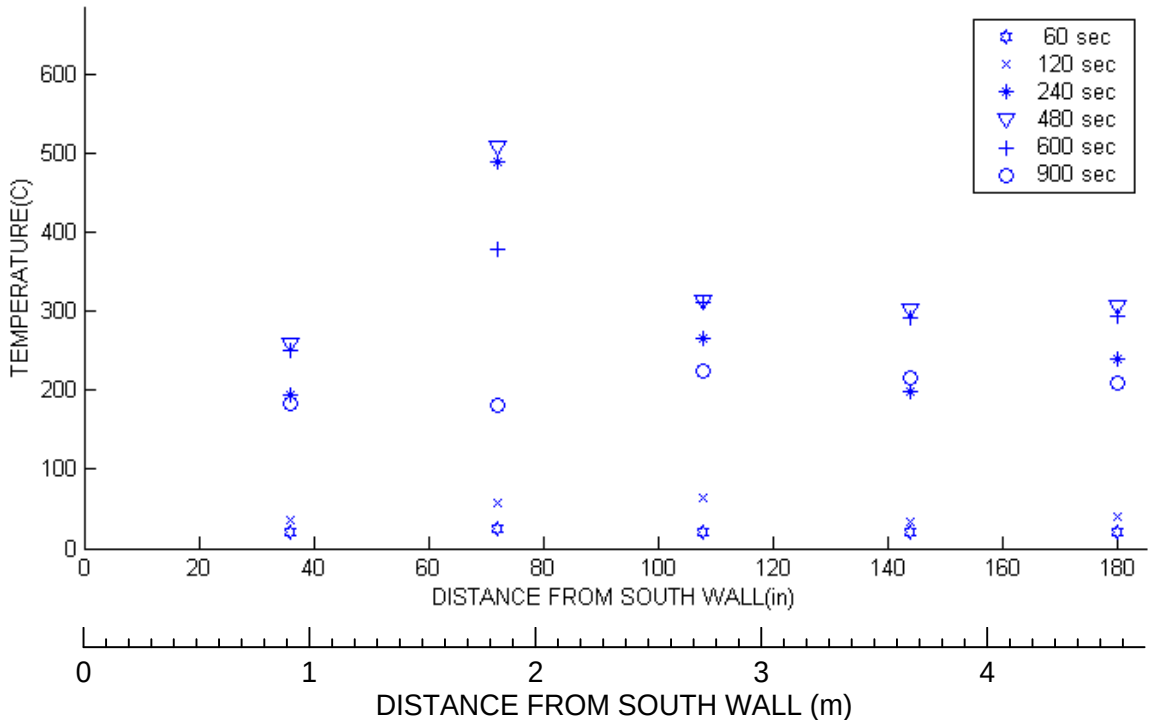

Figure 3.30: Temperature of Thermocouples 8" (203 mm) Below Ceiling, September 30, 2004

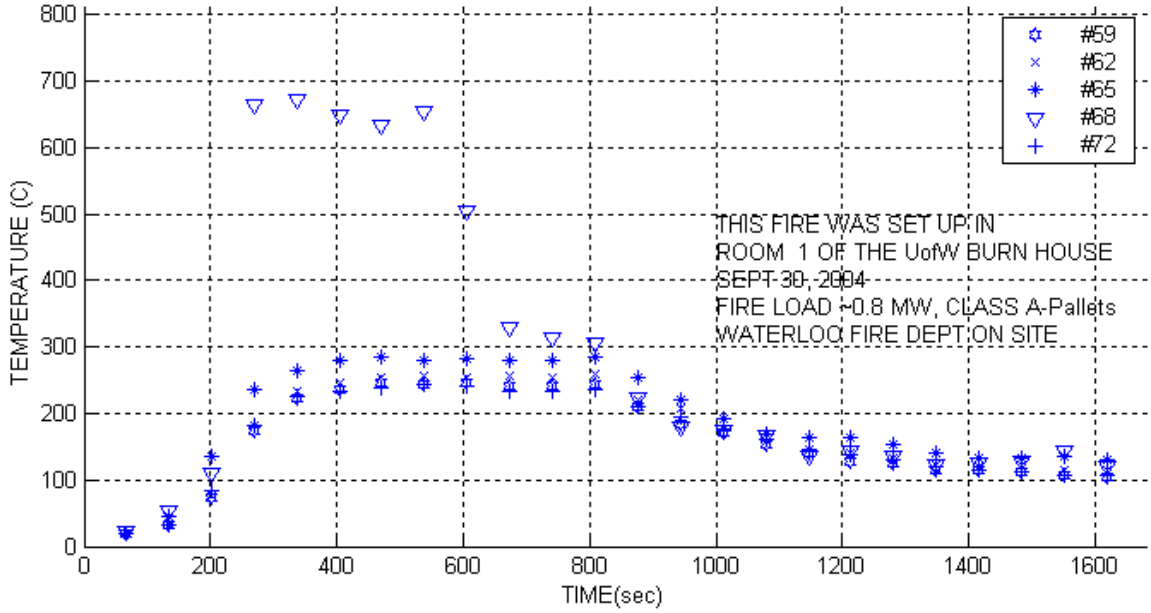

Figure 3.31: Temperature vs Time, Thermocouples 16" (406 mm) Below Ceiling, September 30, 2004

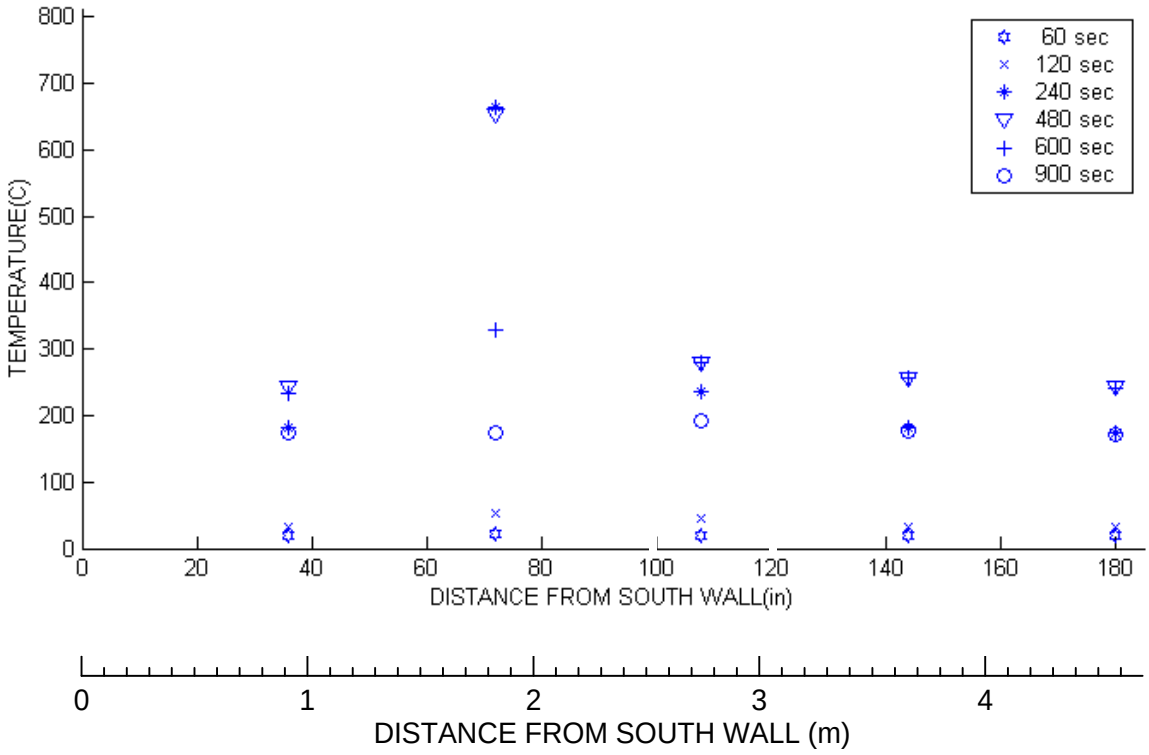

Figure 3.32: Temperature of Thermocouples 16" (406 mm) Below Ceiling, September 30, 2004

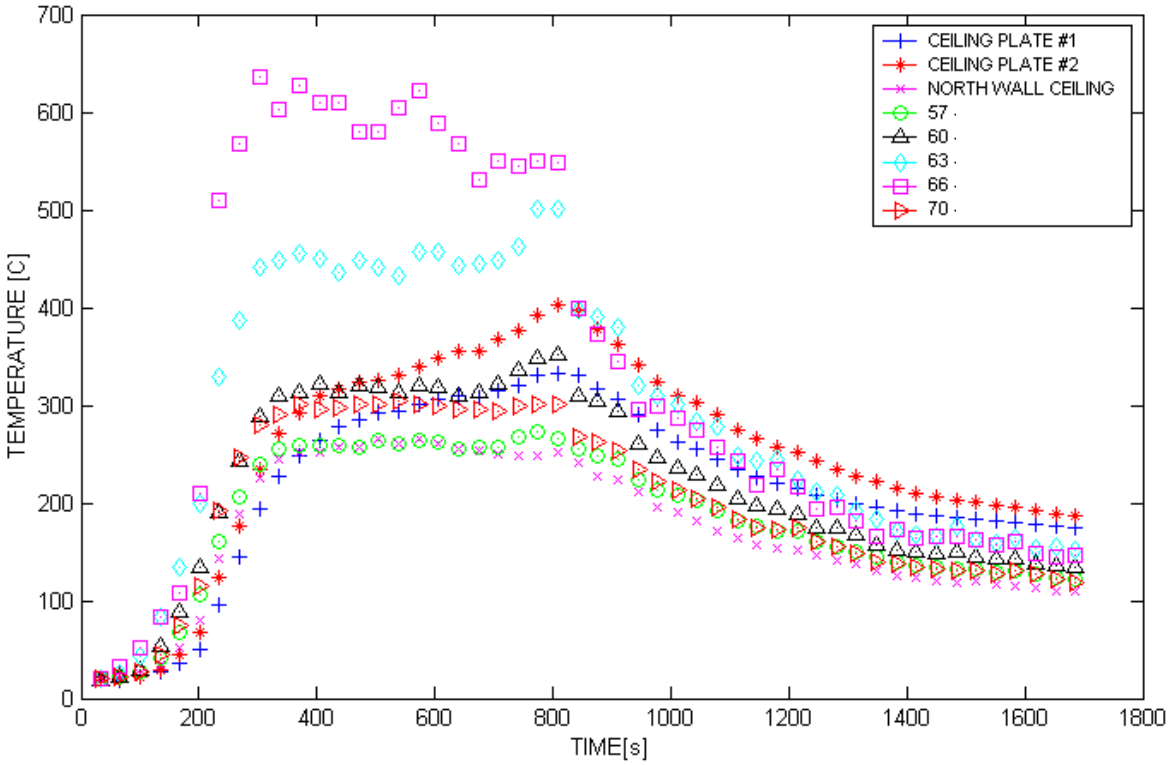

Figure 3.33: Temperature vs Time, All Ceiling Thermocouples, September 30, 2004

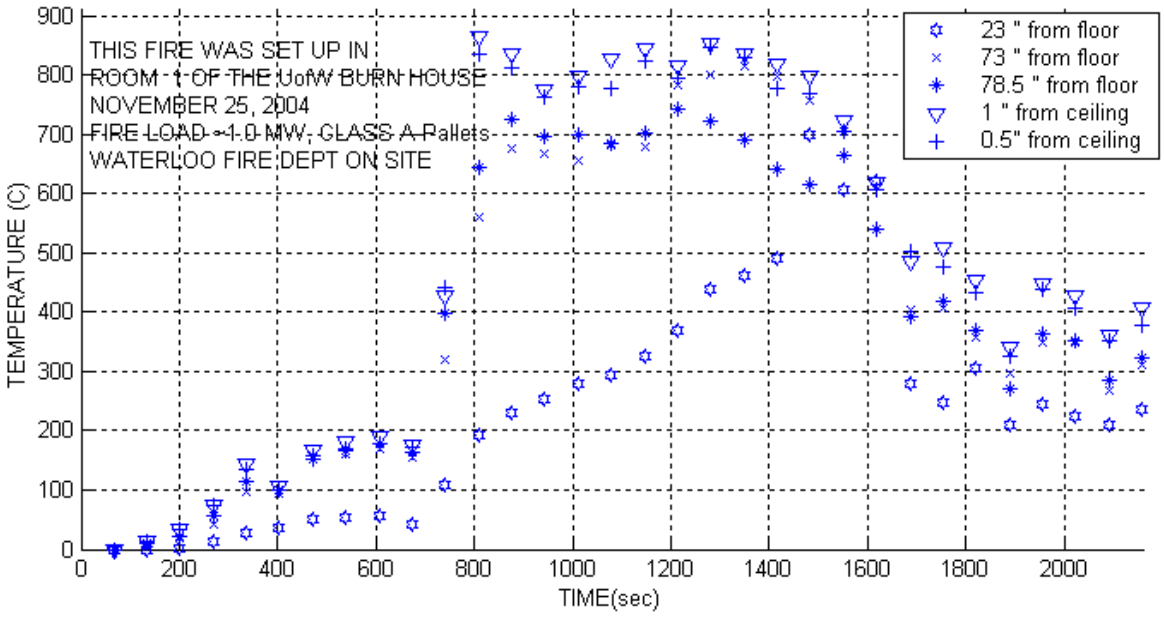

Figure 3.34: Temperature vs Time, Rake 1, November 25, 2004

Legend with SI Units

23” (0.584 m) from floor
73” (1.854 m) from floor
76.5” (1.943 m) from floor
1” (25.4 mm) from ceiling
0.5” (12.7 mm) from ceiling

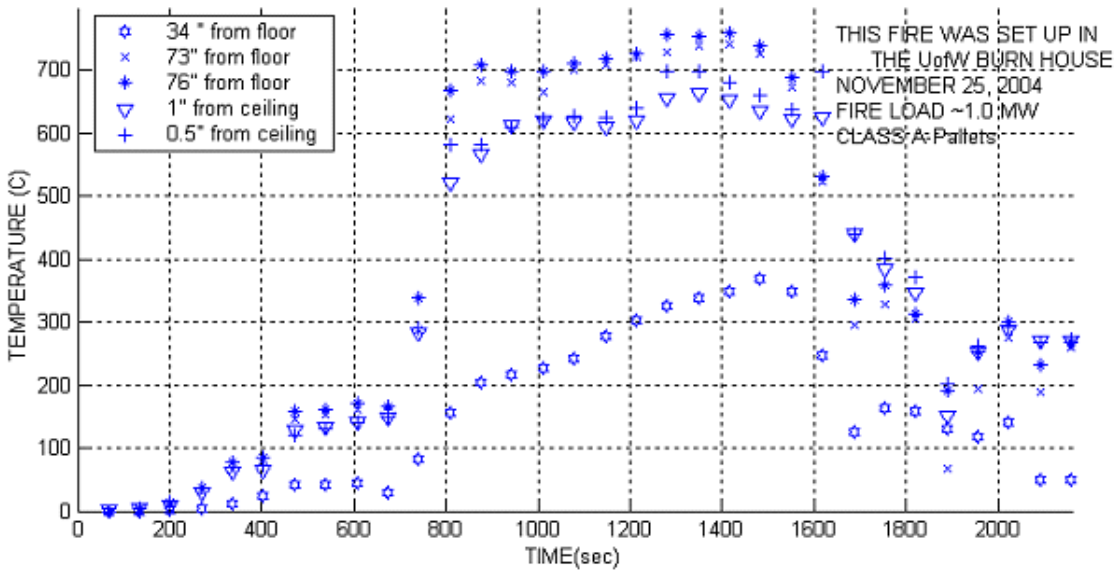

Figure 3.35: Temperature vs Time, Rake 2, November 25, 2004

Legend with SI Units

34” (0.864 m) from floor
73” (1.854 m) from floor
76” (1.930m) from floor
1” (25.4 mm) from ceiling
0.5” (12.7 mm) from ceiling

Figure 3.36: Digital Video Images of Fire, November 25, 2004

Figure 3.37: Fully Developed Fire - 1140 seconds, November 25, 2004

Figure 3.38: Onset of Decay - 1522 seconds, November 25, 2004

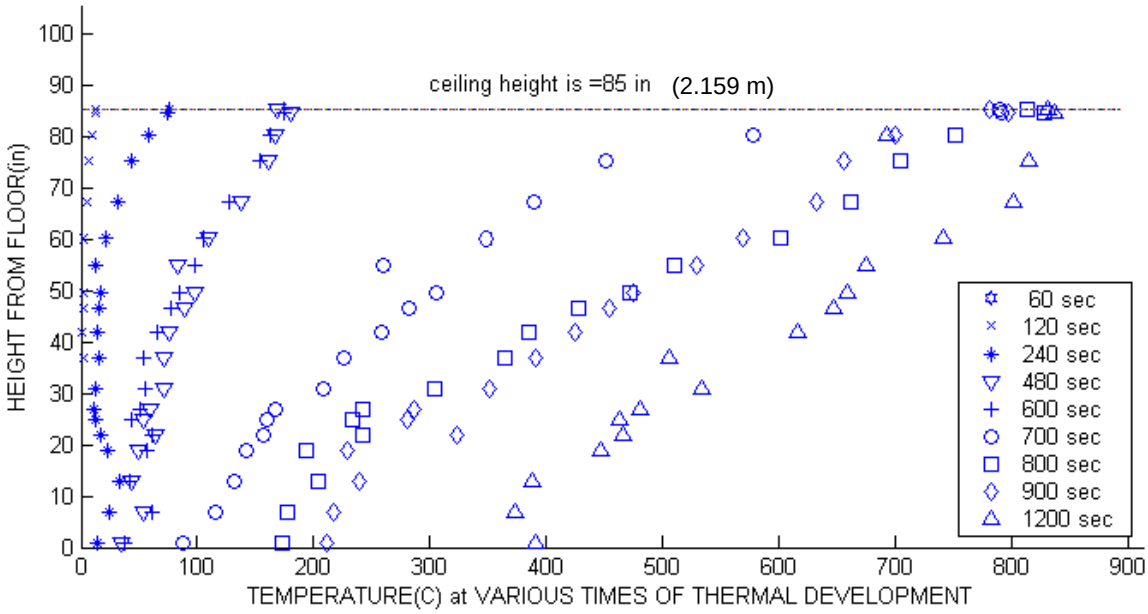

Figure 3.39: Temperature Stratification, Rake 1, November 25, 2004

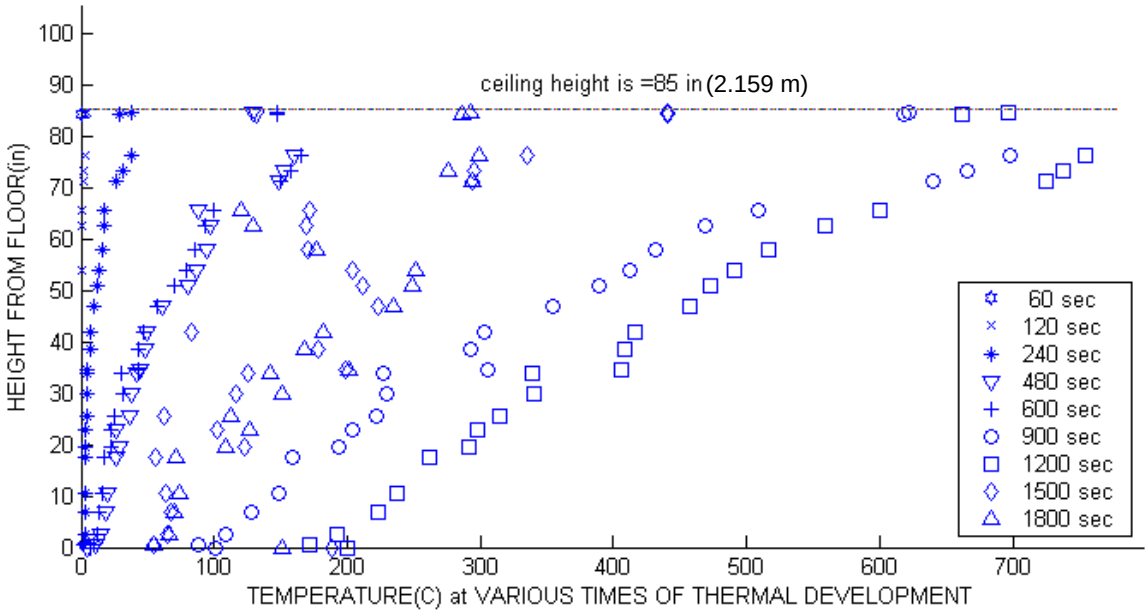

Figure 3.40: Temperature Stratification, Rake 2, November 25, 2004

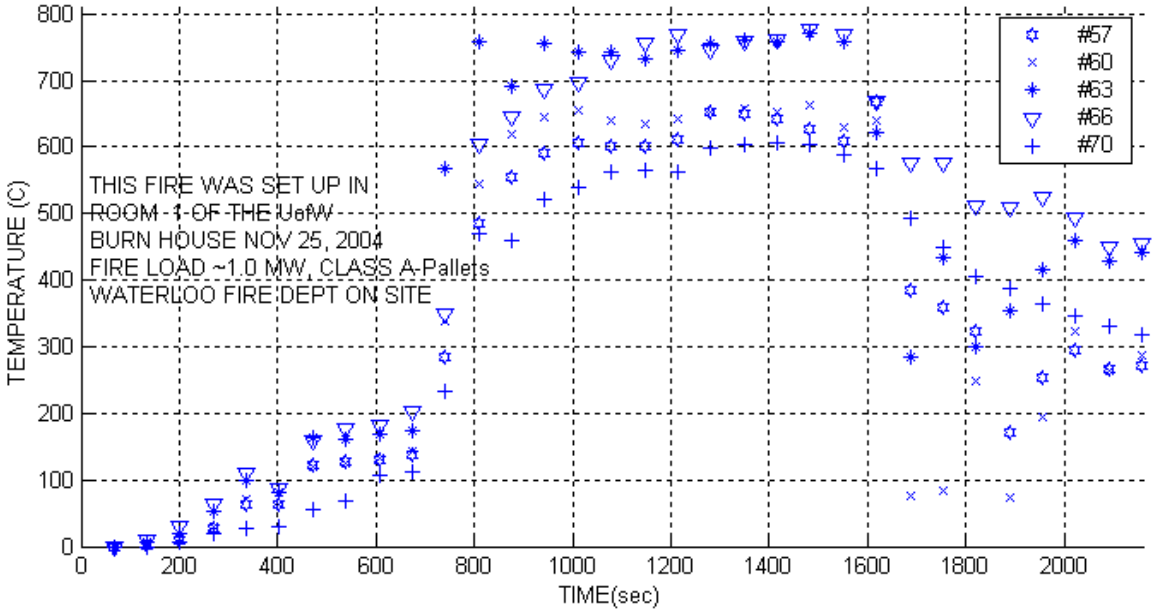

Figure 3.41: Temperature vs Time, Ceiling Thermocouples (Centre Plane), November 25, 2004

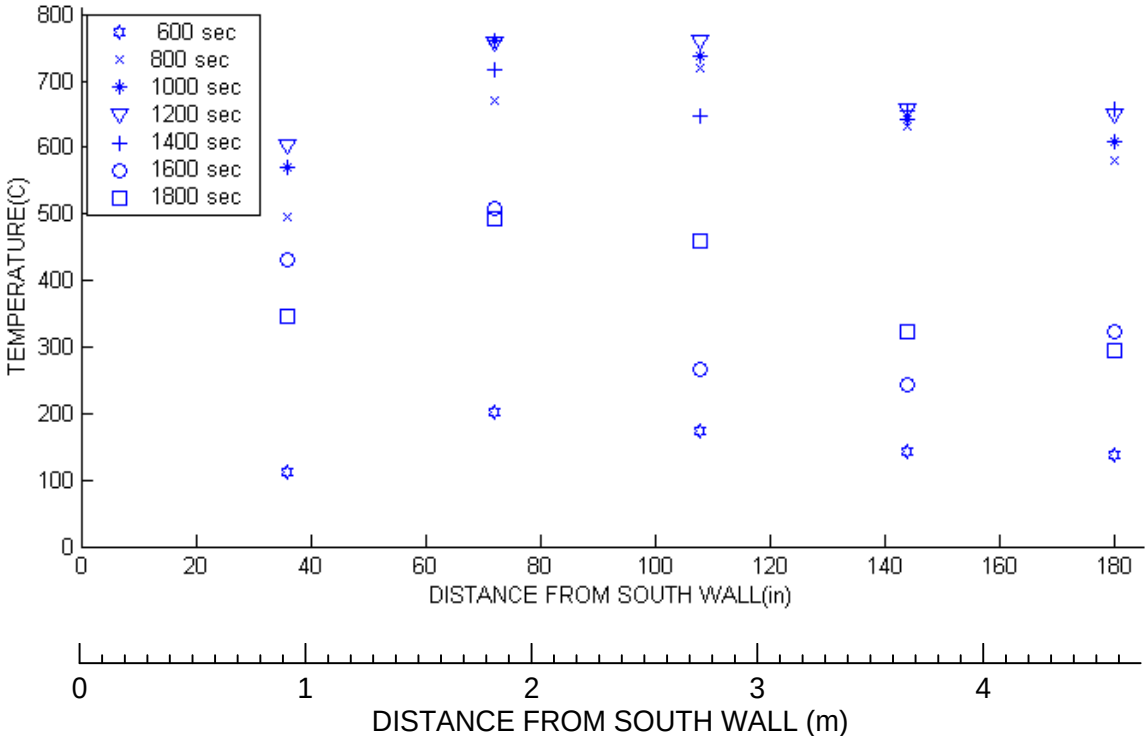

Figure 3.42: Temperature of Ceiling Thermocouples (Centre Plane), November 25, 2004

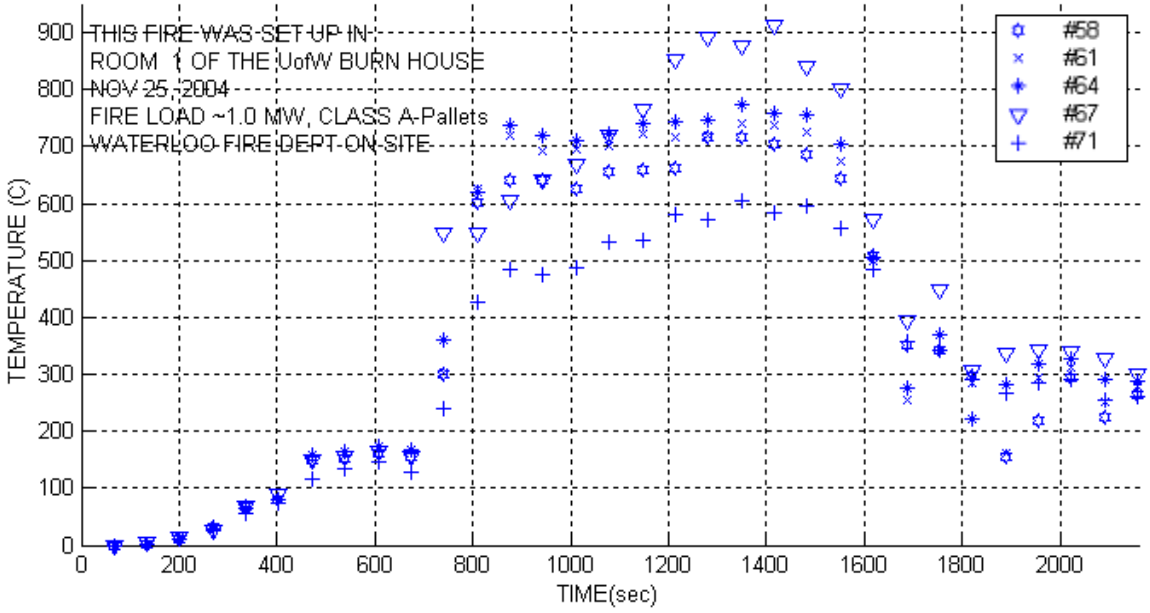

Figure 3.43: Temperature vs Time, Thermocouples 8" Below Ceiling, November 25, 2004

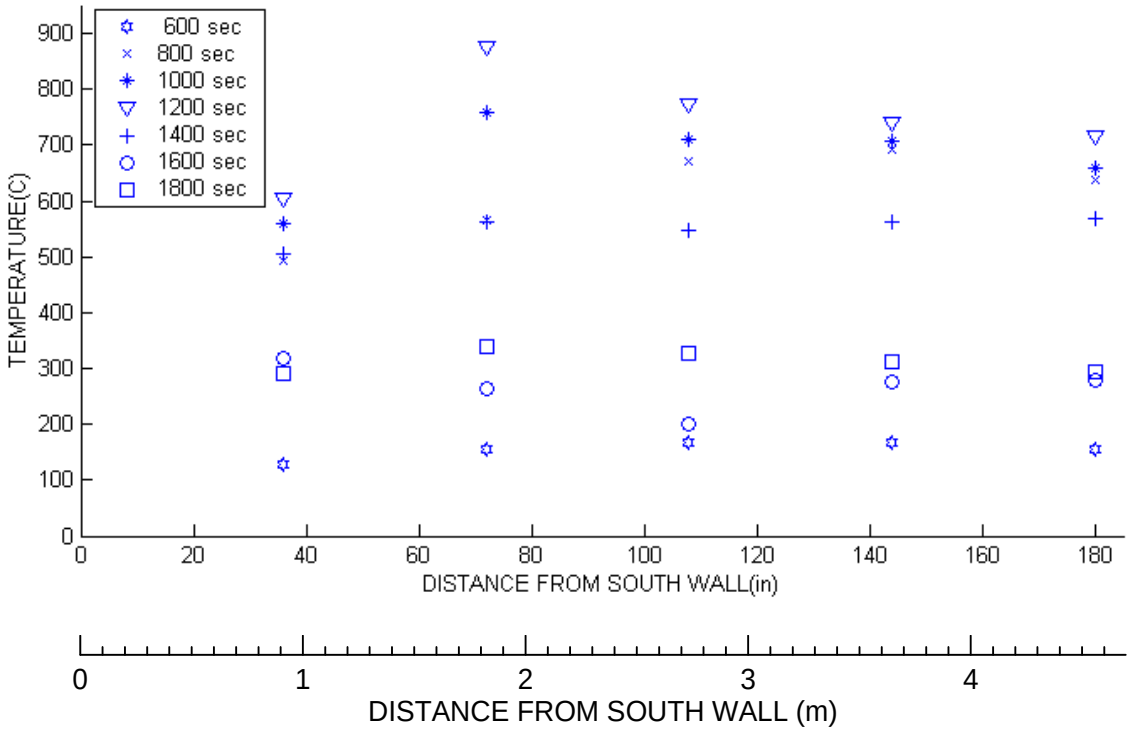

Figure 3.44: Temperature of Thermocouples 8" (203 mm) Below Ceiling, November 25, 2004

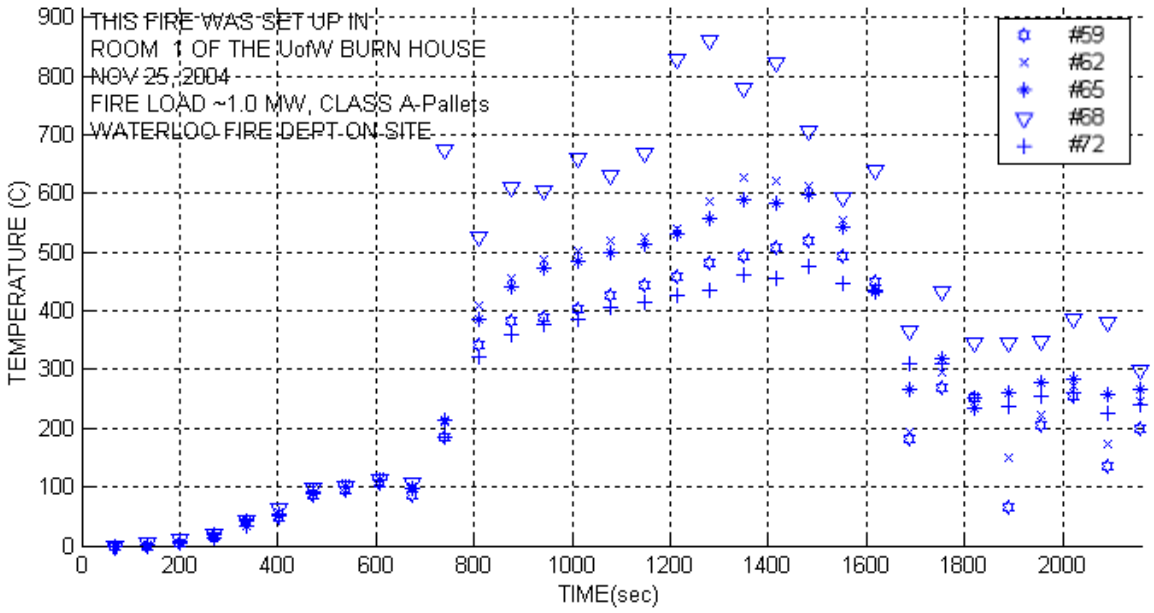

Figure 3.45: Temperature vs Time, Thermocouples 16" (406 mm) Below Ceiling, November 25, 2004

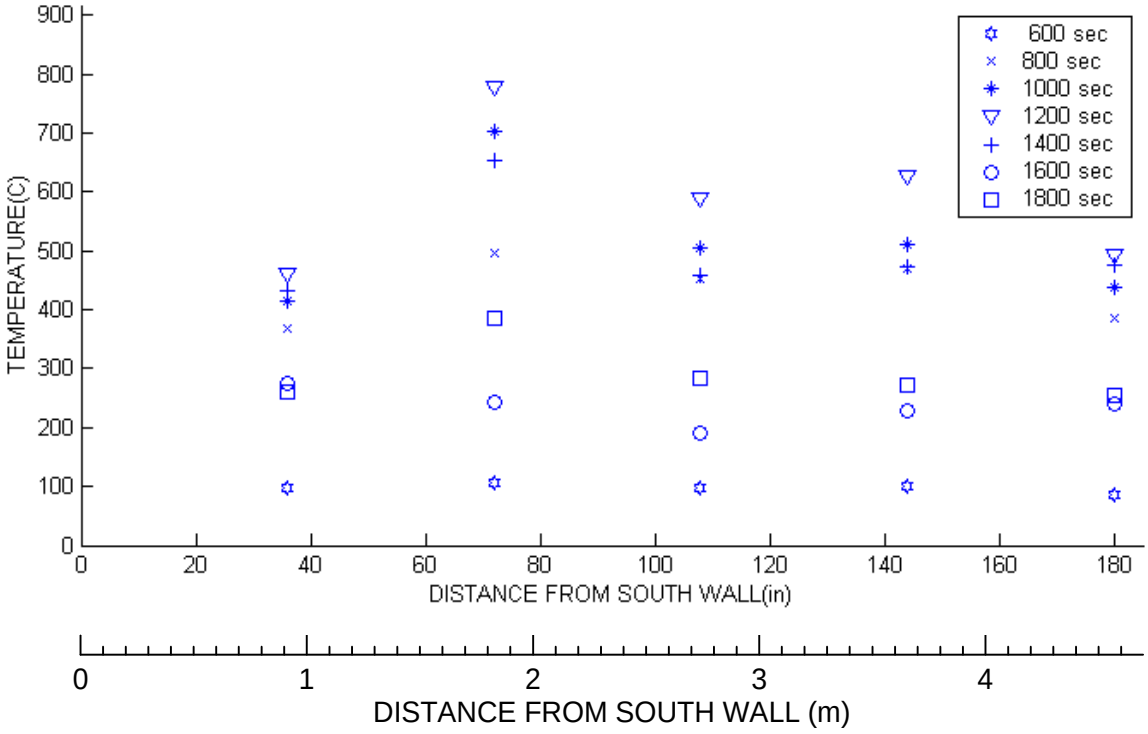

Figure 3.46: Temperature of Thermocouples 16" (406 mm) Below Ceiling, November 25, 2004

CHAPTER FOUR

Discussion of Experimental and CFAST Results

This chapter will provide a discussion of the results presented in Chapter 3. Sources of experimental error and uncertainty will be examined, followed by comparisons of data from the present Burn House experiments and from previous University of Waterloo fire studies as well as to CFAST predictions of the fire experiments. The purpose of these comparisons will be to identify key similarities between sets of experimental results, and demonstrate that the Burn House fire behaviour is similar to that of real structural fire experiments.

4.1 Discussion of Experimental Results

4.1.1 Systematic Errors

Time Response Error

When temperature measurements are made under non-steady-state conditions, it is important to determine the transient response of the measuring device. Measurement accuracy may be adversely affected by fluctuating air flow patterns [50]. In this case, thermocouples used to obtain temperature data will experience a *thermal lag*[18] at the junction (bead) when exposed to a temporal change of the environment. This transient response (or time constant) for a thermocouple bead can be estimated using the following equation [51]:

$$\tau = \frac{mc}{hA} \qquad [\text{s}] \qquad (4.1)$$

where h is the convection coefficient (W/m^2K) of the environment, c is the specific heat capacity of the bead (J/kgK), A is the surface area of the bead (m^2) and m is the mass of the bead (kg)given by:

$$m = \frac{4}{3}\rho\pi r^3 \qquad [\text{kg}] \qquad (4.2)$$

where ρ is the density (kg/m^3) of the thermocouple material.

[18] Thermal lag describes a material's transient (time) response when exposed to an unsteady environment. For example, a material with high thermal mass (high heat capacity and low conductivity) will have a high thermal lag.

The thermocouple wire used in these experiments was 0.02" (0.51 mm) in diameter with a bead diameter of approximately 60 to 80 μm. The density and specific heat capacity for these K-type thermocouples is 8610 kg/m^3 and 523 J/kg·K, respectively [52].

The convection coefficient for the thermocouple bead can be estimated using a correlation from Whitaker [53]:

$$h(\mathrm{Re}, T_g) = (2.0 + 10.4\sqrt{\mathrm{Re}} + 0.06\,\mathrm{Re}^{2/3})\,\mathrm{Pr}^{0.4} + (\frac{k_g}{d}) \cdot (\frac{\mu}{\mu_s}) \ \ [\mathrm{W/m^2K}] \qquad (4.3)$$

All properties are evaluated at the gas temperature (1100 K was used in this case), except for μ_s, which is evaluated at the surface temperature (300 K) of the thermocouple. The corresponding Reynolds number for the flow in the burn room was estimated using a low velocity (1m/s).

The resulting convection coefficient (h) for the thermocouple is approximately 2180.49 W/m^{2}K using an 80 μm bead diameter. Using this value, the time constant (time response) of the thermocouple is determined to be 0.0275 s (27.5 ms) from Equation 4.1, which is much less than the one second sampling rate set on the datalogger. A study on thermocouple compensation in combusting flows, performed at the University of Waterloo, shows that the time response of a K-type thermocouple bead of size 71 μm, in a low velocity flow (1 m/s) produced a time constant of approximately 30 ms when exposed to a temperature of 1100 K via laser heating [54]. Alternately, this same thermocouple produced a time constant of approximately 56 ms when exposed to a temperature of 1100 K via resistive heating methods. These results further support the argument that the time response of the thermocouple bead used in these experiments will be less than the one second sampling rate of the data acquisition system. The transient error will be reduced due to the faster response of the thermocouple than the system,

however, the flow temperatures in the room will still change more quickly than the thermocouple can respond, therefore the measured temperature will not be completely accurate. In addition, since the sampling rate of the datalogger has been shown to be slower than the time response of the thermocouples, this will mean that not all temperature measurements will be captured by the data acquisition system. The slower sampling rate will mean that that the time temperature curve will be shifted in time.

Figure 4.1 demonstrates the logged thermocouple response over the linear (fully developed) portion of Experiment #4. The mean of these temperatures (represented by the dashed green line) was plotted to help illustrate the relatively small magnitude and consistency of temperature fluctuations. With a sampling rate of 1 Hz, it is unlikely that a major event or sudden change in temperature occurred that was *not* captured by the instrumentation or at the very least, reflected in subsequent temperature measurements. In addition, the experiments presented in this work are concerned with temperature changes over relatively large time scales and any information not captured by the datalogger or due to the lagged response of the thermocouples will not have a significant impact on results. As a result, these errors will not be accounted for in this study. In the case where it would be necessary to resolve information over smaller time scales (i.e. heat fluxes), the error associated with the difference in sampling and measuring rates, as well as the time response of the thermocouples would have to be considered in more detail.

Although a detailed analysis of thermal lag for the Burn House experiments will not be given, it should be noted that thermal lag effects *can* be very substantial when larger diameter probes are used. Literature shows that there is a growing tendency for fire researchers to use larger diameter thermocouples where the effects of thermal lag must be accounted for [55].

Thermocouple Error Due to Radiative Heat Transfer

In general, thermocouple junction error can be determined with reasonable accuracy, however, the bigger problem lies in the fact that the junction temperature of a thermocouple is not necessarily equal to the surrounding (gas) temperature, which is usually the quantity that is to be determined. Differences between the junction and surroundings can be associated to a number of different sources, such as heat conduction, or reactions at the surface of the bead, however, radiative effects are a significant cause of thermocouple error and are of particular importance in fire studies [55].

While radiative effects *will* be significant, no attempt was made to determine this error or account for it in the results of these experiments, as it is not the primary focus of this work. In addition, this task is time consuming and complex and this topic is the focus of numerous on-going research activities at various institutions [32, 54, 55, 56]. A brief discussion of a study performed by researchers at NIST on the radiative error of bare-bead thermocouples will be offered to provide some indication of the level of radiative error that may be expected in the fire experiments presented in this study.

In 1999 researchers at NIST reported on a study of the radiative error of bare-bead, single and double shielded aspirated thermocouples in various compartment fire environments [56]. The purpose of the report was to describe idealized models of thermocouples, demonstrate the differing behaviour in the upper and lower layers, to describe ways of reducing radiative errors through use of aspirated thermocouples and to provide researchers with an approach for developing their own models for aspirated thermocouples [56].

The experiments were performed in a 40% scale model (38 in (0.97 m) x 38 in (0.97 m) x 57.4 in (1.46 m)) similar to the ISO Standard Enclosure for Full Scale Room

Rests of Surface Products. Heptane and natural gas fires were used producing heat release rates between 200 kW and 800 kW, with the heptane fires achieving flashover. As part of the study, idealized models of the relevant heat transfer processes for bare bead thermocouples were developed. The energy balance used for the bare thermocouple bead with no shields or aspiration was:

$$T_b^4[\varepsilon_b\sigma] + T_b[h_{bU}] - [\varepsilon_b\sigma T_\infty^{\ 4} + h_{bU}T_g] = 0 \qquad (4.4)$$

Figure 4.2 shows the calculated responses for 0.06" (1.52 mm) diameter bare bead thermocouples. The calculated behaviours are qualitatively similar to those observed experimentally in the NIST study [56]. The figure demonstrates that the thermocouple bead behaves differently in the upper and lower layer of a room fire. In the upper layer, the percent error for a given gas temperature is relatively insensitive to the temperature of the surroundings decreasing gradually to zero as T∞ approaches Tg. In this region, the percent error increases with increasing Tg. Overall, the error is less than 25% until T∞ approaches Tg. In contrast, in the lower layer, the percent error is a strong function of both Tg and T∞, increasing more and more rapidly with increasing T∞ when the latter value is relatively high. In this region, the percent error decreases with increasing Tg. The most extreme errors occur in the lower layer when Tg is at its lowest assumed value (300 K) and T∞ is at its highest (1400 K), which would most likely be encountered during a fully involved room fire [56].

From this information, it can be assumed that the degree of error associated with the temperature measurements will vary throughout the course of Experiment #4 and cannot be determined accurately from this information. The error will likely be smallest for upper layer measurements where gas temperatures are generally greater than the surroundings and greatest in the lower layer during full room involvement.

In order to provide a sample estimate of the radiative error for the thermocouples used in this work, it will be assumed that T∞ can be approximated as the temperature observed by the thermocouple located half way up the south wall for Experiment #4 (#56, Figure 3.7). At its maximum, this thermocouple reached approximately 436 ºC (~709K) at 1192 seconds into the fire. This time occurs during fully developed room conditions. The maximum upper layer gas temperature (Tg) measurement was 842ºC (1115K) at this same time, directly above the fire, 8" (203 mm) below the ceiling. Using these values with Figure 4.1, the resulting percent error in temperature measurements will be small. Conversely, the minimum lower layer gas temperature measurement was 152ºC (425K) at this time, resulting in an error of approximately 20% as shown in Figure 4.2.

In addition to the aforementioned, thermocouple error can arise as a result of the effects of aging. Aging can cause thermocouple accuracy to vary, especially after prolonged exposure to temperatures at the extremities of their useful operating range [55]. Improper storage and handling of thermocouples may also cause twisting of the wires which can lead to short circuiting and thus, erroneous measurements. Prior to Experiment #1 the Burn House was instrumented with a rake (Rake 1) comprised of thermocouple wire that had been used in previous fire studies. Some frayed areas were observed on the thermocouple sheathing. As discussed in Chapter 3, the results from Experiment #1 showed some skewed temperature measurements which may have been a result of the poor condition of the wire. New thermocouple wire was purchased and used to instrument another rake (Rake 2) and the rest of the Burn House for subsequent experiments.

4.1.2 Random Error: Experimental Uncertainty and Confidence Interval

An estimate of the experimental uncertainty for the steady-state temperature measurements in this study was made using a sample of the first 70 data points recorded for thermocouples on Rake 2 in Experiment #4. As previously mentioned, the data

acquisition system was started once radio communication from the burn room indicated that the fire was about to be ignited. Assuming the fire had been started within the 70 second sampling time interval, it is likely that a portion of the initial temperature measurements will represent the ambient temperature just before the fire was actually started. The remaining measurements in this sample were also assumed to still be representative of the ambient temperature conditions, as effects of the fire would likely not have propagated throughout the burn room and increased early temperature measurements.

The standard deviation of the sample was calculated by:

$$\sigma = (\frac{1}{n}\sum_{i=1}^{n}(x_i - \bar{x}^2)^{\frac{1}{2}} \qquad (4.5)$$

where n is the size of the sample, (in this case n = 70), $\bar{x}$ is the arithmetic mean of the sample and x_i represents each temperature measurement in the sample from 1 to n = 70.

The upper and lower bound of the confidence interval[19] was calculated using a 95% confidence level for each of the temperature measurements, and is given by:

$$\pm 1.96\frac{\sigma}{\sqrt{n}} \qquad (4.6)$$

[19] The confidence interval represents a range of values around the sample mean that will include the true mean.

The results of these calculations are shown in the following table.

Table 4.1: Mean, Standard Deviation and Confidence Interval for sample Measurements on Rake 2, Experiment #4

Thermocouple #	Distance from Ceiling (inches)	Mean (ºC)	Standard Deviation	Confidence Interval
1	85	-2.294	0.042	0.010
2	84.5	-2.290	0.061	0.014
3	82	-2.268	0.058	0.014
4	78	-2.228	0.075	0.018
5	74	-2.165	0.042	0.010
6	70	-2.151	0.080	0.019
7	67	-2.137	0.078	0.018
8	65	-1.963	0.047	0.011
9	62	-2.710	0.102	0.024
10	59	-2.809	0.094	0.022
11	55	-2.667	0.102	0.024
12	50	-2.623	0.101	0.024
13	46	-2.552	0.131	0.031
14	43	-2.440	0.122	0.029
15	38	-2.440	0.119	0.028
16	34	-2.354	0.156	0.036
17	31	-1.937	0.152	0.036
18	27	-1.861	0.106	0.025
19	22	-1.788	0.116	0.027
20	19	-1.718	0.112	0.026
21	14	-1.583	0.073	0.017
22	12	-1.420	0.127	0.030
23	9	-0.741	0.102	0.024
24	1	0.974	0.514	0.120
25	0	0.091	0.169	0.040

Distance from Ceiling (m) for Thermocouples 1 - 25: 2.159, 2.146, 2.083, 1.981, 1.880, 1.778, 1.702, 1.651, 1.575, 1.499, 1.397, 1.270, 1.168, 1.092, 0.965, 0.864, 0.787, 0.686, 0.559, 0.483, 0.356, 0.229, 0.00254, 0.

As shown in Table 4.1, the greatest standard deviation is 0.514, calculated for thermocouple #24, just below the ceiling. Observation of the corresponding confidence interval shows that a temperature measurement on this particular thermocouple will be 0.974 +/- 0.12 ºC with a 95% confidence level. This result appears to be significantly greater than for the other thermocouples and could likely be due to a faulty thermocouple. The remaining temperature measurements have standard deviations in the range 0.042 to 0.169, with corresponding confidence levels of 0.01 to 0.04, respectively. If it is assumed that these thermocouples are functioning properly, then

for any given steady state temperature measurement there is a 95% certainty that the actual temperature is within four one-hundredths of a degree from this value.

4.1.3 Experimental Comparisons

The purpose of this section will be to present experimental data from previous University of Waterloo fire studies in comparison to the Burn House experimental data. These comparisons will be made to identify time-temperature curve similarities, therefore illustrating the similarities between *real* structural fires and Burn House fires.

Waterloo House Fire Tests vs. Burn House Experiments

Figures 4.3a and 4.3b illustrates data that was provided from 6 of the 9 Waterloo House Fire Tests performed in a residential structure on April 15, 2001 and Burn House experimental data, respectively. Varying sizes of Class A fuels were used for the Waterloo experiments, the largest of which consisted of approximately 5 to 6 wooden pallets. Fires were performed sequentially (Tests 1 – 9); each fire was suppressed, recharged, and then the next fire test was performed. The suppression of the fuel load after each test meant that from the second fire test onward, the room and ambient conditions were wet. In addition, a burn-through on the window during the second test altered the ventilation in the room. The effects of a wet and changing ventilation situation are unknown but could potentially affect the consistency of results from test to test, especially in the initial growth phase. Although an attempt was made to reproduce a series of data during experimentation, Figure 4.3a illustrates the level of variation in time-temperature curves for the Waterloo House Fire Tests.

Comparison of Figures 4.3a and 4.3b show that Waterloo House Fire Test #8 and Burn House Experiment #3 appear to have had similar fire loads based on the peak

temperatures achieved at the end of the growth phase (375 seconds) in addition to the extent (duration) of their growth phases. The data from the growth region of these fires (from ignition, t = 0, to 375 seconds) was re-plotted as shown in Figure 4.3. A least squares quadratic curve was fit to each set of data to illustrate how closely these regions resembled a t-squared[20] growth pattern. The R-squared (R^2) value on the plot is an indicator from 0 to 1 (also known as the correlation coefficient) that reveals how closely the estimated values for the curve fit correspond to the actual data. A curve fit is most accurate when its R-squared value is at or near 1. The R-squared value is calculated using the following equations:

$$R^2 = 1 - \frac{SSE}{SST} \qquad (4.7)$$

$$SSE = \sum (Y_i - \hat{Y}_i)^2 \qquad (4.8)$$

$$SST = (\sum Y_i^2) - \frac{(\sum Y_i)^2}{n} \qquad (4.9)$$

The R-squared values (Waterloo House Fire #8: 0.9841, Experiment #3: 0.9690) in Figure 4.4 show that the quadratic curves fit the experimental data quite well(R=1.0 is a perfect fit) which indicates that the growth phase can be approximated as a function of time, squared, typical of structural (compartment) fire behaviour. As well, Experiment #3 shows relatively steady temperatures were achieved throughout the fully developed stage of the fire which is again, typical of compartment fire behaviour.

[20] As discussed in Chapter 2, compartment fire growth can generally be approximated to having a parabolic growth rate, called a t-squared fire.

Observation of Figures 4.3a and 4.3b once again, shows that Waterloo House Fire Test #1 and Burn House Experiment #4 appear to have similar fire growth rates and peak fire temperatures, indicating that they may have had comparable fuel loads. The growth region for these experiments was re-plotted in Figure 4.5. Observation of the growth phase for Waterloo House Fire Test #1 shows that fire temperatures peaked at approximately 210 seconds, and again at approximately 360 seconds, after a brief drop in temperature. Detailed information of burn room observations for Waterloo House Fire Test #1 was not provided and therefore it is unknown what event may have caused this 'dip' in temperature at 210 seconds;however it may have been caused by early suppression or ventilation effects. This event was omitted from the comparison to Burn House Experiment #4 in Figure 4.5 by excluding data past 210 seconds. The duration of the growth stage for Experiment #4 was estimated from 600 seconds to 830 seconds and from ignition (t = 0) to 210 seconds for Waterloo House Fire Test #1.

The R-squared values displayed in Figure 4.5 (Waterloo House Fire #1: 0.9504, Experiment #4: 0.9939) indicate that the growth regions for both fires can be well approximated by t-squared curves. Burn House Experiment #4 shows an exceptionally good fit to the least squares quadratic curve.

HFOS Test #1 vs. Burn House Experiments

Data from the living room thermocouple rake for the University of Waterloo HFOS–I fire study (Edmonton, 1991) was plotted with Burn House experimental data from Rake 2 as shown in Figure 4.6. Thermocouple measurements from 9 and 10" below the ceiling on each of the rakes were plotted for the HFOS-I and Burn House experiments, respectively.

Observation of Figure 4.6 shows similar growth rates for Experiment #3 and the HFOS-I burn, with a slightly longer incubation period observed for Experiment #3. Maximum temperatures of approximately 300 ºC were achieved just before 300 seconds

for Experiment #3. Observation of the HFOS-I data indicates that the fire was suppressed at roughly 260 seconds.

Experiment #1 appears to have a similar growth rate as HFOS-I data until approximately 200 seconds. At this time the temperatures begin to deviate as the Experiment #1 fire continues to grow at a slower rate for the next 200 seconds. At 400 seconds into the burn, the Experiment #1 fire begins to burn quickly again, reaching peak temperatures of almost 700 ºC by the end of the growth phase (approximately 430 seconds). In comparison, a maximum temperature of only 440 ºC was observed for the HFOS-I fire where it had then been suppressed.

In Figure 4.7 the growth regions for both HFOS- I and Experiment #3 have been plotted, along with least squares curve fits of the data. The correlation coefficient for both sets of data is 0.9887 which demonstrates that growth rates for each experiment are equally represented by their respective quadratic curve fits. The overall correlation coefficient suggests that these growth regions can be well represented by a t-squared growth rate.

4.1.4 Estimation of Growth Rates – Experiment #3 and #4

As discussed in Chapter 2, the growth region of a compartment fire will, in general, be of the form:

$$\dot{Q} = \alpha_f (t - t_o)^2 \qquad \text{[kW]} \qquad (2.1)$$

where $\dot{Q}$ is the rate of heat released during the fire in kilowatts, α_f is the fire growth coefficient (kW/s^2) and t_o (s) is the incubation period. The growth coefficient can be

estimated from the quadratic equation representing the growth region of the fire. Expanding Equation 2.1, the curve will be of the form:

$$\dot{Q} = \alpha_f t^2 - 2\alpha_f t t_o + \alpha_f t t_o^2 \quad [\text{kW}] \qquad (4.10)$$

When t_o is at (or close to) zero in Equation 4.10, the coefficient, α_f, will be the corresponding growth rate coefficient of the fire. The growth regions of Experiments #3 and #4 were plotted at the origin ($t_o = 0$) along with a least squares quadratic curve fit. A growth coefficient of 0.0036 kW/s^2 was obtained from the equation of the quadratic curve fit for Experiments #3 as shown in Figure 4.8.

Figure 4.3b shows that Experiment #4 grows slowly from ignition to approximately 450 seconds into the fire, which will be termed 'Growth Stage A'. At this point, temperatures in the burn room level off and stay relatively constant for approximately 150 seconds. The fire then begins to burn much more rapidly, growing again, and temperatures have peaked to 748ºC by 850 seconds. This second growth region will be defined as 'Growth Stage B'. These events correspond to the smouldering[21] fire and the subsequent addition of fuel, as discussed in Chapter 3. Figures 4.9 and 4.10 show the least squares quadratic curve fits for Growth Stages A and B, respectively. From these equations, coefficients of 0.0009 and 0.0191 kW/s^2 were obtained.

Comparing these growth coefficients to those presented in Table 2.1 shows that the growth coefficient for Experiment #3 corresponds to slow to medium growth fire. The coefficient for Growth Stage A of Experiment #4 is much less than that for a slow growth fire, which coincides with observations that the fire began to smoulder in Experiment #4. The coefficient for Growth Stage B of Experiment #4 corresponds to a medium to fast growth fire.

[21] Smouldering events are generally ignored and included as part of the incubation period of a fire.

4.2 CFAST Model Results and Discussion

The CFAST compartment fire model was chosen to simulate and predict the fire behaviour in the Burn House. The purpose of this chapter is to outline the steps taken to modeling the fire in CFAST and to discuss the results of the simulations and compare to experimental results. From these comparisons, the veracity of the model as a predictive tool will be discussed along with its potential for use in future fire scenario predictions.

Experiments #3 and #4 were modelled in this study. Observation of the experimental results showed that Experiment #3 appeared to be the best controlled burn; lower burn room temperatures were achieved in addition to relatively steady temperatures throughout the fully developed region, making it the simplest of the four experiments to model. This was likely a result of a small, single-source fuel load.

Experiment #4 was also modelled using CFAST. This experiment was chosen in anticipation that the actual burn events observed could be simulated – the ignition of the ceiling and wall materials. Much higher burn room temperatures were achieved due to full room involvement and this would hopefully be reflected in the CFAST model results.

4.2.1 Estimation of Model Inputs

As described in Chapter 2, CFAST is a two-zone model capable of predicting the environment in a multi-compartment structure subjected to a fire. It calculates the time-evolving distribution of smoke and fire gases and the temperature throughout a building during a user-specified fire. CFAST requires the following user inputs:

1. Geometric and material properties of enclosure surfaces.

2. Ventilation opening geometry: Window and door configurations are specified and can be modelled to open or close at specific times during the fire.

3. Initial ambient gas properties (including relative humidity, temperature).

4. Two of: Heat Release Rate (HRR), Pyrolysis Rate or Heat of Combustion. Generally, HRR and Heat of Combustion are specified as they can be readily estimated from the literature when the fuel load is well specified.

The room size and sources of ventilation (outside door, exterior windows) were specified to their exact dimensions in the burn room. Interior doors and windows were sealed off in the burn room, and therefore were not specified in the model.

Once the room configurations have been entered into the model, enclosure surface types must either be selected from the built-in materials database or created using the thermophysical properties of the material. Any type of construction or combination of materials (up to three layers) can be entered, provided the properties can be specified. Table 4.2 lists the thermophysical properties used as model inputs for the burn room lining materials. These properties were taken at 300 K as the temperature dependence of these properties cannot be specified in CFAST. The error associated with these estimates is discussed in the next section.

Table 4.2: Thermophysical Properties of Lining Materials @ 300 K, Room 1 [53, 57]

Material	Density, ρ [kg/m^3]	Thermal Conductivity, k [W/m◦K]	Specific Heat Capacity, C_p [kJ/kg◦K]
Cement Board	1152	0.227	1.090
Plywood	545	0.12	1.215
Steel (sheet)	7800	50.2	0.460

The model inputs required for the ambient gas properties were taken from the database at the University of Waterloo's weather station for each experiment [58]. (Chapter 3, Table 3.2)

The Heat of Combustion for the wood pallet fuel source was estimated to be 19,500 kJ/kg [5].

As discussed in the previous section, the growth rate of a compartment fire will generally be a function of time-squared. Using the growth coefficients estimated for Experiments #3 and #4 in the last section (See Table 4.3) the heat release rate for the growth region could be estimated. Research has shown that the shape of the heat release rate curve will govern the shape of the predicted time-temperature curve for a compartment fire [4]. Conversely, knowledge of the temperature evolution of a fire will provide an indication of the corresponding heat release rate profile. Time to peak (maximum) and steady temperatures will coincide with times to peak and steady heat release rates [4]. The duration of the growth stages and steady-state regions were observed from time-temperature plots from Rake 2 for both experiments. Figures 4.11 and 4.12 show the heat release rate curves generated for Experiments #3 and #4, respectively. A maximum heat release rate of 0.44 MW was obtained for Experiment #3 and 1.22 MW was used for Experiment #4. These curves were input into the CFAST model.

Table 4.3: Growth Coefficients used to Estimate the Growth Region of Heat Release Rate Curve.

Experiment	Growth Coefficient, α_f (kW/s)
September 30, 2004	0.0036
November 30, 2004	0.0009
November 30, 2004	0.0191

Comparison of the heat release rate curves to the time-temperature plots of the experiments shows that the decaying region of the fires has not been accurately modelled. In the actual experiments, the fire has been suppressed (or exhausted) prior to this stage and after this the temperatures in the burn room decrease at a slow rate. (This slow decay rate can be attributed to thermal inertia in the Burn House.) The temperature evolution in the burn room during the decay stage of the fire is not of interest in this study and has therefore, for simplicity, been modelled to decay at a rate similar to that at which the fire grows. This will have a negligible effect on the model predictions of interest in this study.

4.2.2 CFAST Model Results

This section will present the CFAST model temperature predictions obtained from the fire simulations of Experiments #3 and #4.

It should be noted that a limitation of the CFAST model is that temperature results can only be displayed as layer temperatures (upper or lower) and ceiling, floor or wall temperatures. Layer temperatures are resolved by averaging the temperature measurements over the height of each layer. The boundary between layers is referred to as the interface height. In order to be able to compare results, the experimental data needed to be averaged over the burn room upper and lower layers. This was accomplished using CFAST's prediction of interface height. Figures 4.13 and 4.14 illustrate the interface layer heights, as determined by CFAST, for Experiments #3 and #4, respectively. The error associated with these estimates will be discussed in the next section.

Comparison of CFAST Model and Experiment #3 Results

Experimental and model estimates for upper and lower layer temperatures, as well as CFAST ceiling temperatures are shown in Figure 4.15 for Experiment #3.

Observation of the growth regions for the upper layer temperature profiles shows that the growth rate is slightly steeper for the experimental results. Predicted CFAST model temperatures are 13 ºC higher at the end of the growth stage (approximately 350 seconds) than for Experiment #3. At this time, a maximum temperature of 238 ºC is predicted by CFAST, whereas actual maximum temperatures are 225ºC. From 350 seconds until the end of the fully developed region (840 seconds) the CFAST model shows a gradual increase in upper (and lower) layer temperatures. At roughly 600 seconds into the simulation, model and experimental temperatures begin to differ more substantially, as model temperatures continue to escalate while experimental results level off.

Figure 4.15 shows that ceiling temperatures predicted by the CFAST model are comparable to the temperatures predicted in the lower layer of the burn room. CFAST ceiling temperatures reach a maximum of 199ºC. The location of the predicted ceiling temperature measurement in the burn room simulation is unknown for the CFAST model.

Figure 4.15 also shows that CFAST has predicted much higher lower layer temperatures than observed for Experiment #3. The maximum lower layer temperature predicted by CFAST is 187 ºC at 840 seconds into the burn. At this time, actual lower layer temperatures in the burn room are only 116 ºC

Comparison of CFAST Model and Experiment #4 Results

Experimental and model estimates for upper and lower layer temperatures, as well as CFAST ceiling temperatures are shown in Figure 4.16 for Experiment #4.

A comparison of the upper layer temperatures shows that, while both experimental and model results have similarly shaped profiles, the CFAST model predicts a much shorter incubation period. Temperatures begin to grow soon after ignition and at a slightly steeper growth rate than for Experiment #4. This results in slightly higher upper layer temperature predictions throughout the initial growth phase (Growth Phase A). Temperatures begin to level off sooner (at 400 seconds) for the actual experimental results to around 100ºC. At 500 seconds, CFAST upper layer temperature predictions level off to approximately 150ºC. The second growth stage (Growth Stage B) begins at 640 seconds for Experiment #4 and 700 seconds for the CFAST model. At the end of this stage (780 and 860 seconds), peak temperature measurements for Experiment #4 and the model are 385ºC and 445 ºC, respectively. This corresponds to a difference of 60ºC in temperature predictions. Both upper layer temperature curves continue to escalate beyond these points.

Figure 4.16 shows model predictions of the ceiling temperatures for Experiment #4. CFAST predicts a maximum ceiling temperature of 581 ºC, almost 80º higher than the maximum experimental upper layer temperature. Maximum CFAST ceiling temperatures are approximately 30 ºC cooler than upper layer temperatures predicted by the model.

Observation of Figure 4.16 shows that the lower layer temperatures have once again been significantly overpredicted by the CFAST model. CFAST predicts a maximum lower layer temperature of 505 ºC at 1560 seconds. At the same time, actual lower layer temperatures are 216 ºC.

It should be noted that the CFAST model predicted the occurrence of a flashover in the burn room at approximately 1492 seconds into the simulation for Experiment #4. Visual observations of the burn room during Experiment #4 indicated a thickening of the upper thermal layer down to about 2" (50.8 mm) from the floor and flaming of all combustible material throughout the room by approximately 1140 seconds into the fire (Figure 3.37), which are both typical observations of a flashover occurrence.

4.2.3 CFAST Model: Sensitivity Analysis

In this section, six sources of potential error for the CFAST model predictions will be discussed. The first four sources of error relate to user-specified inputs for the model: heat release rate, vent configuration, thermophysical properties (of burn room lining materials) and ambient conditions. A sensitivity analysis has been performed for each variable, using the CFAST model results obtained for Experiment #3 as a reference case. The error associated with estimating layer heights and average temperatures will be discussed briefly in addition to model limitations and assumptions. The results of this analysis are presented as maximum temperatures predicted and percent difference in temperature from the reference case. These percentages are presented in terms of relative temperatures, which are the difference between the maximum CFAST predicted temperatures and the ambient temperature observed during Experiment #3, 15.4 ºC (Table 3.2). The percent difference is then calculated by dividing the relative temperature value by the relative temperature of the reference case.

Heat Release Rate – Sensitivity Analysis

Figure 4.17 illustrates the changes in CFAST temperature predictions as a result of varying heat release rate (HRR) inputs. The upper and lower layer temperature predictions for Experiment #3 (0.44 MW) are shown in comparison to upper and lower layer temperatures for simulations using 0.53 and 0.35 MW maximum heat release rates.

These changes correspond to a twenty percent increase and decrease in maximum (peak) heat release rates, respectively.

As shown in Figure 4.17, the model results are quite sensitive to a change in HRR. For the reference case maximum upper layer temperatures are predicted to be 288ºC and lower layer temperatures are predicted to be 187 ºC. As shown in Figure 4.17, maximum upper and lower layer temperatures increase by 31ºC (11 – 18%) in addition to a slight change in the slope from the reference case, for a corresponding twenty percent increase in peak HRR. Conversely, upper and lower layer temperatures decrease by 36 ºC with a twenty percent reduction in peak HRR, corresponding to a reduction of 13 – 21% in model predictions of layer temperatures. This information is summarized in the following table. Bolded values represent the reference case.

Table 4.4: Variation in CFAST Predictions: Heat Release Rate

	Maximum Temperature (ºC)	Relative Temperature Difference (%)
HRR = 0.44 MW, Upper Layer Temperature	**288**	-
HRR = 0.44 MW, Lower Layer Temperature	**187**	-
HRR = 0.53 MW, Upper Layer Temperature	319	+11.3
HRR = 0.53 MW, Lower Layer Temperature	218	+18.1
HRR = 0.35 MW, Upper Layer Temperature	252	-13.2
HRR = 0.35 MW, Lower Layer Temperature	151	-20.9

Vent Size - Sensitivity Analysis

As discussed in Chapter 3 and in Appendix B, a door and window were kept open to the ambient for the duration of Experiment #3 to allow for ventilation to the burn room. The configuration of these openings was put into the CFAST model in order to simulate Experiment #3. The effect of the size of the openings (and thus amount of airflow into and out of the burn room) on temperature predictions was analysed by varying the width of the window and door in the CFAST model. Table 4.5 summarizes the changes for this sensitivity analysis.

Table 4.5: Vent Configurations for CFAST Sensitivity Analysis

	Vent	Sill (m)	Soffit (m)	Width (m)	Area (m^2)
Experiment #3	Door	0.0	2.03	0.152	0.310
	Window	0.8	1.80	0.152	0.152
Doubled Vent Width	Door	0.0	2.03	0.305	0.619
	Window	0.8	1.80	0.305	0.305
20 % Increase in Vent Width	Door	0.0	2.03	0.122	0.247
	Window	0.8	1.80	0.122	0.122
20% Decrease in Vent Width	Door	0.0	2.03	0.183	0.371
	Window	0.8	1.80	0.183	0.183

Figure 4.18 illustrates the effects of altering the vent widths on upper and lower layer temperature predictions. As shown in Figure 4.18, there is very little change in upper layer temperature (4ºC) by altering vent width by twenty percent. Temperatures in the lower layer vary by approximately 10.5% from the reference case when the vent width is altered by twenty percent. The greatest variation in maximum temperature predictions is observed for both layers when the vent width is doubled; the maximum upper layer temperature decreases by almost 20ºC (6.9%) and lower layer temperatures decrease by almost 80 ºC (46%).

The following table summarizes the maximum temperatures predicted for each of the scenarios along with the relative temperatures. Bolded values represent the reference case (Experiment #3). All maximum temperatures were observed at 840 seconds into the simulation.

Table 4.6: Variation in CFAST Predictions: Vent Width

Vent Configuration	Maximum Temperature (ºC)	Relative Temperature Difference (%)
Experiment #3: U. Layer	**288**	-
Experiment #3: L. Layer	**187**	-
Double Vent Width: U. Layer	269	-6.9%
Double Vent Width: L. Layer	108	-46%
80% Vent Width: U. Layer	292	+1.5%
80% Vent Width: L. Layer	205	+10.5%
120% Vent Width: U. Layer	284	-1.5%
120% Vent Width: L. Layer	169	-10.5%

Thermophysical Properties of Lining Materials - Sensitivity Analysis

The accuracy of the model predictions is affected by how well the user specifies the thermophysical properties of the materials used in the study. There is a higher level of uncertainty in the predictions of the model if the properties of real materials and real fuels are unknown or difficult to obtain [59].

Figure 4.19 shows the variation in upper and lower layer temperature predictions when the thermal conductivity of the inside wall lining material (Durock) is doubled and then halved. The following table summarizes the maximum temperature predictions of the model along with the percent variation of these predictions from the reference case (Experiment #3). All maximum temperatures were observed at 840 seconds.

Table 4.7: Variation in CFAST Predictions: Thermal Conductivity of Durock

Thermal Conductivity	Maximum Temperature (ºC)	Relative Temperature Difference (%)
Upper Layer Temperature (k = 0.227 W/mK)	**288**	-
Lower Layer Temperature (k = 0.227 W/mK)	**187**	-
Upper Layer Temperature (k = 0.454 W/mK)	268	-7.3
Lower Layer Temperature (k = 0.454 W/mK)	171	-5.8
Upper Layer Temperature (k=0.114 W/mK)	312	+8.8
Lower Layer Temperature (k=0.114 W/mK)	205	+10.4

As shown in Table 4.7, the largest change in temperature predictions is observed as an increase in upper layer temperatures by 24ºC when the thermal conductivity is halved. Overall, the variation in maximum temperature predictions is relatively small for any change in thermal conductivity performed in this study and is likely not a key contributor to error in temperature predictions.

Ambient Conditions – Sensitivity Analysis

The effects of ambient conditions on the prediction of upper and lower layer temperatures was studied by adjusting three user-specified variables in the CFAST model as shown in Figure 4.20. The following table summarizes the changes for these ambient conditions and the resulting maximum temperature predictions for each layer, along with the percent variation between the reference case (Experiment #3) and each simulation. All maximum temperatures were observed at 840 seconds.

Table 4.8: Variation in CFAST Predictions: Ambient Conditions

Variable Change	Maximum Temperature (ºC)	Relative Temperature Difference (%)
Experiment #3 Upper Layer Temperature	**288**	-
Experiment #3 Lower Layer Temperature	**187**	-
Wind Speed (2 to 10 m/s) Upper Layer Temperature	288	-
Wind Speed (2 to 10 m/s) Lower Layer Temperature	187	-
Ambient Temp. (288 to 303K) Upper Layer Temperature	299	+4
Ambient Temp. (288 to 303K) Lower Layer Temperature	206	+11
Rel. Humidity (76 to 100%) Upper Layer Temperature	288	-
Rel. Humidity (76 to 100%) Lower Layer Temperature	187	-

As shown in Table 4.8 and Figure 4.20, the only change in upper and lower layer temperature predictions occurs when the outside ambient temperature is increased by 15ºC. This corresponds to a relative temperature increase of 4 and 11% for the upper and lower layer, respectively. Overall, upper layer temperatures are less affected by large changes in ambient temperatures.

Experimental Upper and Lower Layer Estimations

As previously discussed, the temperature outputs from CFAST are displayed as *layer* temperatures. One of the major limitations inherent in the two-zone model is the assumption of stratification of the gas layers into a hot *upper* layer or cold *lower* layer. The zone model concept, by definition, implies a sharp boundary between these layers,

called the interface height. Therefore, the layer temperature is determined from the average of all the temperatures above (upper) or below (lower) this interface height.

In order to compare to the model predictions, the experimental data had to be averaged over an estimated upper and lower layer. This required an estimate of the interface height in the burn room. It was difficult to identify a developing interface height from the temperature stratification plots presented in Chapter 3 for the experimental results. As well, the boundary between layers will not actually be a sharp transition and will occur typically over about 10 % of the height of the compartment which can be larger in weakly stratified flows, making it hard to pinpoint an exact value [59].

For comparison purposes, the interface height obtained from the CFAST model predictions was taken to also be the interface height in the burn room and used to determine the average upper and lower layer temperatures. This method assumed that the interface predictions from the model were accurate.

No exact definition or mathematical equation exists that can accurately define an interface height for a given fire scenario or experiment. It is therefore not possible to quantify the error associated with the CFAST prediction of interface height, or similarly, the error associated with using this as a reference for upper and lower layer temperature estimates.

CFAST Model Assumptions

Studies typically show CFAST model predictions to be within 10 to 25% of experimental results, which is considered reasonably accurate for the purposes of estimating global trends in fire behaviour [59]. The degree of accuracy achieved with a

model will be directly affected by the accuracy of the model inputs and as well of course the degree of numerical and physical approximations adopted. Some of these issues are discussed in the next section [59].

The main error related to model assumptions and numerical approximation attributed to CFAST is that this model belongs to the class of zone models which assume that each compartment can be divided into two layers, a hot upper layer and a colder lower, each of which is internally uniform in temperature and composition [59]. Beyond basic zone assumptions, the model incorporates a combination of established theory (conservation equations), empirical correlations where there are data but no theory and approximations where there are neither. A widely used assumption is that the estimated error from ignoring the variation of thermal properties of structural materials with temperature is small. While this information would be fairly simple to add to the model code, data are scarce over a broad range of temperatures, even for the most common materials [59]. An extensive description of these errors has been well documented in a technical reference produced by NIST [59]. A report by Lundin (1997) [60] also discusses errors associated with an older version of the CFAST model and their effect on the prediction of temperatures from a comparison to experimental results.

4.2.4 Discussion of Model Results

CFAST version 3.1.7 was used in this study. The following table summarizes the difference between model temperature predictions and experimental results for maximum upper and lower layer temperatures in Section 4.2.2.

Table 4.9: Difference between Maxiumum Temperatures for Model Predictions and Experimental Results

	Temperature Difference: Upper Layer Temperatures (ºC)	Temperature Difference: Lower Layer Temperatures (ºC)
Experiment #3	13	71
Experiment #4	60	289

As shown in Table 4.8, the best agreement between experiment and prediction was for the upper layer temperatures for both experiments. Upper layer temperature comparisons were made at the end of the growth stage. The results showed that CFAST over-predicted upper layer temperatures for both experiments. Similar observations were identified in Poole [4] with regards to CFAST's tendency to over-predict upper layer temperatures. A detailed discussion is provided in this work on the physical processes in the room which may affect these predictions, such as CFAST's treatment of heat release rate specification and the addition of heat to the upper gas layer. Overall the CFAST model shows general agreement in upper layer temperature measurements for this study.

Over-prediction of lower layer temperatures was also observed in this study, however, the discrepancies in these estimates was much greater than for upper layer temperatures. Lower layer temperatures were over-predicted by 71ºC for Experiment #3 and by 289ºC for Experiment #4.

Some of the variation in layer temperature predictions can be attributed to the methods used to estimate interface height. As previously discussed, there is no sharp boundary between upper and lower gas layers and no mathematical equation exists that can pinpoint the location of this interface for a specific fire scenario. Using CFAST's interpretation of layer height as a means to determine the upper and lower layer

temperature estimates for the Burn House experiments will no doubt incorporate errors which cannot be quantified. This method, however, is the only means of providing a comparison to model layer predictions. The accuracy of these comparisons could potentially be improved if interface heights for the actual experiments can be ascertained. This information could potentially be resolved from temperature stratifications over the course of a well controlled experiment so that the developing layer height could be observed. This task would be difficult, however, due to the number of uncontrollable burn room variables which could affect results and could not be anticipated such as instrumentation difficulties, ambient effects or ventilation leaks.

Inconsistencies between experiment and model lower layer temperatures could also have been affected by the way the Burn House was configured in CFAST. The Burn House experiments were modelled as a multi-room configuration but the burn room geometry was specified such that there were only two vent openings to the ambient with no other ventilation pathways defined. In actual experiments, gases could have vented through leaks in doors and windows to the adjoining room, hallway or through other openings in the burn room which were not accounted for in the model. This could somewhat explain the cooler lower layer temperatures observed for experimental results due to the influx of fresh air from additional sources of ventilation.

As discussed in a technical reference guide provided by NIST [59], one of the limitations of the CFAST model is that downward wall flow has not been included in calculations for mixing of smoke and gases in the lower layer of the compartment [59]. The result of this would be an underestimate of lower layer temperatures, which does not coincide with the observations found in this study. Other effects are considered to be predominant over the exclusion of this flow in CFAST calculations.

The results of the CFAST sensitivity analysis showed that the accuracy of model predictions relies strongly in how well the user can specify properties and burn room

geometry. It has been shown that modelling errors of 10 – 25% can generally be expected, which is reasonable for use as an initial predictor of fire behaviour. From the comparisons to experimental data, the CFAST model demonstrated error within this range for upper layer temperature estimates only. Overall, the sensitivity analysis showed that errors in this range can typically be expected for user-specified variables.

Heat release rate is the single most important factor for specifying a fire which means that the more accurately it can be estimated, the more closely the temperature predictions will resemble experimental results. The sensitivity analysis showed that varying the heat release rate by twenty percent can generate differences of up to 31ºC in upper layer temperature predictions and differences of up to 36ºC for lower layer temperature estimates. Similar results have also been observed in a sensitivity analysis performed by Poole [4].

Simplistic methods based on known experimental data were used to estimate the heat release rates for Experiments #3 and #4 in this study. Validated pyrolysis and heat release models are not yet available for most fuels therefore correlations developed from experiment are still required to make quantitative heat release predictions in the absence of experimental data. Incorporating empirical correlations for estimates of heat release rate could prove to be more accurate, however, correlations are often developed for specific fuel compositions and geometries and cannot always be directly applied to slightly different fuel assemblies or fuel loads with varying orientations. Furthermore, correlations for estimating solid fuel heat release have been developed but for fuels with known moisture content. In addition, correlations for heat release rates for smouldering fuels do not exist. As a result, there is no completely accurate method available for specifying the heat release rate of a given fire and it is up to the discretion of the individual researcher to determine which method is best and will produce the degree of accuracy required from the model.

A sensitivity analysis was performed to observe the effects of changing the size of vent openings. When the vent width was doubled, lower layer temperatures decreased by 79ºC. This was likely due to an increased influx of cooler, ambient air at the sill of the vent openings. A twenty percent change in vent width corresponded to less than a 20ºC change in lower layer temperatures. The difference in upper layer temperature estimates was small for the same vent configuration changes and was considered to have a negligible effect on these predictions. A discussion on the sensitivity of the CFAST model to a change in vent area is given in Poole [4] which states that a 20% relative decrease in predicted upper layer gas temperature has been observed for a 10% increase in ventilation opening area in a single enclosure fire scenario.

As discussed in the technical reference by NIST [59] it is assumed that the variation of thermal properties of structural materials with temperature is small and has therefore not been accounted for in the model. This assumption comes from a lack of available information on the change in material properties over a broad range of temperatures. The sensitivity of the model to changes in the thermal conductivity of the lining material was investigated. The results showed that a maximum temperature change of 24ºC in upper layer temperatures can be expected when the thermal conductivity of the inside material is halved. Changes in temperature predictions for all other scenarios were relatively small (less than 20ºC).

The sensitivity of the model to changes in ambient conditions was evaluated. The reference case was altered to reflect changes in ambient wind speeds, temperature and relatively humidity. The results of the analysis showed that changing the relative humidity and ambient wind speeds had no effect on burn room temperature predictions.

The ambient temperature was increased by 15 ºC, and as a result, maximum upper and lower layer temperature predictions increased by 11 and 19ºC, respectively. This indicates that when the burn room is slightly pre-heated, the maximum temperatures achieved in the burn room will higher.

Given that CFAST has a large expectancy of error it is worth pointing out that it is still a very useful design tool. It requires low CPU cost, is user friendly, has a support base (NIST), is still widely used, and is remarkably flexible in that a wide range of geometries, ventilation conditions, and construction materials can be modeled. In a live structural fire scenario, +/- 30 % would be considered quite acceptable, a target within the ability of CFAST.

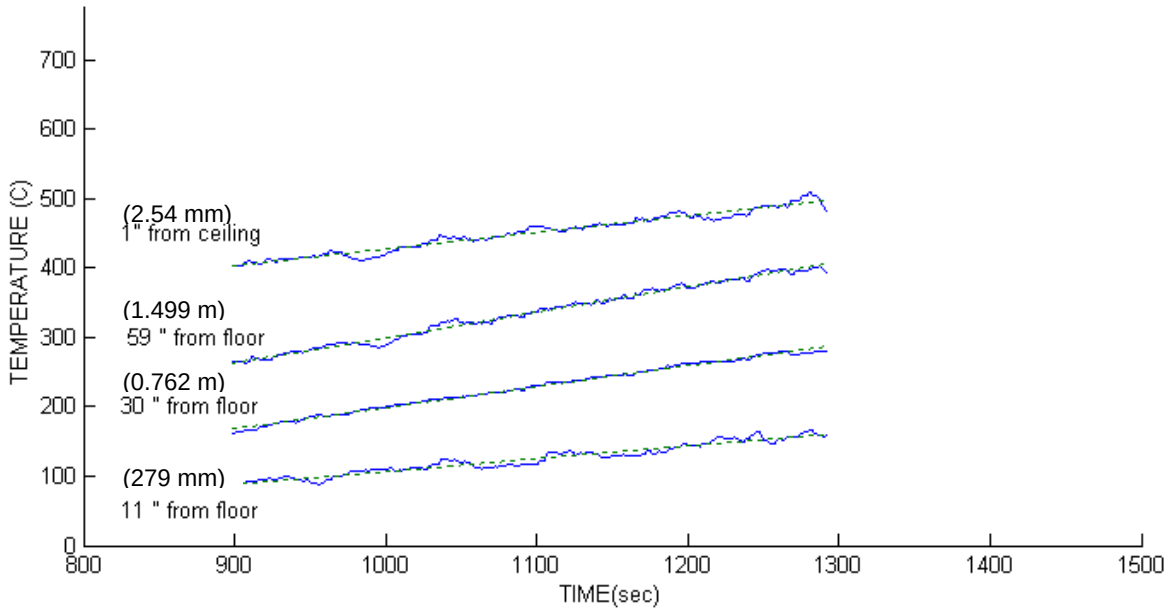

Figure 4.1: Selected Temperature Measurements for Steady State Region of Experiment #4 with Linear (mean) Curve Fit of Data.

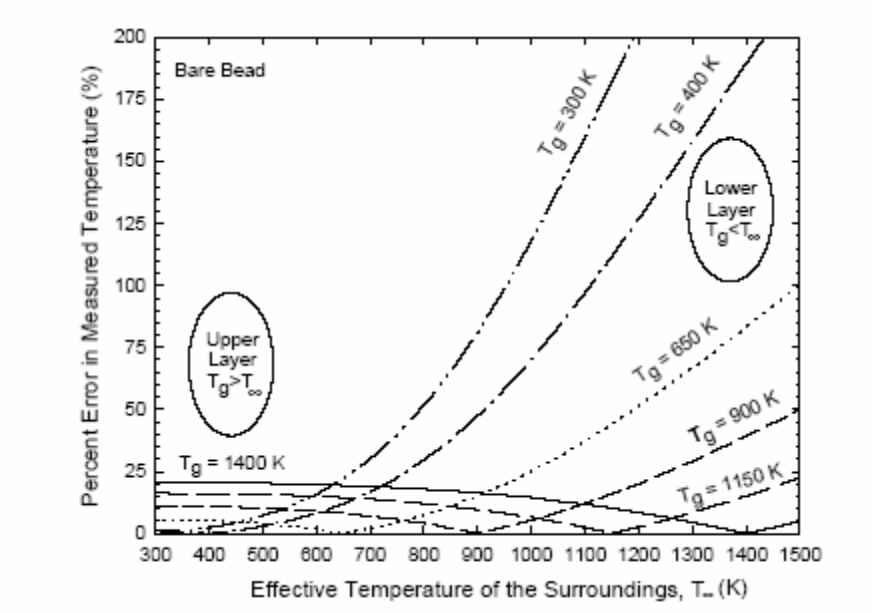

Figure 4.2: Percent Error in Measurement Temperature versus Effective Temperature of the Surroundings for a 0.06" (1.52 mm) Bare-Bead Thermocouple (Reproduced from [56])

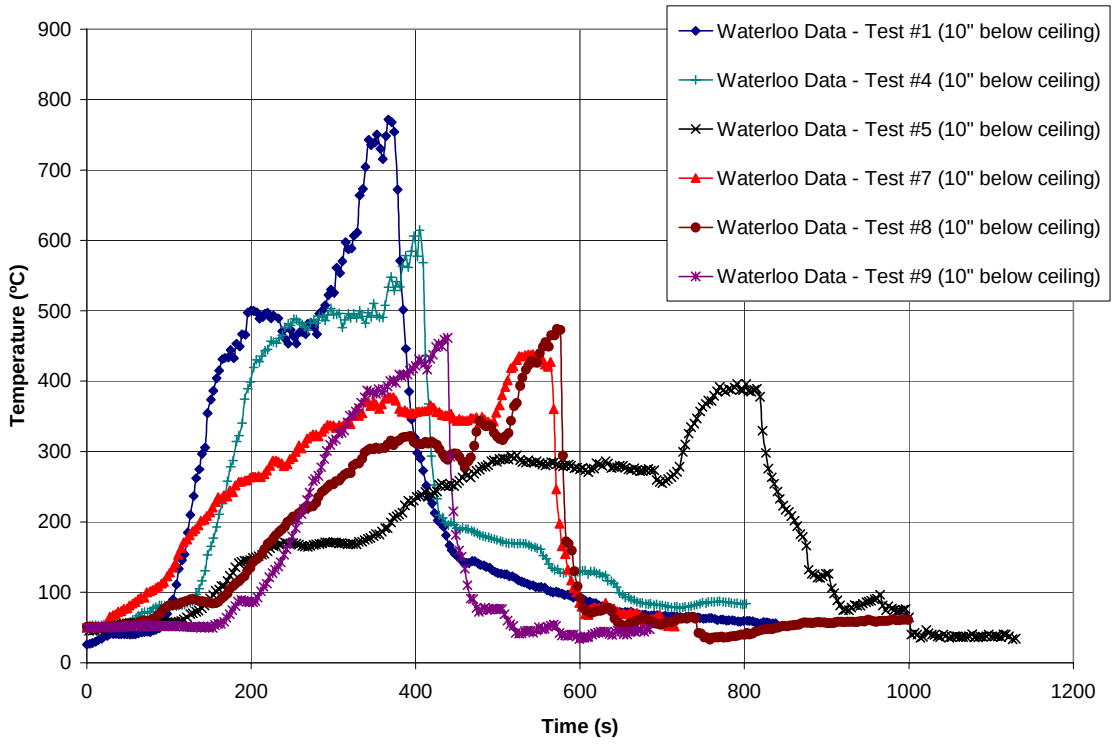

Figure 4.3a: Temperature vs. Time, Waterloo House Fire Test Data (all 254 mm below the ceiling)

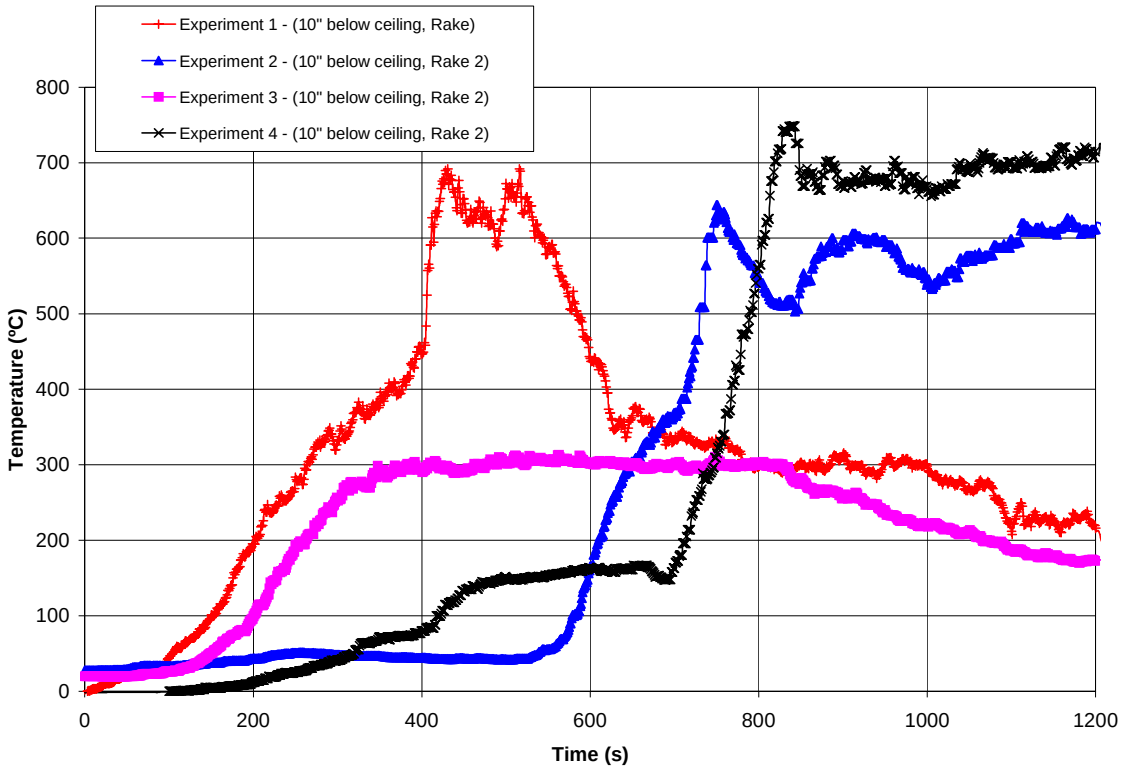

Figure 4.3b: Temperature vs. Time, Burn House Experiment Data (all 254 mm below the ceiling)

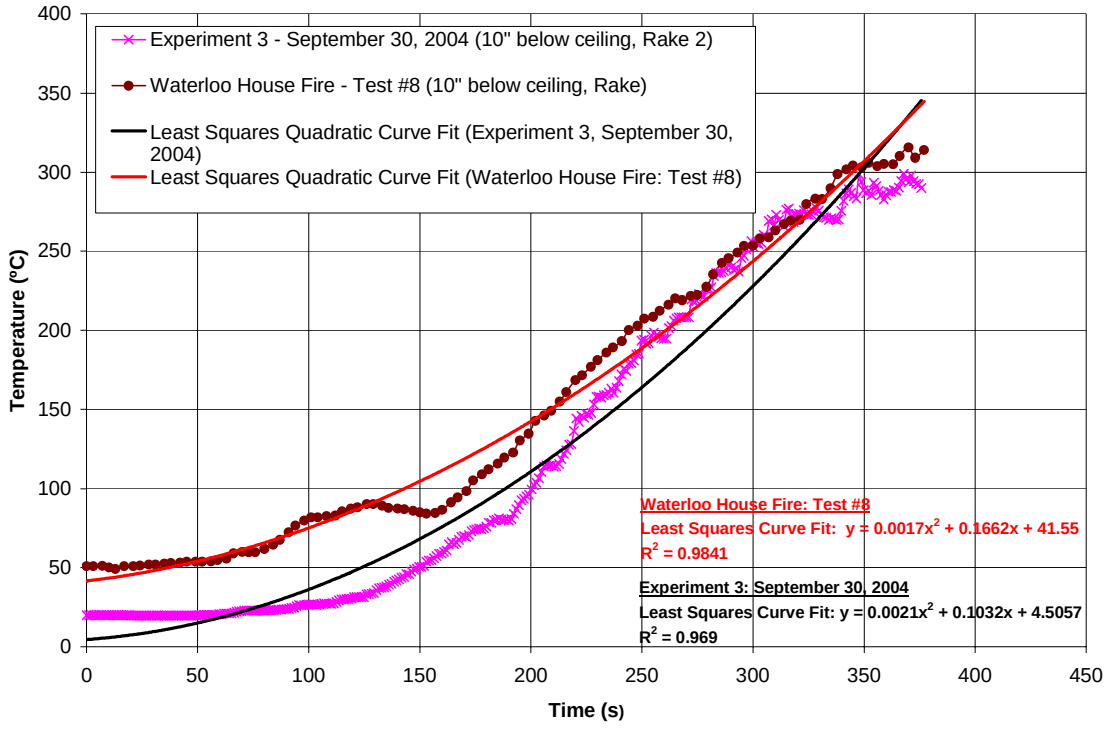

Figure 4.4: Plot of Fire Growth (t^2) Phase and Least Squares Quadratic Curve Fit, Waterloo House Fire Test #8 and Burn House Experiment 3 (all 254 mm below the ceiling).

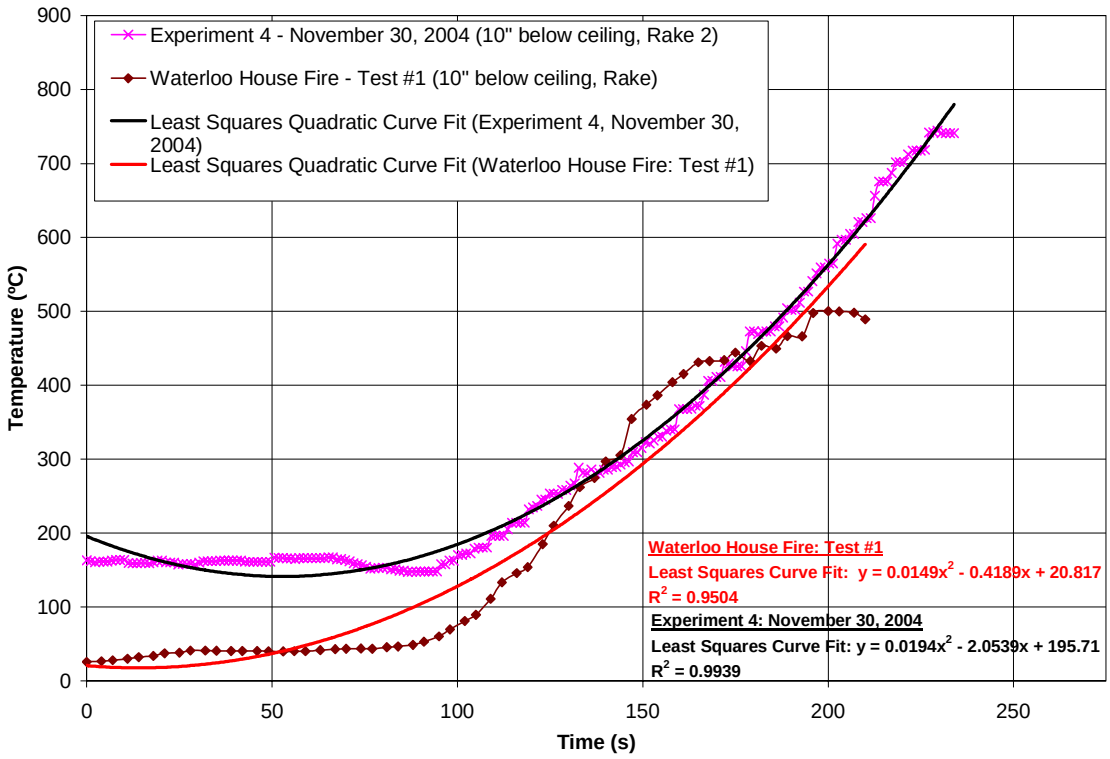

Figure 4.5: Plot of Fire Growth (t^2) Phase and Least Squares Quadratic Curve Fit, Waterloo House Fire Test #1 and Burn House Experiment 4 (all 254 mm below the ceiling).

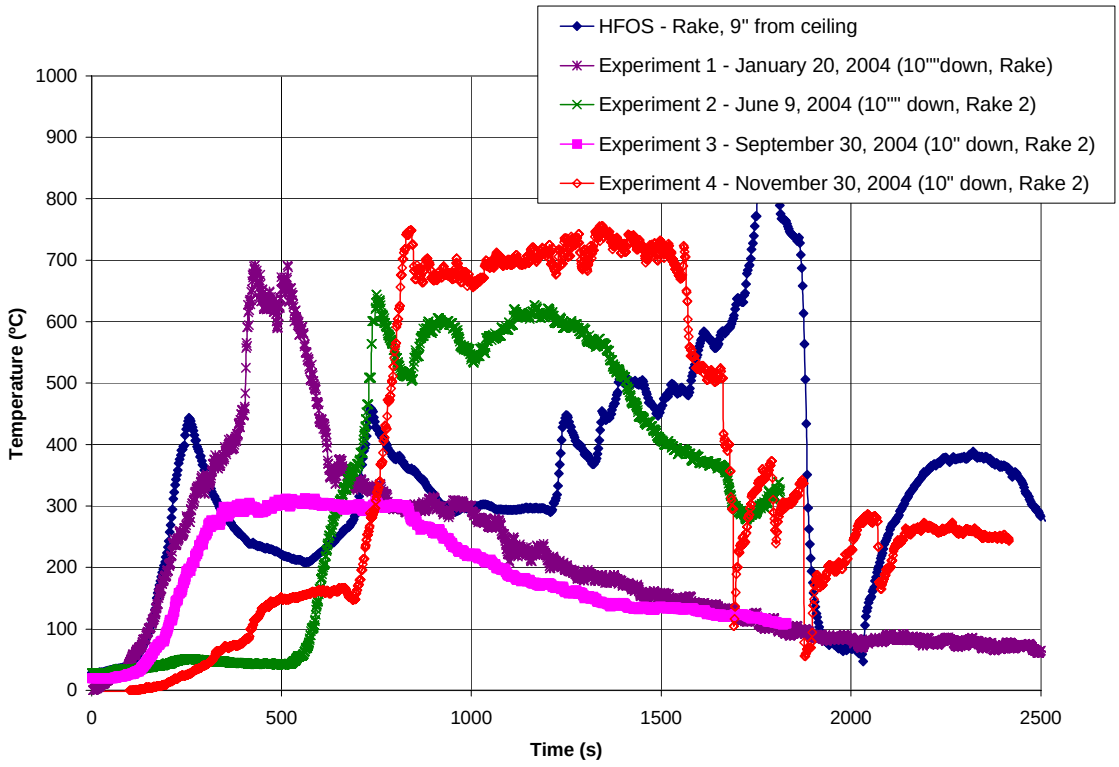

Figure 4.6: Temperature vs. Time, HFOS Fire Test Data and Burn House Experimental Data (HFOS - Rake, 229 mm from ceiling; all others 254 mm down)

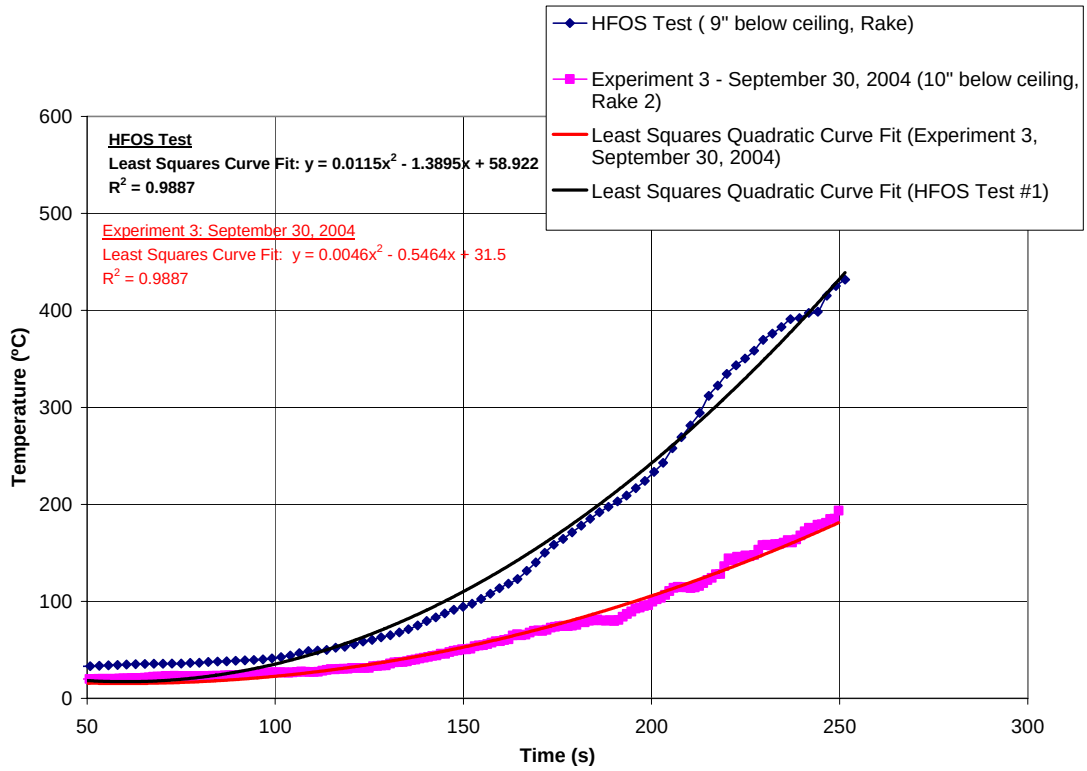

Figure 4.7: Plot of Fire Growth (t^2) Phase and Least Squares Quadratic Curve Fit, HFOS Fire Test and Burn House Experiments 1 and 3 (HFOS - Rake, 229 mm below ceiling; Experiment 3, 254 mm below ceiling).

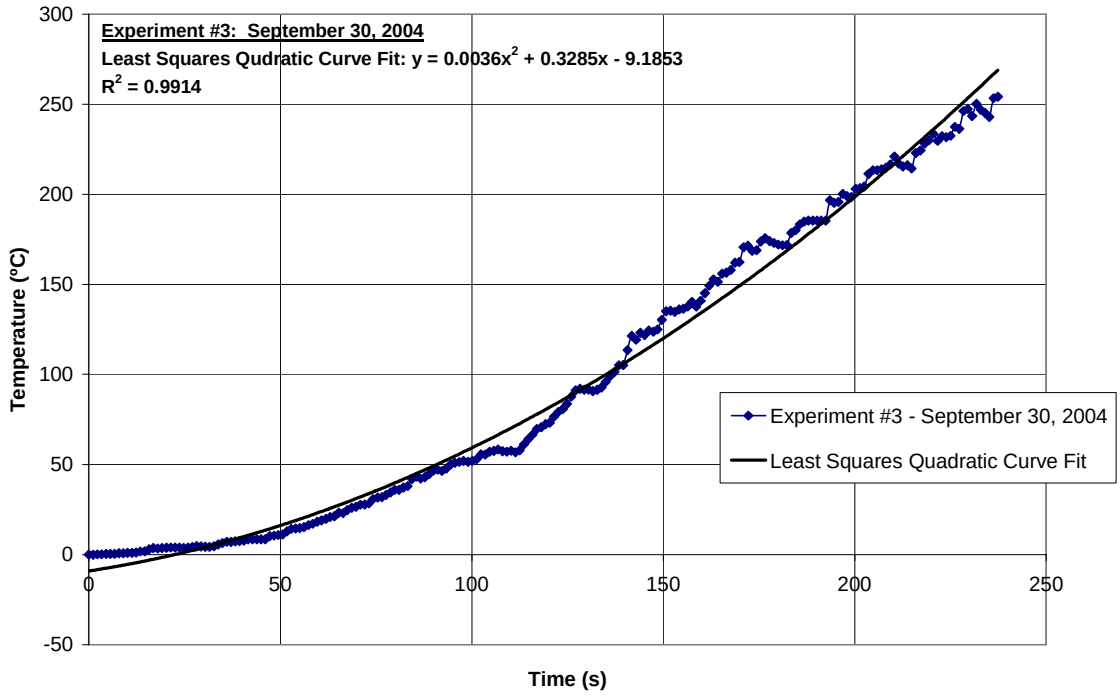

Figure 4.8: Experiment #3 – Estimate of Growth Coefficient

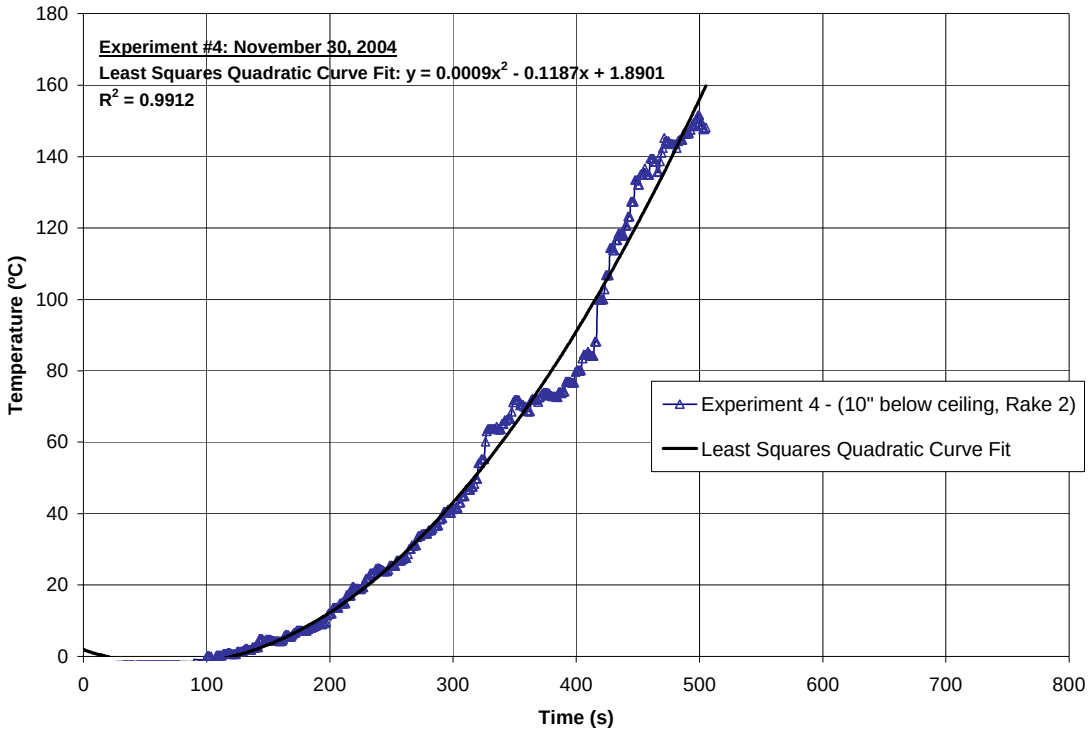

Figure 4.9: Experiment #4 – Estimation of Growth Coefficient A (254 mm below ceiling)

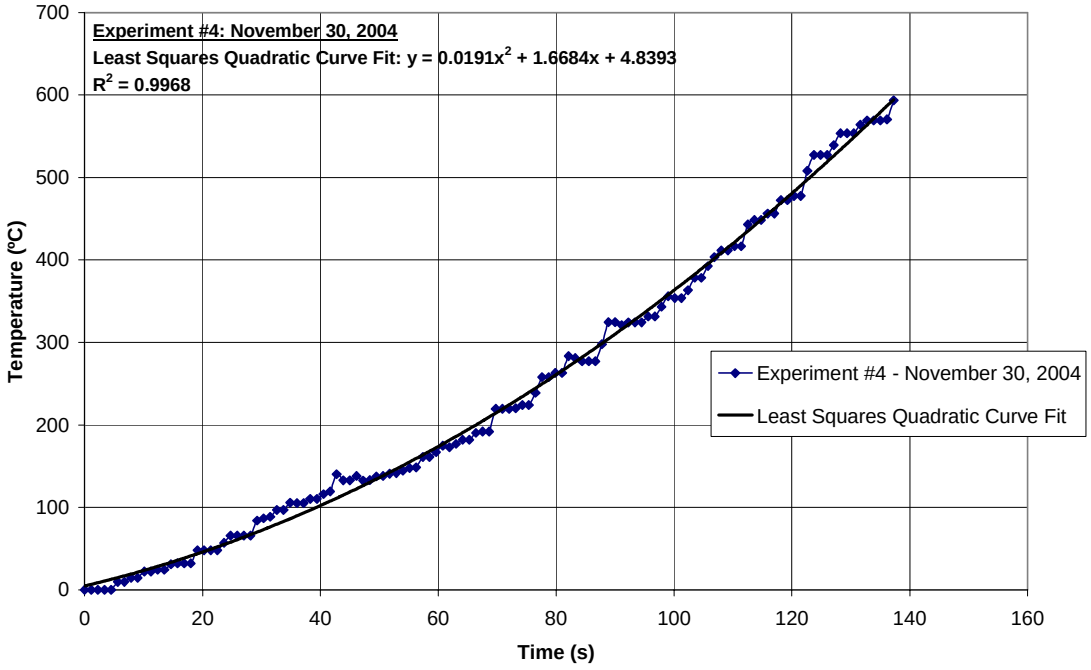

Figure 4.10: Experiment #4 – Estimation of Growth Coefficient B

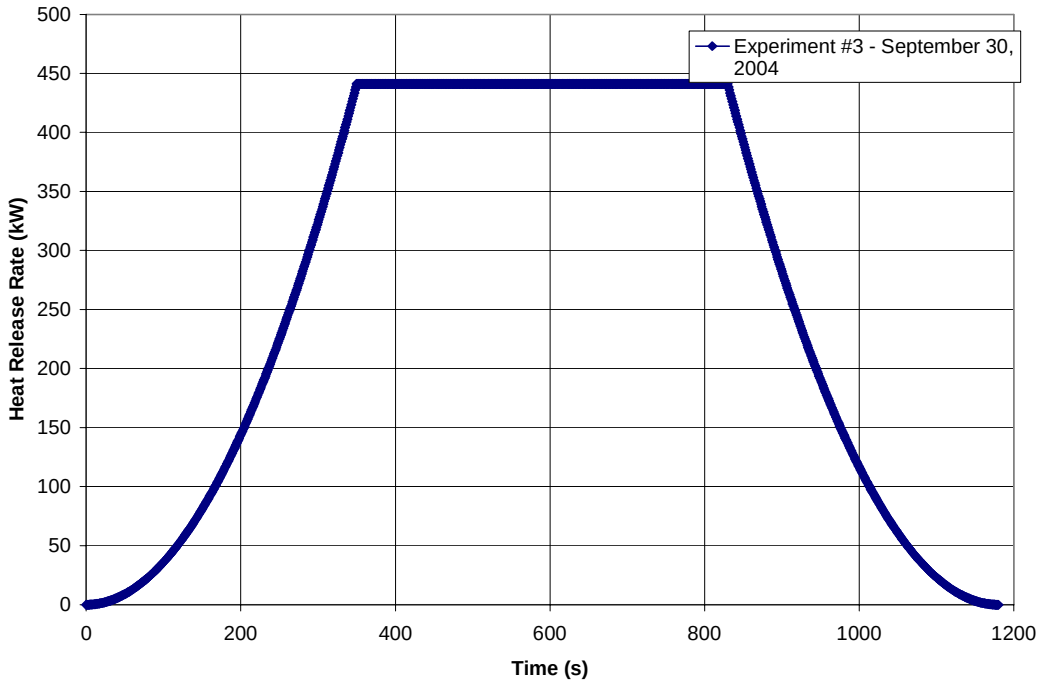

Figure 4.11: CFAST Heat Release Rate Curve – Experiment #3

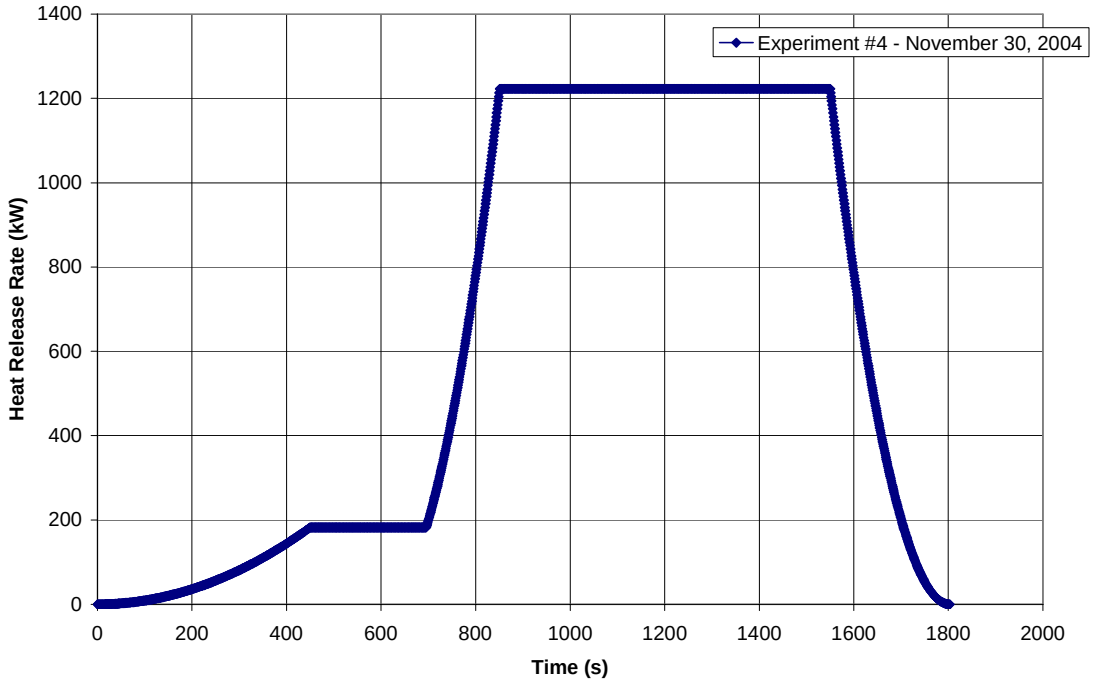

Figure 4.12: CFAST Heat Release Rate Curve – Experiment #4

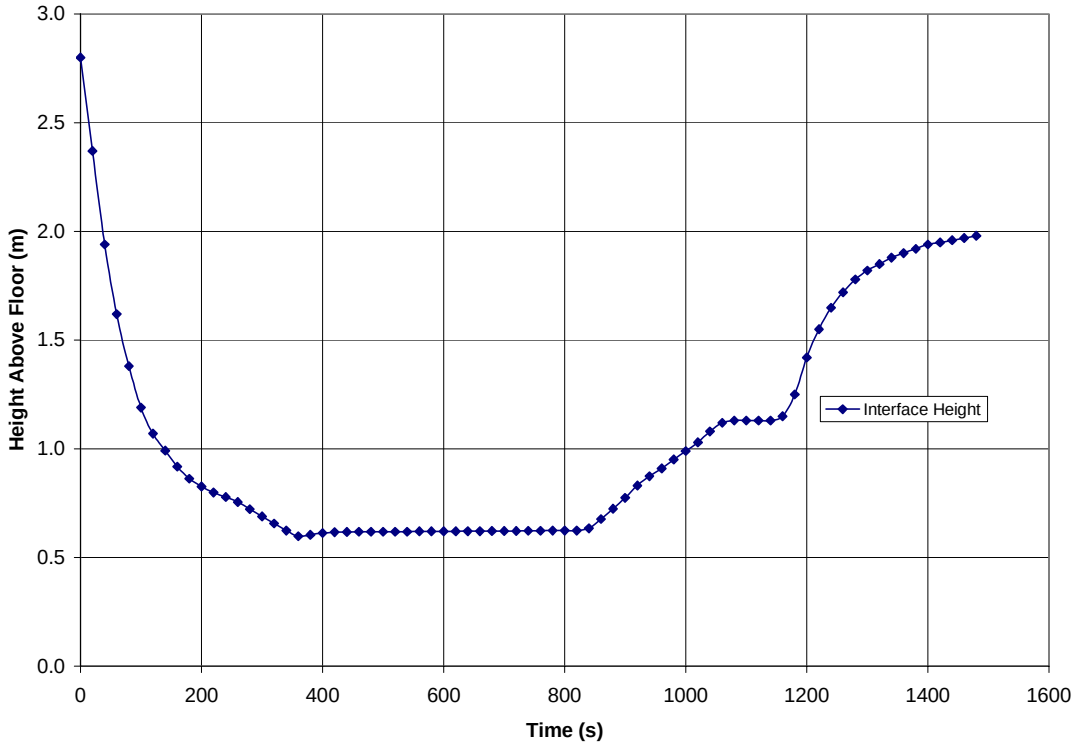

Figure 4.13: CFAST predicted interface height – Experiment #3

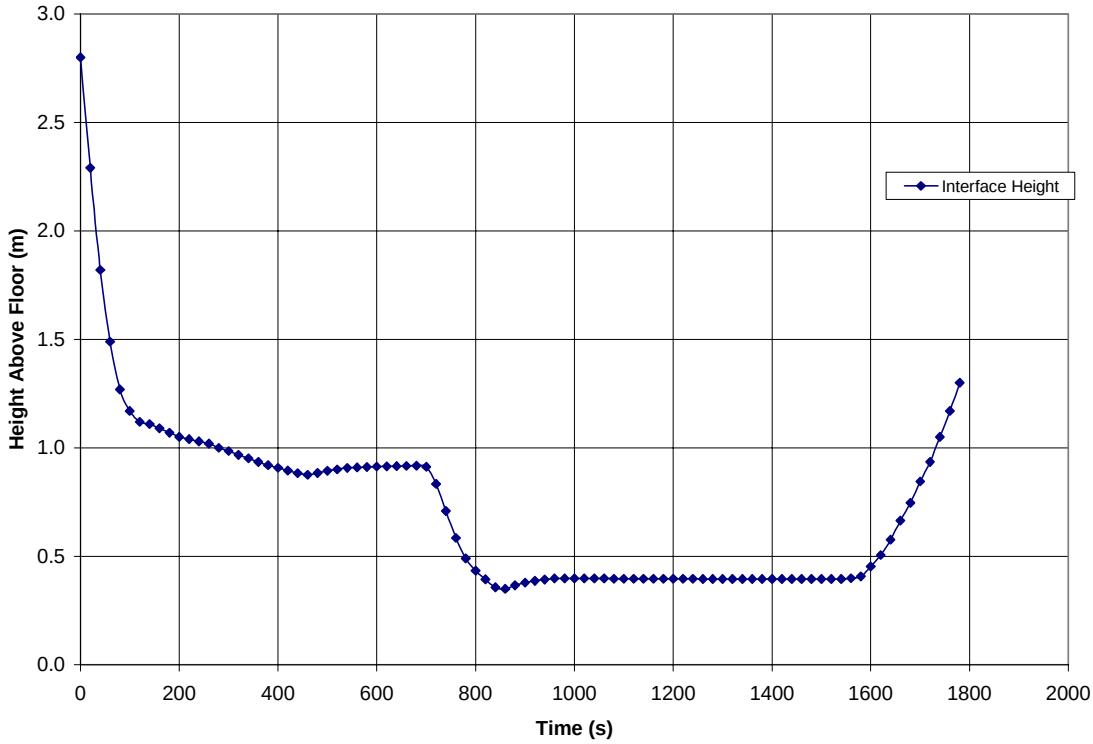

Figure 4.14: CFAST interface height – experiment #4

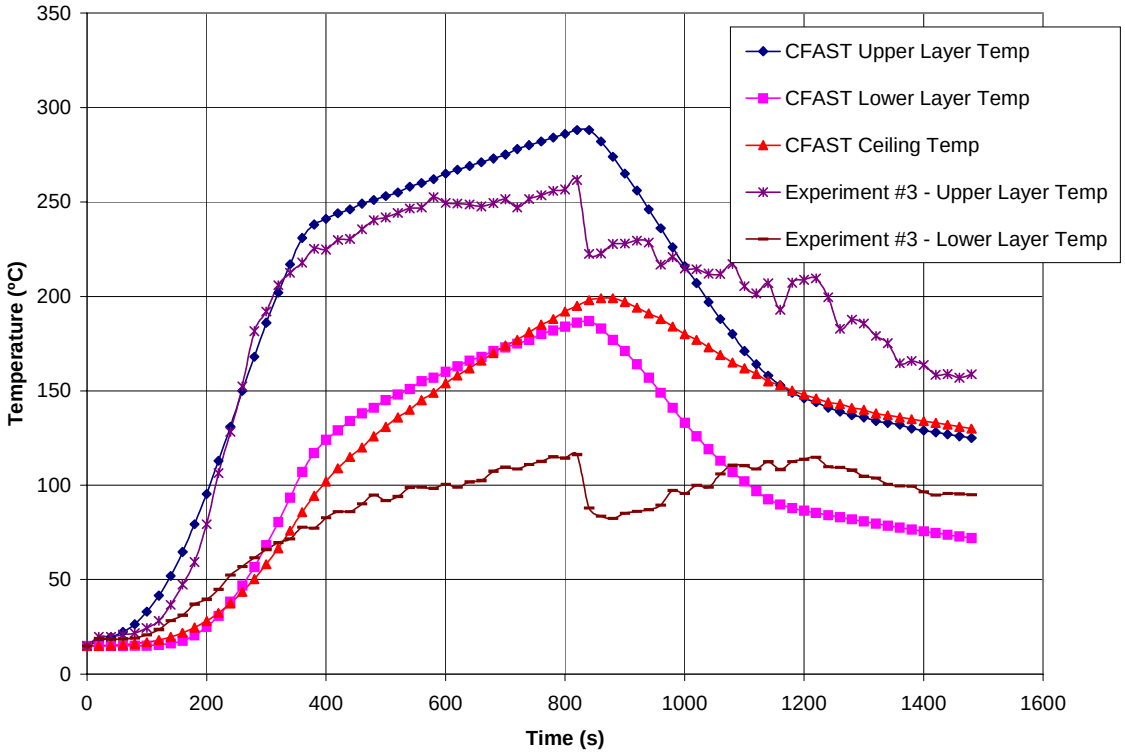

Figure 4.15: CFAST vs Experiment #3

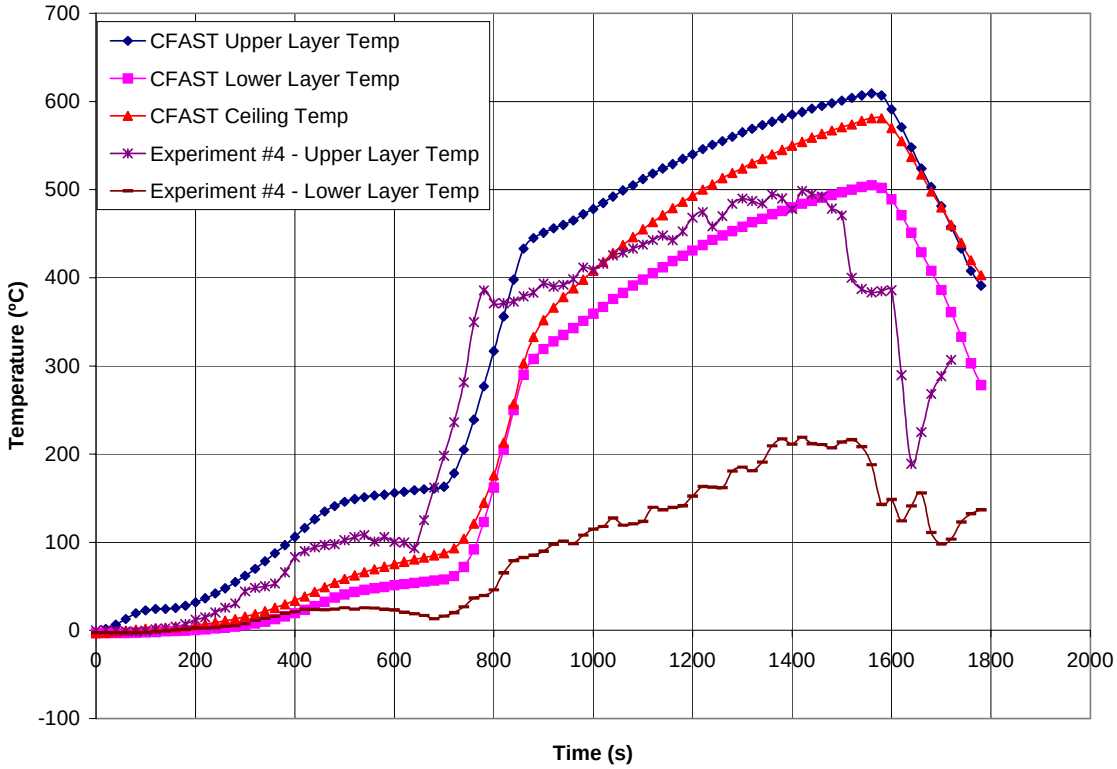

Figure 4.16: CFAST vs. Experiment #4

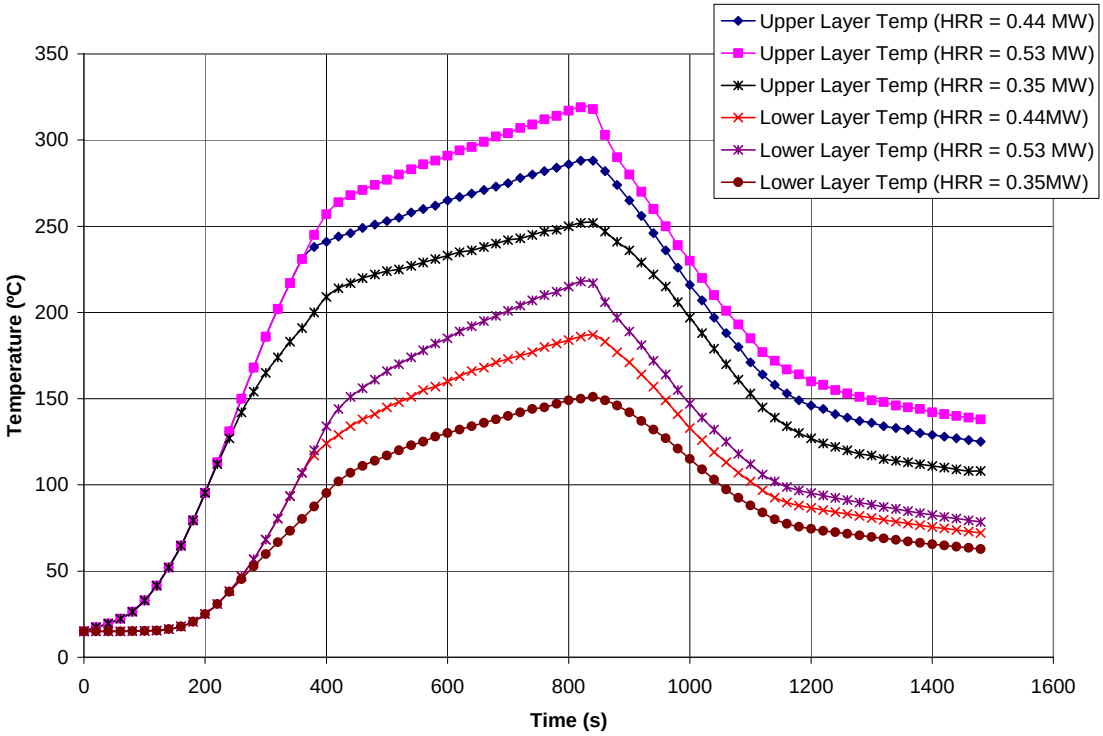

Figure 4.17: Variance in Layer Temperatures with Change in HRR

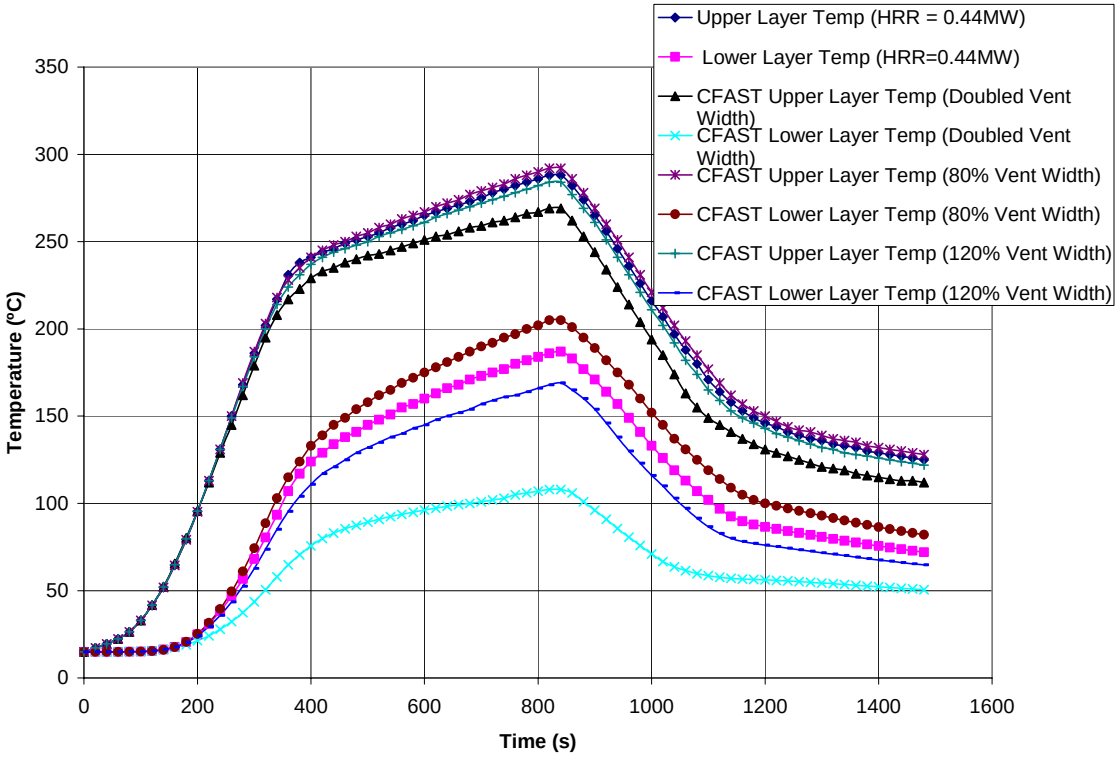

Figure 4.18: Variance in Layer Temperatures with Change in Vent Width

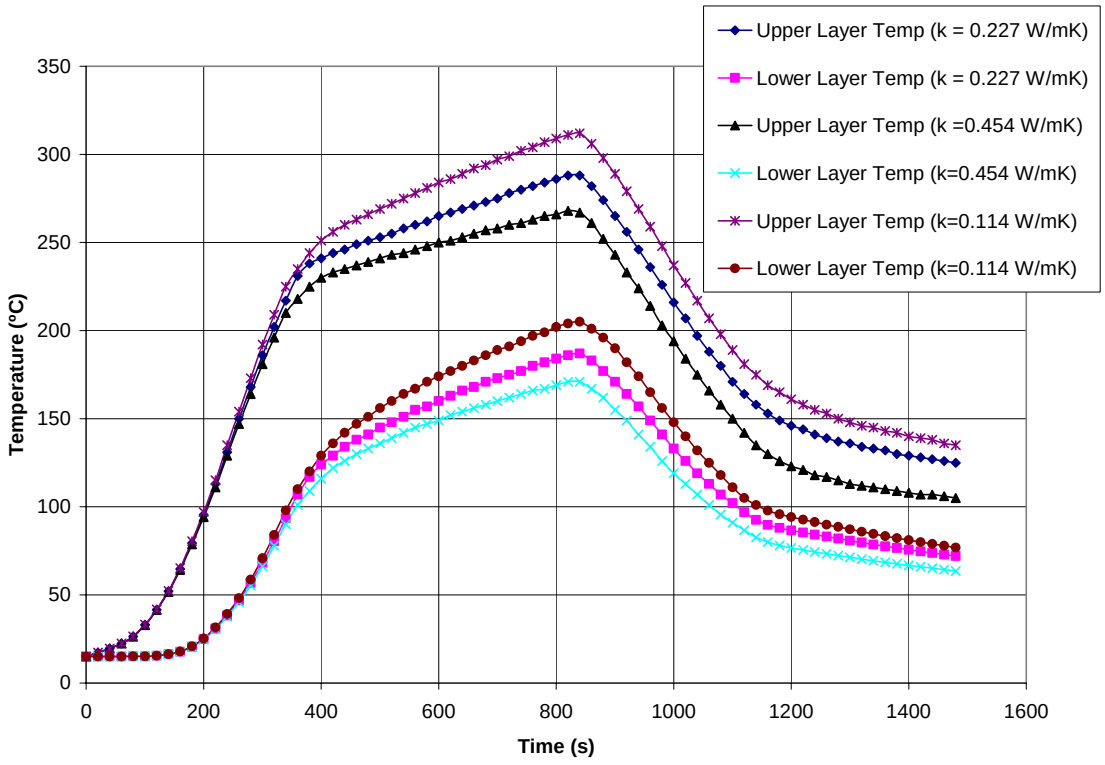

Figure 4.19: Variation in Layer Temperatures with Change in Thermal Conductivity

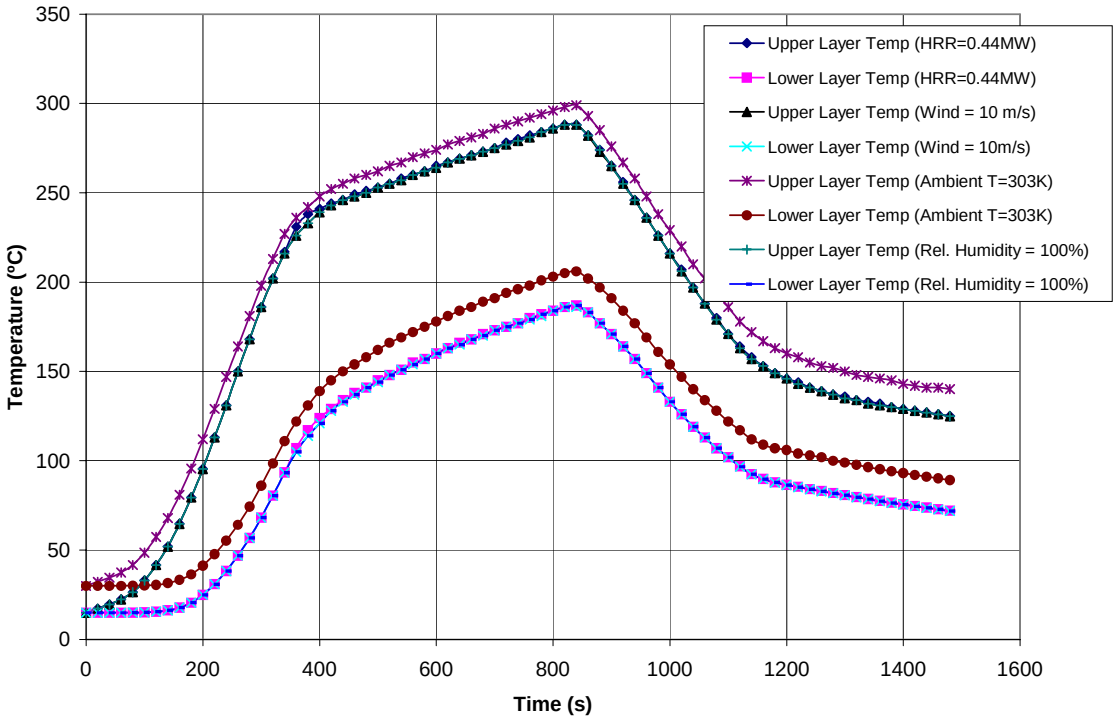

Figure 4.20: Variance in Layer Temperatures with Change Ambient Conditions

CHAPTER FIVE

Conclusions and Recommendations

5.1 Conclusions

The primary objective of this thesis was to report the results of a commissioning study of burn experiments, undertaken in the new University of Waterloo, Fire Research Group Burn House. The purpose was to determine the operating parameters and thermal characteristics of the main burn room as a working model for realistic full scale structural fire tests.

To achieve this objective four full-scale compartment fire tests were designed, instrumented and measured for the purpose of characterizing the thermal behaviour in Room 1 of the University of Waterloo Burn House structure. These initial experiments were conducted to establish that the fire behaviour in the Burn House is representative of residential structural fire behaviour which will provide a basis for future Burn House research activities.

CHAPTER FIVE – CONCLUSIONS AND RECOMMENDATIONS

The first experiment was performed in January, 2004 with a moderate fuel loading comprised mainly of wooden pallets. The fire was allowed to burn to extinction and analysis of the first experimental results indicated the possibility of instrumentation errors which were compensated for in subsequent experiments by replacing and installing additional thermocouple wire. A slightly higher fuel loading was incorporated for the second experiment, which resulted in a larger fire, higher burn room temperatures and subsequent ignition of the plywood ceiling and material located in the adjacent hallway. A well controlled experiment was achieved for the third experiment, by reducing the fuel loading and removing any secondary sources of fuel (such as the plywood ceiling) that could potentially be ignited. Much lower burn room temperatures were achieved and results demonstrated a well behaved temperature history throughout the duration of the burn; very few extraneous events or extreme fluctuations in the temperature profile were observed, making this experiment the most controlled and best behaved fire model. For the fourth experiment, a plywood ceiling layer was added again, this time extending approximately half way down the burn room walls. The fuel loading for this experiment was increased over the previous experiment. The temperature results and visual observations of the burn room indicated full room involvement in fire.

Potential sources of error in these experiments were discussed. Erroneous measurements were attributed to faulty thermocouples as a result of the effects of aging and mishandling in previous experiments. The error associated with these items could not be quantified. A brief discussion was provided regarding the error associated with the time response of the thermocouples. The time response of the thermocouples were calculated to be faster than the sampling rate of the data acquisition system, however, this response will still be slower than the temperature changes of the flow, which will result in temperature measurement inaccuracies. In addition, the slower sampling rate of the data acquisition system will also mean that the time-temperature history of the flow will be shifted slightly in time. Error due to radiation effects was not quantified in this study but will likely be significant and vary throughout the course of the experiments with

changing gas and surrounding temperatures. Measurement error due to radiation effects was estimated to be as large as 20% in the lower layer during fully developed fire conditions. An uncertainty analysis was performed on sample measurements of thermocouples in Rake 2 for Experiment #4. This analysis showed that measurement inaccuracies within +/- 0.04 ºC with a 95% confidence level can generally be expected for steady state temperatures measurements.

A comparative study was made between Burn House experimental results and previous University of Waterloo fire studies. Initial observations indicated that Experiment #3 and Waterloo House Fire Test #8 likely had comparable fuel loadings. This assumption was based on particular curve similarities such as fire growth rate and maximum temperatures achieved during steady state conditions. Least squares quadratic curve fits for both burn experiments illustrated t-squared growth rate patterns, typical of compartment fire behaviour. Additional comparisons were made between Burn House Experiment #4 and Waterloo House Fire #1 and again between Experiment #3 and HFOS-I experimental data. All comparisons demonstrated typical t-squared growth rate patterns. Experiment #3 results showed relatively steady temperatures during fully developed fire conditions.

Experiments #3 and #4 were modelled using a two-zone model, CFAST. Comparisons were made between the present experimental data and model predictions with the intention of establishing the level of confidence in CFAST as an off-the-shelf predictive tool for modelling future Burn House fire scenarios. These comparisons showed that upper layer temperatures can be predicted reasonably well with the model. Results of these comparisons showed that lower layer temperatures were grossly and consistently over-predicted by the CFAST model.

A sensitivity analysis was undertaken to explore the variation in predicted model results with a change in user specified variables. The analysis demonstrated that differences in predicted temperatures will typically be small (less than a 20ºC change) for variations in user specified variables, with the exception of predicted lower layer temperatures when vent widths are doubled and for all temperature predictions when heat release rates are varied by 20%. In the former, a 79ºC decrease in lower layer temperature was observed for a doubling in vent width. This is likely due to an increase of fresh ambient air at the sill of the openings. In the latter, upper and lower layer temperature predictions increased by 31ºC and 36ºC for variations in heat release rates of 20%.

The heat release rate is the single most important physical input to CFAST that needs to be defined to model a fire. The accuracy of model results will strongly depend on the user's ability to define the heat release rate curve. The methods incorporated in this study were based on experimental observations. Use of empirical correlations is possible, but these have often been developed for specific fuel configurations only.

Other potential sources of variation in model predictions were discussed and include assumptions and limitations inherent in the model such as the specification of the physical processes in the burn room derived from theoretical equations (conservation), empirical correlations and experimental data. CFAST is a two-zone model which incorporates the assumption that the burn room can be approximated by two large control volumes within which temperatures and properties are considered to be spatially uniform.

5.2 Recommendations for Future Experimental Work

The Burn House is part of a unique testing facility which has the capability of testing a vast number of variables relating to structural fire behaviour. This study was focused on performing an initial set of experiments that were designed to study the thermal development in one room of the Burn House. The information obtained from the experiments in this study can be used as a reference for future experimental work.

In this section, a list of potential recommendations for future research activities have been provided as they pertain to further experimental investigation of the fire characteristics and behaviour of the Burn House:

1. As previously discussed, one of the main features of the Burn House structure is that it can be positioned outside the facility and exposed to ambient conditions or it can be placed inside the test facility itself. Experiments should be carried out inside the facility to assess the effects of ambient conditions on fire behaviour in the Burn House.

2. Fire behaviour in other rooms inside the Burn House should be studied.

3. Forced ventilation scenarios using the Burn House's unique wind generation system should be studied.

4. Further research should be aimed at determining the development of an interface height during fire growth. This could be accomplished through additional experimentation and collection of more detailed temperature stratification data in conjunction with a visual analysis of layer development and mathematical analysis of temperature stratification curves. This will aid in determining a more

realistic indication of upper and lower layer heights for use with CFAST model predictions.

5. Studies should be performed to determine changes in fire behaviour when varying fuel type and sizes, configurations and burn room linings.

6. Sampling of burn room gases to determine concentration of toxic and non-toxic combustion products should be performed in future experimental work.

7. Evaluation of the predictive capabilities of more sophisticated fire models, (for example, Fire Dynamics Simulator (FDS)) for use in future Burn House experimentation and analysis.

5.3 Summary of Major Conclusions

The following provides a summary of the main conclusions established in this work as they relate to the stated objectives of this thesis.

1. A comparison of fire growth during the initial growth period against other structural fire data showed that Burn House fire behaviour is typical of residential structural fire behaviour. To this end, it is assumed from the results of this study that the Burn House structure will continue to produce results much the same as can be expected from a real residential structure.

2. Comparisons of data with predictions from the CFAST fire growth model showed reasonably consistent agreement in upper layer temperature results, which gives a good level of confidence in the use of CFAST as an overall

predictor of upper layer temperature predictions for future burn house experimentation. Continued use of the model and incorporation of the suggested recommendations for resolving an interface height to aid in future comparisons will further improve the confidence of the model's use and in its predictions.

3. As discussed in this work and in a supplementary report provided in Appendix B, there was no visual indication or observation that the Burn House structure suffered any loss of structural integrity due to the exposure of high fire temperatures in these experiments. In addition, the wall and ceiling liners of the burn room were considered to have been more than adequate as thermally protective barriers. Although the cement board liner experienced considerable damage after these four experiments, it is anticipated that by completing the suggested recommendations outlined in Appendix B that at least 10 burn experiments could be achieved from a single installation of liner materials.

4. Although the Burn House was constructed with the intent of withstanding repeated fire testing, some consideration should be given to suggested operating parameters (i.e. fuel load) for future research activities based on the results of the experiments presented here. As previously mentioned, observations during this study indicated that there was no loss of structural integrity to the Burn House and, in addition, the lining material proved to adequately protect the surface of the burn room; therefore the fuel loadings and configurations studied throughout these experiments can be considered to be within safe operating limits. From estimated heat release curves and CFAST predictions, the maximum fuel loading was for Experiment #4 which was approximately 1.2 MW in size with an additional sacrificial ceiling layer as a secondary source of fuel. The ability of the Burn House and its subsequent lining materials to withstand fuel loads higher than this cannot be determined; however, CFAST can be utilized to predict expected burn room upper layer temperatures as an initial indication. For the

time being, it is recommended that the fuel loads in the burn room not exceed the loads that have already been tested. Other types of fuel sources not considered in this study may be chosen for future experimental work; however, careful consideration should be given to anticipated heat release, burn room temperatures and expected fire damage. Lastly, future burn experiments should not be performed in the absence of burn room protective liners, as recommended in Appendix B.

REFERENCES

[1] Council of Canadian Fire Marshals and Fire Commissioners. (2001) Annual Report: Fire Losses in Canada. [online] Available from: http://www.ccfmfc.ca/stats/en/report_e_01.pdf [Accessed January 2005]

[2] Barnett, Jonathan R. (1997) Fire: *Encarta Online Encyclopedia*. [online] Available from: http://encarta.msn.com/text_761563809__15/Fire.html [Accessed January 2005]

[3] Forintek Canada Corp. (2002) Fire Safety – A Wood Frame Building Performance Fact Sheet. [online] Available from: www.forintek.ca [Accessed January 2005]

[4] Poole, Gordon Murray. (1995) *An Experimental Investigation of Hot Layer Development in Structures Subjected to Interior Fires.* M.A.Sc. Thesis, University of Waterloo.

[5] Drysdale, D. (1998) *Introduction to Fire Dynamics. Second Edition*. ISBN: 0 471 97290 8. United Kingdom: John Wiley and Sons Ltd.

[6] Naruse, T. & Hasemi, Y. (2000) Wind Effect of Fire Behaviour on Compartments. *Fifteenth meeting of the UJNR Panel on Fire Research and Safety,* San Antonio, Texas, U.S.A., March 1 – 7, 2000, (2) pp.399-405.

[7] (2001) Experimental Study of Fire Ventilation During Fire fighting Operations. *Fire Technology*, (37) pp.69-85.

[8] Poreh, M. & Trebukov, S. (2000) Wind Effects on Smoke Motion in Buildings. *Fire Safety Journal*, (35) pp.257-273.

[9] Sekine, T. (1997) Behaviour of Wind Blown Crib Fires. *Thirteenth Meeting of the UJNR Panel on Fire Research and Safety*, Gaithersburg, Maryland, U.S.A., March 13-20, 1996. (1).

[10] Weisinger, Jennifer. (2004) *Characterization of the University of Waterloo Live Fire Research Facility Wind Generation System.* M.A.Sc. Thesis, University of Waterloo.

[11] Walton, William D. & Thomas, Philip H. (2002) Estimating Temperatures in Compartment Fires. *SFPE Handbook of Fire Protection Engineering, Second Ed.* [online]. 6(3) pp.134-147. [online] Available from: http://fire.nist.gov/bfrlpubs/fire95/PDF/f95044.pdf [Accessed January 2005]

[12] Reneke, Paul & Jones, Walter (2001) A comparison of CFAST Predictions to USCG Real-Scale fire Tests. *Journal of Fire Protection Engineering.* 11(1) pp.43-68

[13] Peacock, R., Forney, G., Reneke, P., Portier, R. & Jones, W. (1993) *CFAST: The Consolidated Model of Fire and Smoke Transport. Technical Note 1299*. Gaithersburg, Maryland: Building and Fire Research Laboratory, NIST.

[14] Floyd, J. & Wolf, L. (1998) *Evaluation of the HDR Fire Test Data and Accompanying Computational Activities with Conclusions from Present Code Capabilities, Volume 3: Test Description and CFAST Validation for T51 Wood Crib Fire Test Series. Report NUMAFIRE:03-98*. College Park, Maryland: Department of Materials and Nuclear Engineering, University of Maryland.

[15] Klote, J. (2002) Design Fires, What You Need to Know: *HPAC Engineering*. [online] Available from: http://www.hpac.com/member/feature/2002/0209/0209klote.htm [Accessed January 2005]

[16] Lee, E., Yuen, R., Lo, S. & Lam, K. (2002) *Probabilistic Inference with Maximum Entropy for Prediction of Flashover in a Single Compartment Fire*. Hong Kong: Department of Building and Construction, City University of Hong Kong.

[17] Thomas, P. (2004) SFPE Classic Paper Review: Fire Behaviour in Rooms by Kunio Kawagoe. *Journal of Fire Protection Engineering*. (14) pp. 5-9.

[18] Sugawa, Osami. (1996) *Thirteenth Meeting of the UJNR, NIST: Progress report on Full Scale Fire Test in Japan*, Tokyo: Centre for Fire Science and Technology, University of Tokyo.

[19] Ministry of Construction, Japan. (2002) *Building and Research Institute.* [online] Available from : http://www.kenken.go.jp/english/ [Accessed January 2005]

[20] Weckman, E.J., Dale, J.D., Strong, A.B., & Ackerman, M. *HFOS (House Full of Sprinklers) I, Part 2: Development of a Living Room Fire in an Unsprinklered Single Family Residence*. Unpublished report. Department of Mechanical Engineering, University of Waterloo.

[21] Putorti, A., Walton, W.D., Twilley, W.H., Deal, S. & Albers, J.C. (1995) Santa Ana Fire Department Experiment at 1315 South Bristol, July 14, 1994. Technical Note. *Fire Technology*, (1) pp. 63-76.

[22] Poole, G., Weckman, E.J & Strong, A.B. (1995) *Hot Layer Development in Structural Fires: Experiment and Prediction*. Unpublished report. Department of Mechanical Engineering, University of Waterloo.

[23] Daniels, J. (2003) *Report on the Stratification Analysis During Growth Phase of a Class A House Fire*. Unpublished report. Department of Mechanical Engineering, University of Waterloo.

[24] Putorti, A. & McElroy, J. (1998) Full Scale House Fire Experiment for InterFIRE VR, May 6, 1998. Gaithersburg Maryland: Building and Fire Research Laboratory, NIST.

[25] National Research Council. (2005) *Construction Innovation, Volume 10: Carleton and NRC Team up to Expand Fire Research Facilities*. [online] Available from: http://irc.nrc-cnrc.gc.ca/pubs/ci/v10nol/v10nol_5_e.html [Accessed April 2005]

[26] Department of Civil Engineering, University of Canterbury. (1995) *Student Research Reports*. [online]. Available from: http://www.civil.canterbury.ac.nz/fire/fe_resrch_reps.html [Accessed June 2004]

[27] Neilsen, C. (2000). *An Analysis of Pre-Flashover Fire Experiments with Field Modelling Comparisons*. M.A.Sc. Thesis, University of Canterbury.

[28] Yii, E. (2002). *Modelling the Effects of Fuel Types and Ventilation Openings on Post-Flashover Compartment Fires.* Ph.D. Thesis, University of Canterbury.

[29] Weaver, S. (2000). *A Comparison of Data Reduction Techniques for Zone Model Validation.* New Zealand: University of Canterbury.

[30] Nyman, J. (2002). *Equivalent Fire Resistive Ratings of Construction Elements Exposed to Realistic Fires*. M.A.Sc. Thesis, University of Canterbury.

[31] Wastney, C. (2002) *Performance of Unprotected Steel and Composite Steel Frames Exposed to Fire.* M.A.Sc. Thesis, University of Canterbury.

[32] *Building and Fire Research Laboratory Publications.* (2005) [online] Gaithersburg, Maryland: National Institute of Standards and Technology. Available from: http://fire.nist.gov/bfrlpubs/ [Accessed November 2004]

[33] Milke, J.A. & Hill, S.M. (1996) BFRL Publications Online. *Full Scale Room Fire Experiments Conducted at the University of Maryland.* [online] Available from: http://fire.nist.gov/bfrlpubs/ [Accessed November 2004]

[34] Mingchun, L., He, Y. & Beck, V. (1996) *Application of a Field Model and Two-Zone Model to Flashover Fires in a Full-Scale Multiroom Single Level Buildling*. Victoria, Australia: Victoria University of Technology.

[35] Mingchun, L., & Beck, V. (1995) *A study of Non-Flashover and Flashover Fires in a Full-Scale Multi-Room Building*. Victoria, Australia: Victoria University of Technology.

[36] Svensson, Stefan. (1996) *Rapport Raddningstjanstavdelningen R53-132/96, Live Fire Tests using Explosive Cutting Frame and Positive Pressure Ventilation*. Sweden: Swedish National Testing and Research Institute.

[37] Svensson, Stefan. (1996) *Rapport Raddningstjanstavdelningen R53-159/96, Live Fire Tests with Fire and Smoke Ventilation in a Small Apartment*. Sweden: Swedish National Testing and Research Institute.

[38] Svensson, Stefan. (1996) *Rapport Raddningstjanstavdelningen R53-147/96, Simulation of Smoke and Fire Ventilation using CFAST*. Sweden: Swedish National Testing and Research Institute.

[39] Swedish National Testing and Research Institute Published Reports. (2005) [online] Sweden: Swedish National Testing and Research Institute. Available from: http://www.sp.se/fire/br_reports.HTM [Accessed October 2005]

[40] Walton, William D. (2002) Computer Fire Models for Enclosures. *SFPE Handbook of Fire Protection Engineering Third Edition*, 7(3) pp.189-193.

[41] Bounagui, A. & Bénichou, N. (2003) *Literature Review on the Modeling of Fire Growth and Smoke Transport*. Ottawa, Canada: Institute for Research in Construction, National Research Council Canada.

[42] Quintiere, J.G. (1995) Compartment Fire Modeling. *SPFE Handbook of Fire Protection Engineering, National Fire Protection Association*. pp.3-125.

[43] Fowkes, N.D. (1975). *A Study of Room Fire development: The Second Full-Scale Bedroom Fire Test of the Home Fire Project. Technical Report. No 21011.4.* Rhode Island, USA: Factory Mutual Research Corporation. pp.8-50.

[44] Zhuman, F. & Hadjisophocleous, G. (2000) A Two Zone Fire Growth and Smoke Movement Model for Multi-Compartment Buildings. *Fire Safety Journal.* (34) pp.257-285.

[45] National Institute of Standards and Technology. *Wooden Pallet Fire*. [online] Available from: http://www.fire.nist.gov/fire/fires/pall/pa.html [Accessed January 2004]

[46] Rehm, R.G., Hamins, A., Baum, H., McGratten, K. & Evans, D. (2002) BFRL Publications Online. *Community Scale Fire Spread, NISTIR Report 6891*. [online] Available from: http://fire.nist.gov/bfrlpubs/fire02/PDF/f02019.pdf [Accessed November 2004]

[47] Iding, Robert. (2003) *Calculating Structural Response to Fire.* [online] Society of Fire Protection Engineering, Issue 18. Available from: http://www.pentoncmg.com/sfpe/articles/idingfpe%20spring%2003.pdf. [Accessed March 2005]

[48] Blagojević, M. & Petković, D. (2001) *Detecting Fire in Early Stage – A New Approach. Working and Living Environmental Protection*. [online] Version 1, Volume 2. Available from: http://facta.junis.ni.ac.yu/facta/walep/walep2001/walep2001-03.pdf [Accessed March 2005]

[49] The MathWorks. *Matlab*. (Version 6, Release 12.1). (2001) The MathWorks, Inc. 3 Apple Hill Drive, Natick, MA.

[50] Picotech Technology Ltd. (2000) *Thermocouples – A Quick Guide*. [online] Available from: http://www.azom.com/details.asp?ArticleID=1208 [Accessed January 2005]

[51] Holman, J.P. (1994). *Experimental Methods for Engineers, Sixth Edition*. ISBN: 0-07-029666-9. USA: McGraw-Hill, Inc.

[52] MatWeb. (2005). *MatWeb, Material Property Data.* [online] Available from: http://www.matweb.com/search/SpecificMaterial.asp?bassnum=NHOS0 [Accessed January 2005]

[53] Incropera, F.P., & DeWitt, D.P. (2002). *Fundamentals of Mass and Heat Transfer, Fifth Edition.* ISBN: 0-471-38650-2. USA: John Wiley & Sons, Inc

[54] Weckman, E.J., Strong, A.B. & Heuser, M. (1991) *Temperature Compensation in Combusting Flows*. Unpublished report. Department of Mechanical Engineering, University of Waterloo.

[55] Francis, J. (2004) Radiant Network Models of Thermocouple Error in Pre and Post Flashover Compartment Fires. *Fire Technology.* (40) pp.277-294.

[56] Blevins, L.G. (1999) *Behaviour of Bare and Aspirated Thermocouples in Compartment Fires.* Advanced Fire Measurements Group, NIST. Gaithersburg, Maryland.

[57] USG Corporation. (2003). *Durock Brand Cement Board, Submittal Sheet 09300*. [online] Available from: http://www.usg.com/USG_Marketing_Content/usg.com/web_files/Documents/Pr

od_Data_and_Submittal_Sheets/DrckCement_Board-Submittal_Sheet_CB399.pdf [Accessed November 2005]

[58] *University of Waterloo Weather Station Data Archives*. (2005) [online] 1998-2005. Waterloo, Ontario, Canada: University of Waterloo. Available from: http://weather.uwaterloo.ca/info.htm. [Accessed November 2004]

[59] Jones, W., Peacock, R., Forney, G. & Reneke, P. (2004) *Consolidated Model of Fire Growth and Smoke Transport (Version 5), Technical Reference Guide. Special Publication.* Gaithersburg, Maryland, USA: National Institute of Standards and Technology, (Report 1030).

[60] Lundin, J. (1997) *Uncertainty in Smoke Transport Models.* Department of Fire Lund, Sweden: Lund Institute of Technology, Lund University, (Report 3086).

APPENDIX A

Sample MatLab Program Files

EXPERIMENT #3: SEPTEMBER 30, 2004

```
%   ------------------------------------------------------------
%
%   ANALYSIS OF BURN HOUSE DATA
%
%   ------------------------------------------------------------------

%       ----------------------------------------------------
%       Initialization
%
clc
clear
%
%       ----------------------------------------------------

%load the data

a=load('09_04_Rake2.csv');   % THIS IS THE ORIGINAL Sept/04 BURN DATA
FILE

time = a(:,2);
[m1,n1]=size (a)   % m1 rows ; (time steps),  n1 columns ;  (t/c
stations)

%   ------------------------------------------------------------

% FIND THE MAXIMUM TEMPERATURE IN THE DATA FILE
%
tmax=max(a(:,3:n1));
ttmax=max(tmax)
%
%-------------------------------------------------------------------------
-------
%       SET up plotting-time increments;  File 'a'  has m1 time steps
at 1 sec intervals
%
%       dt= plotting time increment integer multiple of recording
timestep
%
```

```
dt=60
it=1
itt=0
    while  it <= m1;
            itt=itt+1;     % itt = no. of plot times
         opt(itt)=time(it);   %  opt=designated  O/P times as
determined from data length ,m1, and specified time interval ,dt.
        it=it+dt;
    end

[mopt,nopt]=size(opt);
%
%       ------------------------------------------------------------
%
%      " kk "    -SET up T/C plot stations based on  file
%                   columns in MATRIX 'a'
%                -the max number is n1 else any number
%                   can be specified.
%
%      " kkloc " -SET up positions in 'inches' from the floor
%                   for each entry of the RAKE position designated by "
kk "
%                   - these are used for plotting the 'stratification'
curves
%
%      " tcloc " -SET up 'descriptors' for each entry of " kk "
%                 NOTE: there must be a 'descriptor' for every
%                 entry of the "kk" matrix


kk=[3 4 5 6 7 8 9 10 11 12 13 14 15 16 17 18 19 20 21 22 23 24 25 26
27];
kkloc=[0 0.5 2.5 7 10.5 17.5 19.5 23 25.5 30 34 34.5 38.5 42 47 51 54
58 62.5 65.5 71 73 76 84 84.5];

tcloc=strvcat( '      0 " from floor  ', ...
'       1/2 " from floor   ' , ...
'       2.5 " from floor   ' , ...
'       7 " from floor   ' , ...
'       10.5 " from floor   ' , ...
'       17.5 " from floor   ' , ...
'       19.5 " from floor   ' , ...
'       23 " from floor   ' , ...
'       25.5 " from floor   ' , ...
'       30 " from floor   ' , ...
'       34 " from floor   ' , ...
'       34.5" from floor   ' , ...
'       38.5 " from floor   ' , ...
'       42" from floor   ' , ...
'       47 " from floor   ' , ...
'       51 " from floor   ' , ...
'       54 " from floor   ' , ...
```

```
'       58 " from floor   ' , ...
'       62.5" from floor   ' , ...
'       65.5" from floor  ', ...
'       71" from floor  ', ...
'       73" from floor  ', ...
'       76" from floor  ', ...
'       1" from ceiling  ', ...
'       0.5" from ceiling ');


[mkkloc,nkkloc]=size(kkloc)
%       set ceiling height  " ch "
ch=85.

[mkk,nkk]=size(kk)
%
%       ------------------------------------------------------
%
%         " jj "-SELECT WHICH STATIONS TO BE GRAPHED;
%           -Choose which entries of matrix "kk" that
%            are to be plotted (-relative to position in matrix)
%
jj=[11 22 23 24 25 ]
[mjj,njj]=size(jj)

%   ------------------------------------------------------------

%          " ssym "-Set up print symbol matrix
%                  - there are 32 specified now;
%                  -add more as required.
%
ssym=strvcat('h ','x ','* ','v ','+ ','o ','s ','d ','^ ','p ', 'h ','x
','* ','v ','+ ', 'o ', 's ','d ','p ','h ','x ','* ','v ','+ ','o ')
[mssym,nssym]=size(ssym)
sym1=strvcat(ssym(1:njj,1))
%
%   ------------------------------------------------------------
%   ------------------------------------------------------------
%
%           " tp" set up plot time matrix based on " dt "
%           -  this assumes data records are at 1 sec intervals!

    for n=1:nopt-1
        tp(n)=n*dt;
    end
%
%   ------------------------------------------------------------
%
%       Set up for  FIG(1)
%
figure(3)
subplot(5,1,2:5)
```

```
hold on
grid on

    for i=1:njj
        plot(a(tp,2),a(tp,jj(i)+2),sym1(i))  % the '2' factor in
'jj(i)+2'
%                                               is because columns of
data matrix 'a'
%                                               are shifted two columns
from
%                                               their positions in
matrix 'kk'
end

        legend(tcloc(jj(1:njj),:),1)
        set(legend,'fontsize',6)

        tstring=sprintf('%s\n%s\n','FIG(3).  TEMPERATURE vs TIME PLOTS
FOR SELECTED  ',' T/C POSITIONS on the VERTICAL RAKE 2');
        h=title(tstring)
        set(h,'fontsize',10)
        xlabel('TIME(sec)')
        ylabel('TEMPERATURE (C)  ')

        axis([0 dt*nopt 0 ttmax+20])

        tstring=sprintf('%s\n%s\n%s\n%s\n%s','THIS FIRE WAS SET UP IN
','ROOM  1 OF THE UofW BURN HOUSE','SEPT 30, 2004','FIRE LOAD ~1.0 MW,
CLASS A-Pallets','WATERLOO FIRE DEPT ON SITE')

        h=text(1500,500,tstring)
        set(h,'fontsize',6)
hold off

% ------------------------------------------------------------------
%
%       SET UP FOR PLOTTING STRATIFICATION TIME DEVELOPMENT OVER TIME
%
%-------------------------------------------------------------------
-
%
%   ---------------------------------------------------------
%
%       " kkt "= TIMES TO PLOT STRATIFICATION CURVES (in SECONDS)
%       "strkkt" required because I don't know how to set up
%               the legend otherwise!
%
kkt=[60 120 240 480 600 900 1200 1500]
strkkt=strvcat(' 60 sec','120 sec','240 sec','480 sec', ...
    '600 sec','900 sec','1200 sec','1500 sec')
```

```
[mkkt,nkkt]=size(kkt)
sym2=strvcat(ssym(1:nkkt,1))

%   ------------------------------------------------------------
%   SET UP FIGURE (2)
%
figure(4)

subplot(5,1,2:5)

tstring=sprintf('%s\n%s\n','FIG(4).  TEMPERATURE STRATIFICATION, RAKE
2, TEMPERATURE (C) vs HEIGHT (in)', ...
    'FOR SELECTED TIMES OF FIRE DEVELOPMENT')
h=title(tstring)
set(h,'fontsize',10)

hold on
axis([0 ttmax+20 0 ch+20])

for i=1:nkkt
    plot(a(kkt(i),3:27),kkloc(1,1:nkkloc),sym2(i))  %this vector length
has to make # of rake entries
end

xlabel('TEMPERATURE(C) at VARIOUS TIMES OF THERMAL DEVELOPMENT')
ylabel('HEIGHT FROM FLOOR(in)')

legend(strkkt(1:nkkt,:),4)
set(legend,'fontsize',6)

ceil=linspace(0, ttmax,500);
plot(ceil,ch,'--')

tstring=sprintf('%s%d%s','ceiling height is =',ch,' in')
h=text(300,90,tstring)

hold off
```

EXPERIMENT #4: NOVEMBER 25, 2004

```
%   ------------------------------------------------------------
%
%   ANALYSIS OF BURN HOUSE DATA
%
%   ------------------------------------------------------------

%       ----------------------------------------------------
%       Initialization
%
clc
clear
%
%       ----------------------------------------------------

%load the data

a=load('11_04_Rake2.csv');   % THIS IS THE ORIGINAL Nov/04 BURN DATA
FILE

time = a(:,2);
[m1,n1]=size (a)   % m1 rows ; (time steps),  n1 columns ;  (t/c
stations)

%   ------------------------------------------------------------

% FIND THE MAXIMUM TEMPERATURE IN THE DATA FILE
%
tmax=max(a(:,3:n1));
ttmax=max(tmax)
%
%-------------------------------------------------------------------------
-------
%       SET up plotting-time increments;  File 'a'  has m1 time steps
at 1 sec intervals
%
%       dt= plotting time increment integer multiple of recording
timestep
%
dt=60
it=1
itt=0
    while  it <= m1;
            itt=itt+1;     % itt = no. of plot times
         opt(itt)=time(it);   %  opt=designated  O/P times as
determined from data length ,m1, and specified time interval ,dt.
        it=it+dt;
    end
```

```
[mopt,nopt]=size(opt);
%
%       ------------------------------------------------------------
%
%      " kk "    -SET up T/C plot stations based on  file
%                   columns in MATRIX 'a'
%                -the max number is n1 else any number
%                   can be specified.
%
%      " kkloc " -SET up positions in 'inches' from the floor
%                   for each entry of the RAKE position designated by "
kk "
%                   - these are used for plotting the 'stratification'
curves
%
%      " tcloc " -SET up 'descriptors' for each entry of " kk "
%                 NOTE: there must be a 'descriptor' for every
%                 entry of the "kk" matrix


kk=[3 4 5 6 7 8 9 10 11 12 13 14 15 16 17 18 19 20 21 22 23 24 25 26
27];
kkloc=[0 0.5 2.5 7 10.5 17.5 19.5 23 25.5 30 34 34.5 38.5 42 47 51 54
58 62.5 65.5 71 73 76 84 84.5];

tcloc=strvcat( '      0 " from floor  ', ...
'       1/2 " from floor   ' , ...
'       2.5 " from floor   ' , ...
'       7 " from floor   ' , ...
'       10.5 " from floor   ' , ...
'       17.5 " from floor   ' , ...
'       19.5 " from floor   ' , ...
'       23 " from floor   ' , ...
'       25.5 " from floor   ' , ...
'       30 " from floor   ' , ...
'       34 " from floor   ' , ...
'       34.5" from floor   ' , ...
'       38.5 " from floor   ' , ...
'       42" from floor   ' , ...
'       47 " from floor   ' , ...
'       51 " from floor   ' , ...
'       54 " from floor   ' , ...
'       58 " from floor   ' , ...
'       62.5" from floor   ' , ...
'       65.5" from floor  ', ...
'       71" from floor  ', ...
'       73" from floor  ', ...
'       76" from floor  ', ...
'       1" from ceiling  ', ...
'       0.5" from ceiling ');
```

```
[mkkloc,nkkloc]=size(kkloc)
%       set ceiling height  " ch "
ch=85.

[mkk,nkk]=size(kk)
%
%       ------------------------------------------------------------
%
%         " jj "-SELECT WHICH STATIONS TO BE GRAPHED;
%           -Choose which entries of matrix "kk" that
%            are to be plotted (-relative to position in matrix)
%
jj=[11 22 23 24 25 ]
[mjj,njj]=size(jj)

%   ---------------------------------------------------------------

%          " ssym "-Set up print symbol matrix
%                  - there are 32 specified now;
%                  -add more as required.
%
ssym=strvcat('h ','x ','* ','v ','+ ','o ','s ','d ','^ ','p ', 'h ','x
','* ','v ','+ ', 'o ', 's ','d ','p ','h ','x ','* ','v ','+ ','o ')
[mssym,nssym]=size(ssym)
sym1=strvcat(ssym(1:njj,1))
%
%   ---------------------------------------------------------------
%   ---------------------------------------------------------------
%
%           " tp" set up plot time matrix based on " dt "
%           -  this assumes data records are at 1 sec intervals!

    for n=1:nopt-1
        tp(n)=n*dt;
    end
%
%   ------------------------------------------------------------
%
%       Set up for  FIG(1)
%
figure(3)
subplot(5,1,2:5)

hold on
grid on

    for i=1:njj
        plot(a(tp,2),a(tp,jj(i)+2),sym1(i))  % the '2' factor in
'jj(i)+2'
%                                               is because columns of
data matrix 'a'
```

```
%                                                   are shifted two columns
from
%                                                   their positions in
matrix 'kk'
end

        legend(tcloc(jj(1:njj),:),1)
        set(legend,'fontsize',6)

        tstring=sprintf('%s\n%s\n','FIG(3).  TEMPERATURE vs TIME PLOTS
FOR SELECTED  ',' T/C POSITIONS on the VERTICAL RAKE 2');
        h=title(tstring)
        set(h,'fontsize',10)
        xlabel('TIME(sec)')
        ylabel('TEMPERATURE (C)  ')

        axis([0 dt*nopt 0 ttmax+20])

        tstring=sprintf('%s\n%s\n%s\n%s\n%s','THIS FIRE WAS SET UP IN
','ROOM  1 OF THE UofW BURN HOUSE','NOV 25, 2004','FIRE LOAD ~1.0 MW,
CLASS A-Pallets','WATERLOO FIRE DEPT ON SITE')

        h=text(1500,500,tstring)
        set(h,'fontsize',6)
hold off

% ------------------------------------------------------------------------
%
%       SET UP FOR PLOTTING STRATIFICATION TIME DEVELOPMENT OVER TIME
%
%------------------------------------------------------------------------
-
%
%   ------------------------------------------------------------
%
%       " kkt "= TIMES TO PLOT STRATIFICATION CURVES (in SECONDS)
%       "strkkt" required because I don't know how to set up
%               the legend otherwise!
%
kkt=[60 120 240 480 600 900 1200 1500 1800]
strkkt=strvcat(' 60 sec','120 sec','240 sec','480 sec', ...
    '600 sec','900 sec','1200 sec','1500 sec','1800 sec')

[mkkt,nkkt]=size(kkt)
sym2=strvcat(ssym(1:nkkt,1))

%   ------------------------------------------------------------
%   SET UP FIGURE (2)
%
figure(4)

subplot(5,1,2:5)
```

```
tstring=sprintf('%s\n%s\n','FIG(4).  TEMPERATURE STRATIFICATION, RAKE
2, TEMPERATURE (C) vs HEIGHT (in)', ...
    'FOR SELECTED TIMES OF FIRE DEVELOPMENT')
h=title(tstring)
set(h,'fontsize',10)

hold on
axis([0 ttmax+20 0 ch+20])

for i=1:nkkt
    plot(a(kkt(i),3:27),kkloc(1,1:nkkloc),sym2(i))  %this vector length
has to make # of rake entries
end

xlabel('TEMPERATURE(C) at VARIOUS TIMES OF THERMAL DEVELOPMENT')
ylabel('HEIGHT FROM FLOOR(in)')

legend(strkkt(1:nkkt,:),4)
set(legend,'fontsize',6)

ceil=linspace(0, ttmax,500);
plot(ceil,ch,'--')

tstring=sprintf('%s%d%s','ceiling height is =',ch,' in')
h=text(300,90,tstring)

hold off
```

APPENDIX B

A Report: Design and Function of the Burn House Lining

APPENDIX B – REPORT: DESIGN AND FUNCTION OF BURN HOUSE LINING

I, A.B. Strong, hereby give permission to Amanda Klinck, co-author of the report "Design and Function of Wall and Ceiling Liners For the U of W Burn Building" by A. Klinck and A.B. Strong, to reproduce, distribute, and include this report as part of her MASc thesis entitled "An Experimental Investigation of the Fire Characteristics of the University of Waterloo Burn House Structure" at her discretion.

APPENDIX B

FOREWORD: A copy of the report

"DESIGN AND FUNCTION of WALLS AND CEILING LINERS FOR THE U of W BURN BUILDING"

By A. J. KLINCK & A. B. STRONG

is attached to this thesis for the purpose of providing the readers with a more detailed summary of the issues which were considered in determining the liners for the burn room and as well to provide a chronology of observations of how the liners behaved during the succession of the four burns and the steps taken to correct minor deficiencies. Much of the design and construction of the burn room liner was undertaken by one of authors (ABS) and thus the report is considered ancillary to this thesis but is attached to provide information for future researchers and potentially for clarification purposes to readers of this thesis.

DESIGN AND FUNCTION of WALL AND CEILING LINERS FOR THE U of W BURN BUILDING

By A. J. KLINCK & A. B.STRONG

UNIVERSITY OF WATERLOO

FIRE RESEARCH GROUP

WATERLOO, ONTARIO

Nov. 18, 2005

1. INTRODUCTION

The purpose of the U of W burn house was to develop a facility in which multiple and sequential burns could be performed with minimum damage to the burn room(s) and the civil structure. This facility has a welded steel plate and H-beam civil structure and experience with unprotected steel structures undergo serious damage after repetitive exposure to temperatures in the expected test range (up to ~1000 ºC). More importantly it is the intention to evaluate the fire performance of fire preventive materials and paints that are manufactured for the building industry and a suitable sub- structure is required so that these materials can be easily mounted .Thus the purpose of liners in the burn rooms of the steel structure is twofold: firstly to thermally protect the civil structure and secondly to provide a sub structure over the steel so that attached test materials can easily be affixed and that would remain relatively undamaged after the burn. Given the destructive nature of fire it is inevitable that any exposed combustible room materials will need to be replaced either due to damage or by design.

The budget for linings is very minimal and this does not allow for adopting the lining strategy that commercial fire testing laboratories or some of the more modern fire training facilities have (i.e. WRESTRC uses HTL ceramic liners over pagenite board on a concrete civil structure at a cost of about $200.00 sq.ft.). The function and civil structure of the present facility is somewhat unique and the prospect of designing a functional, practical and cheap liner that does not require bringing in specialty trades and /or design teams presented an interesting challenge.

The purpose of this special report is to summarize the present design, the choice of materials used and present, via visual observation and experiences during fire suppression activities, the steps taken to correct problems over the period of four burns.

It is hoped that this summary will benefit future users of the burn house in their research endeavours.

2. DESIGN, MATERIALS AND METHODOLOGY.

The linear expansion coefficient for carbon steel is about 2.4 $x10^{-6}$ / ^{0}C [1]. An estimate of the effect of thermal expansion of the exposed steel plate 2.66 m high from an initial temperature of 20^{0}C to 400^{0}C, using an average vertical temperature suggests a change in length of about 10 mm. This figure is obviously high as the steel temperature is not constant over its extent as is assumed here however there will clearly be differential expansion of the steel sheet from bottom to top and longitudinally along the wall which will severely stress the welded joints between sheets and to the H-beam civil structure. Warping of steel sheets and fracture of welds is inevitable over a series of burns. For this reason it was decided to develop a strategy for thermally protecting the structure with a liner.

A second reason for adding liner is the fact that because of the steel construction of walls and ceiling it is difficult and very time consuming to attach materials to the H-beam frame. A liner would provide for easy attachment of test materials should future experimenters be interested in studying the thermal behaviour of materials exposed to fire.

2.1 The Liner

A plan view of the burn room is shown as Figure 1. For purposes of easy identification in the following discussion the walls are designated N, S, E, and W (North, South, East, and West). Since the fire load is confined to the burn pad it was decided that the walls would be lined continuously from the exterior door on the E side around the S side and up to the W door at the stair entrance. The ceiling liner would cover that area

contained within that boundary. Initially all doors and windows are steel plate except the door leading from the burn room to the hall (NW corner) which is ¾" (19.1 mm) plywood.

The liner consists of three elements the most outer layer which is attached to the steel frame, strapping for accepting fasteners and a fire resistant material to protect the wood sub-wall.

The most difficult task was affixing the outer layer to the steel frame. For strength, holding ability and minimum cost it was decided to use ¾" x 4’ x 8’ (0.0191 x 1.22 x 2.44 m) sheets of plywood (RBS). Nine high strength beam clamps per sheet were attached to the 4" (106 mm) H-beams on the walls and the 8" (212 mm) I-beams on the ceiling. Each plywood sheet was then secured to these clamps with 3/8" x 2" (9.5 x 51 mm) cap screws through a 3/8" (9.5 mm) flat washer. 3/4" x 3 1/2" (19.0 x 81.3 mm) spruce strapping was then attached to the plywood 12" (0.305 m) OC throughout using #10 x 1 ½" (38 mm) steel Robertson head screw to be used as anchor strip for holding fasteners.

For the thermal protective liner, ½" x 3’ x 5’ (0.0127 x 0.910 x 1.520 m) Durock® cement board was chosen. The relevant properties of Durock® are given in Table 1.

Table 1: Relevant Properties of Durock ® Cement Board [2]

Property	Value
Weight	3 psf. (143.6 Pa)
Density	1152 kg/m^3
R value	0.26
k	0.277 (W/m ^oK)
Flame Spread	5
Smoke Index	0

The Durock board was screwed into the strapping with 3/16" x 3 1/4" (4.7 x 82.6 mm) Philips head Tapcon® concrete anchors at approximately 12" (305 mm) intervals over the board. The join seams made by the Durock® sheets were filled with mortar cement as per [2].

As an estimate of its effectiveness a steady state conduction heat transfer calculation was performed. For steady state conditions, the heat flux for a four layer composite wall (which includes the 4" (102 mm) air gap between the plywood and the steel wall but neglects the airspace between the Durock® and plywood) is given by [4],

$$q'' = (T_{hot} - T_{ambient}) \; / \; (h_{hot} + L_{Durock}/k_{Durock} + L_{plywood}//k_{plwood} + L_{air}/k_{air} + L_{steel}//k_{steel} + 1/h_{ambient}) \qquad (W/m^2\,K) \qquad (1)$$

Table 2 shows estimates of material properties and data used in the calculation.

Table 2: Data Used for Surface temperature Calculations [2,3].

k_{Durock}	0.277 W/mK	[2]
L_{Durock}	0.0127 m	
$k_{plywood}$	0.11 W/mK	[1]
$L_{plywood}$	0.019 m	
k_{air}	0.04 W/mK	[3]
L_{air}	0.106 m	
k_{steel}	22 W/mK	[1]
L_{steel}	0.0047 m	
$h_{ambient}$	10 W/m^2 K	Typical for low wind speed
h_{hot}	20 W/m^2 K	Laminar flow estimate of wall jet
$T_{ambient}$	0 ^oC	Typical for winter/spring test
T_{hot}	400 ^oC	Average of observed room temperatures

For the protected wall the heat flux is estimated to be 126. (W/m^2 K) whereas in the case of exposed steel the heat flux is m 2533. (W/m^2 K) . The exterior skin temperature of the steel can be estimated using (from [4]:

$$q'' = h_{ambient} \times (T_{surface} - T_{ambient}) \qquad (W/m^2 K) \qquad (2)$$

which yields 13 ^{0}C for the protected wall and 253 ^{o}C for the unprotected wall. There is clearly error in these calculations as the estimate of the surface conductance is likely to be very tenuous. Nevertheless the estimates show that, relatively, the protective liner vastly lowers the temperature of the steel sheet over a fully exposed steel sheet. It can be noted that although the estimate of 13^{o}C may appear low it was observed that during all four burns the exterior burn house wall was at most luke-warm to the touch confirming qualitatively at least that the estimates are not totally out of order.

In addition to the burn room walls and ceiling the sprinkler pipe at the ceiling on The W wall was boxed in using the same treatment as for the walls and ceiling. The estimated cost exclusive of many hours of labour is \$4.50 ft^2. Figure 2 shows the burn room liner under construction with the plywood, strapping and partial installation of Durock® cement board.

3. OBSERVATIONS, and MODIFICATIONS DURING AND POST BURNS

3.1 Burn #1, Jan. 20/04

3.1.1 Preparation

For this burn the ceiling was lined with a sacrificial liner which was ½" x 4’ x 8’ (0.0127 x 1.22 x 2.88 m) plywood screwed through the Durock® and the ¾" (19.1 mm) plywood with the same 3 ¼" (82.6 mm) Tapcon® concrete screws as used for fastening the Durock® except that a ¼" (6.4 mm) bumper washer was added to the screws to

improve the pull through strength of the plywood. The plywood door at the NW corner was also sheeted with cement board over the top 5’ (1.524 m).

3.1.2 Observations

As discussed in Klinck [5], the ceiling plywood ignited during the burn and was partially consumed. Examination of the room after suppression also showed two minor areas of damage. Firstly, the plywood cover over the N wall window which protected the camera was charred and secondly, some of the mortar in the joints of the Durock® board showed minor spalling in areas where the sacrificial plywood was burned through. All the ceiling plywood was subsequently removed to scrap in preparation for the next burn. (This was adopted as standard practice for all succeeding burns.)

During the removal process it was determined that the Philips head Tapcon® screws were difficult to remove and in many cases the screws were not re-useable. For this reason all future sacrificial liners were attached with the same length Tapcon® screws but with ¼" (6.4 mm) hex heads. Using the appropriate nut driver this greatly improved the installation process and assured that fasteners could be reused over the remaining burns.

3.2 Burn #2, June 9/04

3.2.1 Preparation

The only corrective modification which was undertaken was to thermally protect the plywood on the N wall camera window with Fiberfrax ® DuraBlanket mats, a ceramic fibre which has an operating temperature range up to 1170 ^{o}C [6]. As in burn #1, the ceiling was lined with ½" (12.7 m) plywood as a sacrificial liner. In addition 12"

(0.305 m) plywood strips were added to the top of each wall and the boxed area on the W wall. These were butted against the ceiling.

3.2.2 Observations

The fuel load for this fire was 51.6 kg compared to the first fire (which was slightly lower, 48 kg with the additional combustible plywood on the walls. This produced higher upper layer temperatures and as well the ceiling layer was much thicker.

Suppression required three attempts as minimal water was used so as to minimize the exposure of thermocouples to water and the water load on the ceiling liner which was open at the top because of the ceiling girders. Complicating the suppression activity was the fact that fire had penetrated into and behind the wall at the top right corner of the S window. In addition the boxed in corner had been also been penetrated.

The fire crew had to remove any remaining plywood and break-through the protective liner in each of these areas to reach the burn which resulted in some structural damage to the Duroc® sheets.

About 2 hours after the on duty fire crew left smoke was observed emanating from the top of the door at the NW corner (the hallway) and into room 2 at the ceiling in the SW corner due to a re-kindle of the window fire. The top of the W wall door at the NW corner also rekindled. This required additional suppression (ABS) and an extended period of vigilance but these runners left unattended would have resulted in serious damage to the structure.

The Fiberfrax® mats on the N wall window provided excellent fire protection as no charring to the plywood underneath. When the combustible liner was removed from the remaining areas of the walls and ceiling it was observed that no major damage had occurred to the cement board except as noted above. However the masonry cement

grouting between the cement board joints was breaking out of the joints and exposing the underlayer of ¾" (19.1 mm) plywood next to the steel wall.

A view of some of the damage can be seen in Figure 3. This view is into the SW corner and shows the damage at the top of the S window, the cement board removed from the box protecting the sprinkler pipe and the exposed joints in the cement board on the ceiling. This same view taken prior to this burn is presented by Klinck [5] as Figure 3.13 and can be referenced to ascertain the extent of damage.

3.3 **Burn #3, Sept 30/04**

3.3.1 Preparation.

For this burn two considerations were addressed:

a) repair of the damage that occurred in burn #2 with improvements to protect against further penetration of fire behind the cement board of the liner and to protect the combustible plywood door in the NW corner connecting room 1 and the hallway , and,

b) to conduct a more controlled burn by not installing any sacrificial plywood on the cement board and by reducing the fuel load of the burn.

All damaged cement board and wood was replaced or modified as well as could be done. Any loose masonry cement in the cement board joints was scraped out and all joints were re- grouted with normal drywall compound. This was much easier to apply than the masonry cement.

Since the Fiberfrax® blanket was so effective at protecting the camera window on the N wall it was installed around the S wall window, over the sprinkler pipe box and on

and around the corner of the wood hallway door at the NW corner down to about 60" (0.152 m) using 3 ¼" (82.6 mm) Tapcon® hex head screws through ¼" (6.4 mm) bumper washers on about 12" (305 mm) centers. Figure 3.14 of Klinck [5] shows a view of the fire room prior to the test burn.

3.3.2 Observation.

The full load for this burn was about 38 kg and with no combustible ceiling/wall material the burn this was a rather benign fire. All surfaces appeared unaffected by the burn and no problems were encountered. The exposed dry wall compound held its bond to the cement board and there was no spalling or cracking apparent.

3.4 Burn #4, Nov. 25/04

3.4.1 Preparation.

This burn was anticipated to be the last of the series and it was decided to increase the fire load and the quantity of combustible wall linings to test the ability of this design to protect the steel structure and prevent fire spread to other rooms. The ½" (12.7 mm) plywood sacrificial liner was applied to the ceiling and as well about 3' (0.914 m) down the lined wall. Ceramic bats were installed liberally over any perceived problem areas with the same technique as before. See Figure 3.15 of Klinck [5].

3.4.2 Observations

As anticipated this burn was a severe test of the liner/construction integrity. Although no fire penetration through wall materials occurred the exposed surfaces were stressed but not to failure, except as noted below. Figure 4 shows the view into the SW corner after the burn. The thickness of the thermal layer is evidenced by the tell-tail

vertical strips on the wall and in fact the temperature reached 380 ^{o}C at 24" (0.610 m) above the floor. The ceramic blanket was virtually intact except in areas in which received enough water to totally soak the mat. These blankets have little pull through strength and cannot support the water load when soaked through however this damage was minimal and easy to repair. The dry wall compound remained remarkably intact as can be observed on the ceiling. This survived even after the ceiling sacrificial liner burned off.

Figure 5 shows evidence of one disturbing result. The Durock® cement board placed on the steel wall of the instrumentation shaft on W wall was not protected by any thermal shield. Some hour or so after suppression it was observed that fire had imbedded into the cement board and a smoulder was in progress. In addition the Durock® had lost any residual strength and was brittle to the touch, albeit this area had been exposed to four burns. Figure 5 shows the area of fire penetration in the cement board.

4. CONCLUSIONS AND RECOMMENDATIONS

Overall the chronology of modifications of chosen liner design was successful in achieving its goal in as much as this was a learning experience and modifications were undertaken as problems arose. The thermal shielding of the steel civil structure by the liner was more than adequate. The construction was time consuming but anyone with basic carpentry/masonry skills and physical strength would not be overly challenged. After the 4th burn it would appear that exposed cement board was failing and would need to be replaced. This problem could be alleviated in future by making sure all exposed cement board was covered with ceramic mats. A major positive outcome was the cost. At an estimated \$4.5/ft^2 this cost is relatively minimal to alternative choices. The number of burns that can be performed without major replacement of the liner cannot be determined

but it is anticipated that one should get at least six more burns out of the existing configuration if the following recommendations are adopted.

RECOMMENDATIONS

a) The basic liner construction should be ¾" (19.1 mm) plywood, overlaid with ¾" x 3 ½" (19.1 x 88.9 mm) strapping on using screws and ¼" (6.4 mm) bumper washers on 12" (305 mm) centers and is then covered with ½" (12.7 mm) Durock® cement board ,screwed to the underlying strapping with 3 ¼" (82.6 mm) hex head Tapcon® concrete screws at 12" (305 mm) OC

b) The cement board joints should be filled with drywall compound at temperatures above 15 ^{O}C and allowed to set for 2 or 3 days.

c) If a sacrificial liner is used it should be screwed through the cement board with the appropriate fastener and bumper washers.

REFERENCES

1. Marks Standard Handbook for Mechanical Engineers, 10'th Edition, E.A.Avallone & T. Baumeisster 111, Eds, McGraw Hill, 1996, ISBN 0-07-004997-1
2. Cement Board Systems (Data Sheet), USG Corporation, SA932 09305, www.usg.com/IC//products/C_BOARD/Durock.asp
3. Heat Transfer , A Bejan, John Wiley and Sons, Inc. , 1993, ISBN 0-471-50290-1
4. Fundamentals Heat and Mass Transfer , F.P. Incropera & D.P De Witt, 3'rd Ed., John Wiley and Sons, Inc., 1990, ISBN 0-471-51961-8
5. An Experimental Investigation of the Fire Characteristics of the University of Waterloo Burn House Structure, A.J.Klinck, MASc Thesis, Department of Mechanical Engineering, University of Waterloo, 2006
6. Fiberfrax Blanket and Mat Products, Unifrax Product Information Sheet, Form C-1421,

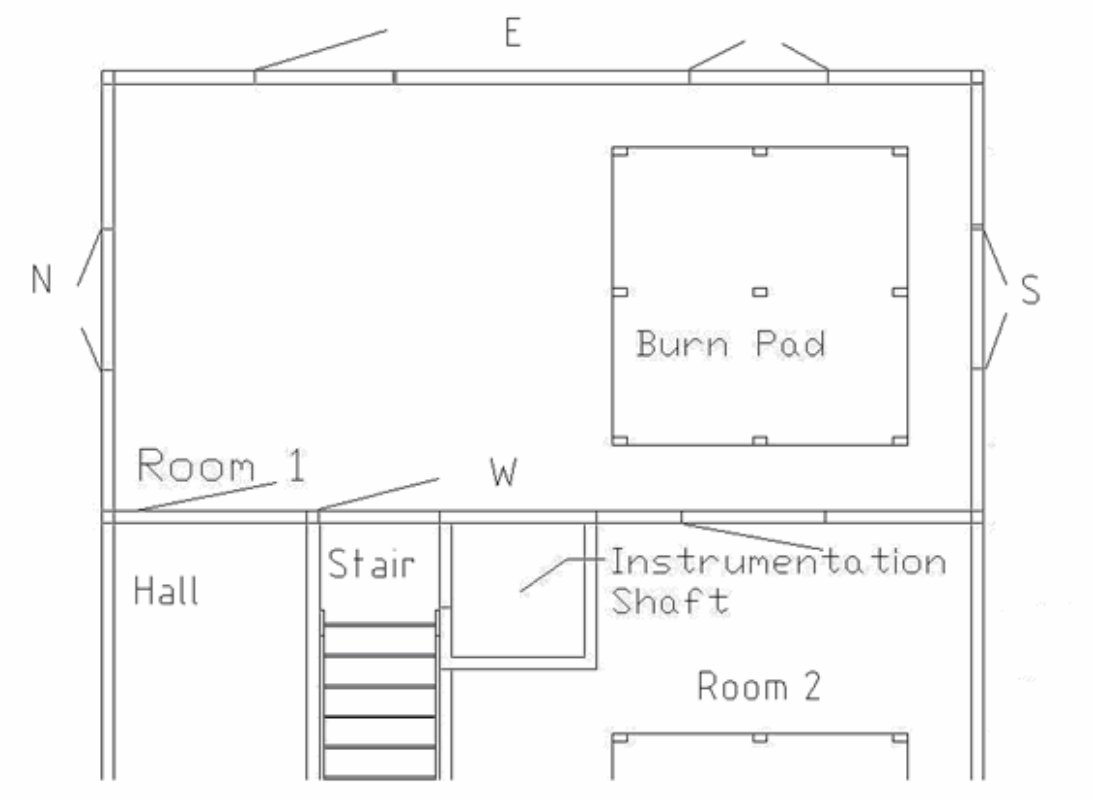

Figure 1: Plan View of Burn Room.

Figure 2: Burn Room Liner under Construction Showing Plywood, Strapping and Partial Installation of Durock Concrete Board. (South Wall in the Background)

Figure 3: Room Damage After the 2nd Burn, June 20/04 Showing the Result of Fire Penetration Through the Wall at the Top Corner of the S Window and the Area of the Boxed in Sprinkler Pipe.

Figure 4: Room Condition after the 4th Burn, Nov. 25/04 with a view into the SW Corner.

Figure 5: Evidence of Fire Penetration into an Exposed Sheet of Durock® Cement Board.